



Coastal Inundation: Tangoio to Clifton

Prepared for

Hawke's Bay Regional Council;
Hastings District Council;
Napier City Council

Prepared by

Tonkin & Taylor Ltd

Date

November 2023

Job Number

1019664 v4



Together we create and sustain a better world

www.tonkintaylor.co.nz

Document control

Title: Coastal Inundation: Tangoio to Clifton					
Date	Version	Description	Prepared by:	Reviewed by:	Authorised by:
09/12/2022	1	Draft issue for Client and Peer Review.	E Beetham; H Blakely	P Knook; R Reinen-Hamill	R Reinen-Hamill
20/04/2023	2	Client and Peer Review comments addressed.	H Blakely; E Beetham	R Reinen-Hamill	R Reinen-Hamill
02/05/2023	3	Peer Reviewed Final Draft.	E Beetham	R Reinen-Hamill	R Reinen-Hamill
30/11/2023	4	Final Report with update memo on post cyclone Gabrielle terrain.	E Beetham	R Reinen-Hamill	R Reinen-Hamill

Distribution:

Hawke's Bay Regional Council	1 PDF copy
Hastings District Council	1 PDF copy
Napier City Council	1 PDF copy
Tonkin & Taylor Ltd (FILE)	1 PDF copy

Table of contents

1	Introduction	1
1.1	Purpose	1
1.2	Scope of works	1
1.3	Terms and Abbreviations	2
2	Physical environment	3
2.1	Site overview	3
2.2	Datums	4
2.3	Geology	4
2.4	Vertical Land Movement	7
2.5	Bathymetry	8
2.6	Topography	10
2.7	Coastal structures and management	13
2.8	Notable coastal inundation events	13
3	Water levels	15
3.1	Astronomical tide	15
3.2	Storm tide levels	15
3.3	Sea level rise	16
4	Wave climate	18
4.1	Wave climate overview	18
4.2	Extreme events for inundation modelling	18
5	Inundation model development	22
5.1	Model description	22
5.2	Model limitations	22
5.3	Model bathymetry	23
5.4	Model parameters	25
5.5	Model calibration	25
5.6	Sensitivity to a 50-year storm or swell event	26
5.7	Terrain changes since Cyclone Gabrielle	27
6	Coastal inundation hazards	28
6.1	Model inputs	28
6.2	Model outputs	29
6.3	Building Code scenario	30
6.4	Areas potentially exposed to static inundation	37
7	Summary	38
8	Applicability	39
9	References	40
Appendix A	Water level analysis	
Appendix B	Wave climate analysis	
Appendix C	Model calibration	
Appendix D	Peer Review Letter	
Appendix E	Comparison of 2020 and 2023 LIDAR in context of the 2022 Clifton to Tangoio Coastal inundation assessment	

Executive summary

Three Hawkes Bay Councils (Hastings District, Napier City and Hawke's Bay Region) commissioned Tonkin & Taylor Ltd (T+T) to investigate coastal inundation hazards between Tangoio and Clifton for the purpose of assessing Building Consent applications.

Building Code compliance was assessed based on a 2% annual exceedance probability event (AEP) with future Sea Level Rise (SLR) from IPCC AR6 scenario SSP5 8.5M over an approx. 80 year timeframe (i.e. 0.77 m at 2100, relative to a 2020 baseline) with additional allowance of Vertical Land Movement (VLM) from NZ SeaRise (2022) predictions. Land subsidence is predicted to occur in all areas of the site, with a large spatial variation. Subsidence north of Napier is predicted to be 0.3 - 0.4 m over the next 80 years, compared to 0.1 - 0.3 m of subsidence south of Napier.

In addition to the 2% AEP event in 2100, the 1% AEP event was considered at 2100 to compare with existing modelled inundation extents, and a 2% AEP event was simulated at present day for sense checking the model results.

Relative sea level rise for 2100 was modelled by adjusting the terrain according to VLM and increasing the water level according to the absolute sea level rise. Terrain levels were informed by recent LiDAR survey in 2020 and a combination of bathymetry surveys and extended beach profiles.

A regional wave hindcast model (operated by Hawke's Bay Regional Council) and data from the Napier Port wave buoy were used to inform the 2% AEP wave event.

Coastal inundation was simulated using the wave forced hydrodynamic model XBeach-GPU. The model was calibrated and tested against field observations of wave inundation during a high energy swell event generated by ex-Tropical Cyclone Pam. The model predicted the observed inundation extent and level at 13 locations between Clifton and Westshore, with a mean absolute error of 0.2 m in the vertical level.

Coastal inundation scenarios were simulated at a spatial resolution of 5 m horizontal with the terrain based on the ground level, without resolving object features such as buildings, trees, and fences. Drainage management networks such as flood gates and pumps were also not resolved.

The resulting coastal inundation outputs were mapped as a raster layers (GeoTIFF) showing the inundation level and extent associated with dynamic coastal processes. Outputs for the coastal inundation level and depth are provided as digital files.

The modelling work undertaken for this assessment, including the draft report has completed a peer review process by Dr Cyprien Bosserelle at NIWA. The peer review letter is appended to Appendix D.

After the modelling work for this project was completed, the region was impacted by Cyclone Gabrielle on 14 February 2023. The coastal terrain was altered in areas of erosion or wave overwash occurred on the gravel barrier, and in areas of silt deposition on the lower catchment. A review of the changes to coastal terrain change during the cyclone was undertaken to assess any implications on the coastal inundation model results. This review is attached as a Memorandum in Appendix E and concludes that the coastal inundation modelling results do not require updating with a post-Gabrielle terrain in the bathymetry.

1 Introduction

1.1 Purpose

Hastings District Council (HDC), Napier City Council (NCC), and Hawke's Bay Regional Council (HBRC) commissioned Tonkin & Taylor Ltd (T+T) to assess coastal inundation for the area between Clifton and Tangoio for the purpose of assessing Building Code compliance. Based on legal advice to HDC by Rice Speir (2021) the most appropriate parameters for assessing building consents are:

- A 2% annual exceedance probability (AEP) event, which is a 50 year annual recurrence interval (ARI).
- A 75 – 80 year economic timeframe (taken to be the year 2100).
- Sea level rise scenario RCP 8.5M.

1.2 Scope of works

A total of three inundation scenarios were agreed for this assessment to assess the Building Code scenario and to test the outputs against present day sea level and the future 1% AEP event:

- The 2% AEP event (50 year ARI) at present day sea level (used for sense checking).
- The 2% AEP event (50 year ARI) for 2100 using RCP 8.5M sea level rise (Building Code scenario).
- The 1% AEP event (100 year ARI) for 2100 using RCP 8.5M sea level rise (comparison to existing).

In accordance with the Ministry for Environment Guidance on Coastal Hazards updated in 2022 (MfE, 2022), we have adopted the latest information on future sea level rise and vertical land movement from NZ SeaRise and IPCC AR6 assessments. The latest information on land elevation (2020 LiDAR) was used to inform land levels and an up-to-date wave climate was established for this investigation.

Coastal inundation was modelled using a wave forced hydrodynamic model XBeach that resolves both static and dynamic drivers of coastal flooding. XBeach is an industry leading wave and hydrodynamic model that is suitable for modelling coastal inundation at a regional scale.

The resulting inundation layers were defined by the maximum water level associated with the following processes that are further defined in Table 1.1:

- Relative sea level rise.
- Storm tide level.
- Wave setup.
- Waves motions at the group frequency (known as surf-beat or infragravity waves).

1.3 Terms and Abbreviations

Table 1.1: Definition of common terms used in this report

Terms	Definition
Coastal inundation	Flooding of land above the typical high tide level that is caused by oceanographic or coastal processes.
Gravity waves	Waves generated by wind blowing on the ocean (waves that people surf on). Short period waves are typically referred to as wind waves (interval between waves ≤ 12 s) and longer period waves are referred to as swell (interval between waves > 12 s).
Surf-beat (or Infragravity waves)	Long period wave motions in the surf zone that are generated by groups of gravity waves. Infragravity waves are 'bound' to wave groups in deep water but are released as 'free' waves in the surf zone (when gravity waves break to form white water). Infragravity waves have a height that scales to the breaking wave height, and a period related to the wave group (30s – 5 min period). Infragravity waves surge through the surf zone and become the main driver of wave runup and inundation at the shoreline, as gravity wave energy is dissipated by the shoreline.
Wave setup	The increase in mean water level (above the still water level) due to the presence of breaking waves. Wave setup occurs landward of the wave breaking point and results in a raised water level at the shoreline that can cause inundation.
Wave runup	The landward reach of waves surging up the shoreline.
Wave overtopping	Wave overtopping occurs when wave runup exceeds the elevation of a coastal barrier, causing waves to flow overland.
Inundation level	The level of the water surface relative to a known datum (NZVD-2016 in this report)
Inundation depth	The depth of water above the ground level. In this assessment the outputs for 2100 are associated with ground levels that are adjusted for vertical land movement.
Vertical land movement	The change in land elevation due to geological processes of subsidence or uplift.
Absolute sea level rise	The increase in the mean level of the sea without reference to land.
Relative sea level rise	The net result of vertical land movement and absolute sea level rise.

Table 1.2: List of symbols and abbreviations

Symbol	Definition	Abbreviation	Definition
H_s	Significant wave height (average of 1/3 largest waves).	SLR	Sea level rise.
H_{m0}	Significant wave height based on wave spectrum.	VLM	Vertical Land Movement.
H_{max}	Maximum wave height.	XBGPU	XBeach-GPU hydrodynamic model.
T_p	Peak wave period.	TC Pam	Ex-Tropical Cyclone Pam (15 March 2015).
T_s	Period of significant waves.		
D_p	Peak wave direction (direction from).		
h	Water depth relative to ground level.		

2 Physical environment

2.1 Site overview

The site extent is between Tangoio and Clifton, which includes Napier City and townships within Hastings District (Tangoio, Whirinaki, Clive, Haumoana, Te Awanga). The coast is approximately 35 km north to south and separated into two discrete littoral cells (see Figure 2.1). The Haumoana cell is located between Cape Kidnappers and Napier Port (Bluff Hill) and is characterised by a gravel barrier at the seaward end and relatively low terrain landward of the barrier. A network of rivers discharges into the Haumoana littoral cell, including the Tukituki just north of Haumoana and a confluence of three rivers that have a complex mouth system between Clive and Awatoto (Clive River, Ngaruroro River, Tutaekuri River).

The Bay View cell is located between Napier Port and Tangoio and is also characterised by a gravel barrier at the coastal edge with low terrain inland. The Bay View cell includes Ahuriri Estuary which flows through Napier City and is trained by stop banks. The Esk River discharges to the coast at the midpoint of the Bay View cell.

All rivers along the site are managed by HBRC to control catchment flooding hazards and a significant network of stop banks have been constructed since the region was first developed.

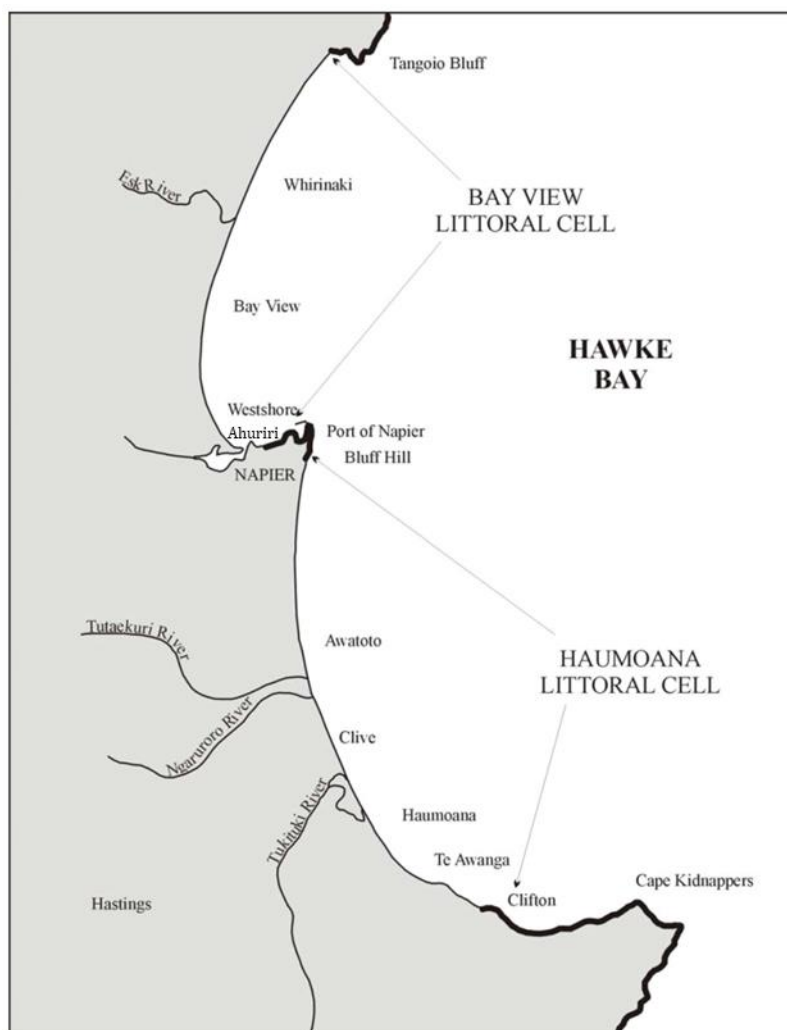


Figure 2.1: Overview of site and Littoral Cells from Komar (2005) with consolidated coast in black.

2.2 Datums

The vertical datum for this project is New Zealand Vertical Datum 2016 (NZVD-16) referred to as RL, and the map projection is New Zealand Transverse Mercator (NZTM, EPSG 2193).

Existing water level datasets from Napier Port are relative to Chart Datum (CD), or Napier Vertical Datum (NVD-62) and can be converted to NZVD16 using offsets in Table 2.1. These conversion values are recommended by MfE Coastal Hazard Guidance (MfE, 2017) for establishing water levels relative to NZVD16. A conversion between Chart Datum and HBRC vertical datum is also provided, which is required for understanding water levels relative to beach profile surveys, as detailed in Beya and Asmat (2021). We also present a conversion between bathymetry data provided by GNS (reference MSL) and NZVD-16 which is outlined in Appendix A.

Table 2.1: Conversion offsets between different vertical datums

Convert from	Convert to	Offset (m)	Reference
CD	NVD-62	-0.9243	MfE (2017)
CD	HBRC Vertical Datum	9.08	Beya and Asmat (2021)
NVD-62	NZVD-16	-0.193	MfE (2017)
GNS model bathymetry (MSL)	NZVD-16	-0.23	This assessment

2.3 Geology

The Hawke Bay region has three major physiographic elements including inland mountain ranges, a central area of lowlands and river valleys, and coastal hill ranges. Figure 2.2 shows that the stretch of coast from Tangoio to Clifton is generally low-lying estuarine deposits (white areas). South of Clifton the shoreline is backed by steep high cliffs (yellow areas). North of Bay View, inland mountains approach the shore (brown). A rock outcrop (Bluff Hill; yellow) is in Napier and separates the shoreline into two the two distinct littoral cells. The coastal ranges are formed predominantly by sedimentary rocks of Cretaceous and Tertiary age, and these include predominance of rock type "papa".

The Hawke's Bay region lies in the most active seismic region of New Zealand (Hull, 1990). The Hawke's Bay region is dominated by the collision of the Australian plate and Pacific plate, with the latter giving way and sliding beneath the Australian plate (Komar and Harris, 2014). Figure 2.2 shows the major faults around the Hawke's Bay (red and black dashed lines). The collision of the two plates have formed and deformed the rocks along the coast and was the cause of the Hawke's Bay earthquake in 1931. This earthquake caused an uplift of about 2 m from Bay View to Tangoio but caused a subsidence in the order of 1 m along the southern end of the Haumoana Littoral Cell (see Figure 2.3)

The 1931 earthquake is a defining event in the development of Napier and Hastings. Prior to uplift, the Ahuriri estuary formed a lagoon, extending inland of Bay View and was navigable for ships, spanning a vast area inside the gravel barrier (Figure 2.4). The seismic uplift event drained the lagoon, which was subsequently managed into farmland and a regional airport. The coastal edge was also uplifted, which lifted the existing gravel barrier that has become developed in sections between Westshore and Tangoio.

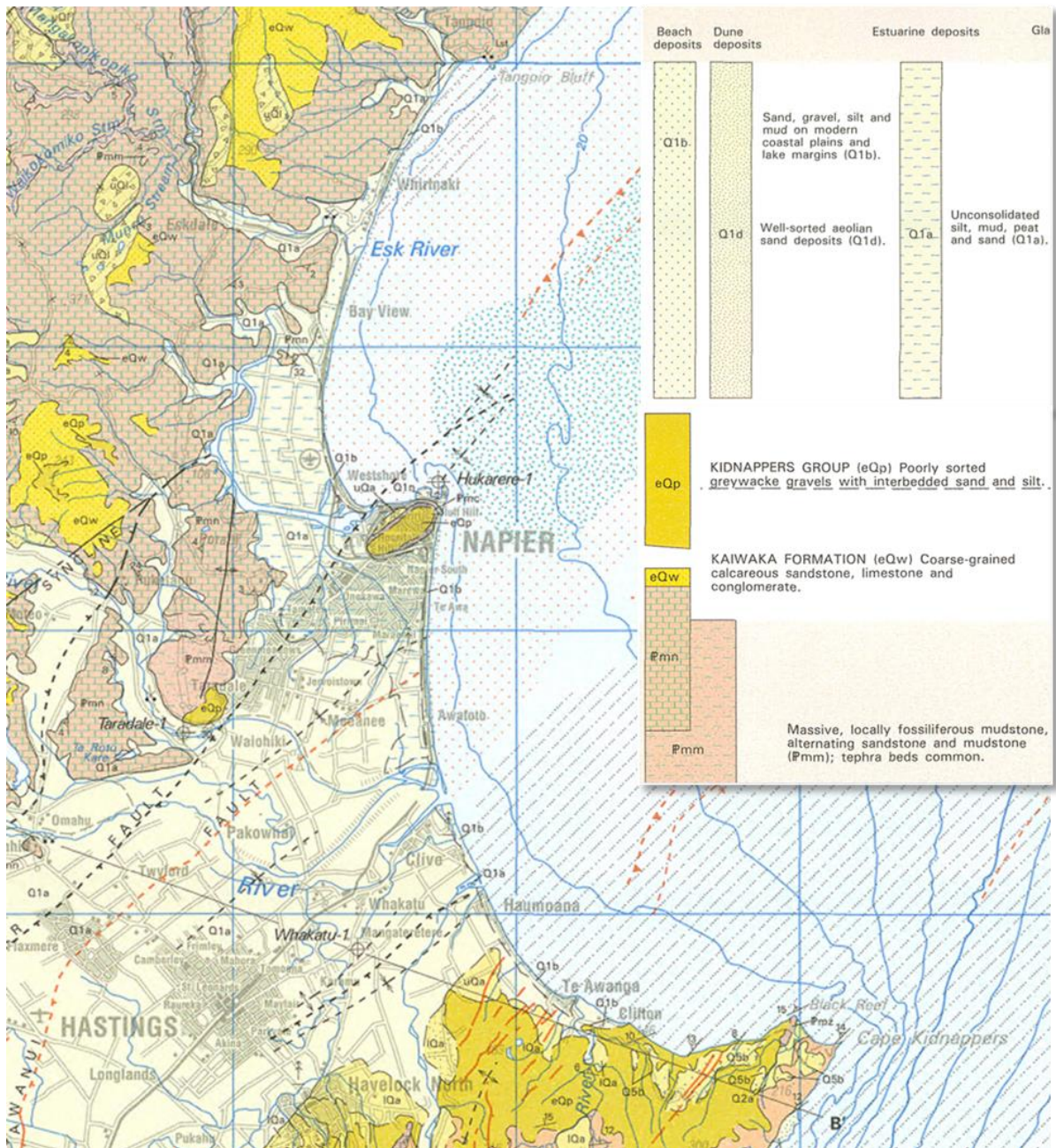


Figure 2.2: Hawke's Bay geology (source: GNS Geology of the Hawkes Bay Area 1:250k QMAP series).

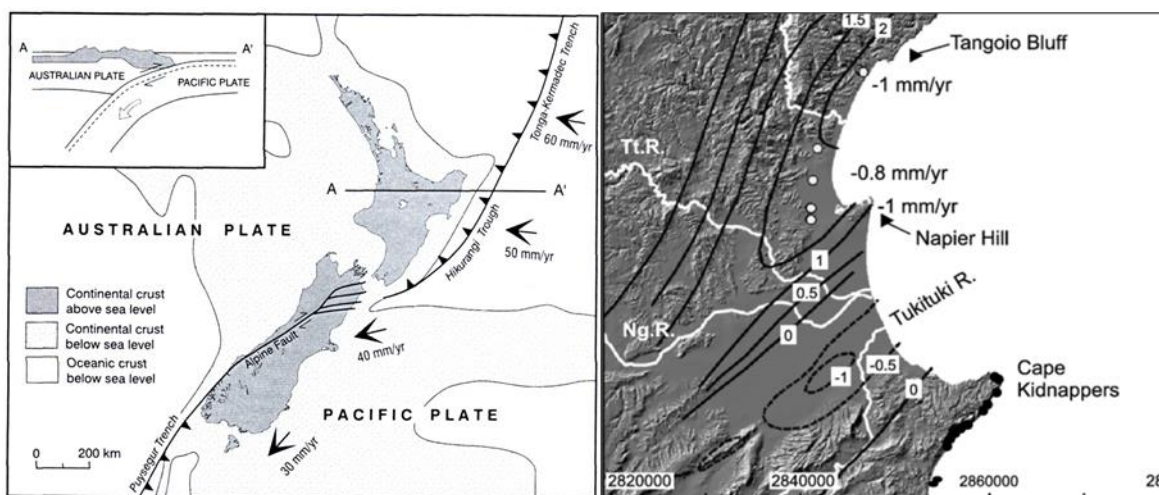


Figure 2.3: Tectonics and geomorphic features of New Zealand. (A) Plate subduction of the Pacific plate occurring at the Hikurangi Trough closest to Hawke's Bay (Source: Aitken, 1999). (B) Land changes resulting from the 1931 earthquake with sudden change in black contours (contour values in white boxes are in m) and the resulting long-term subsidence in mm/yr (Source: Hull, 1990).

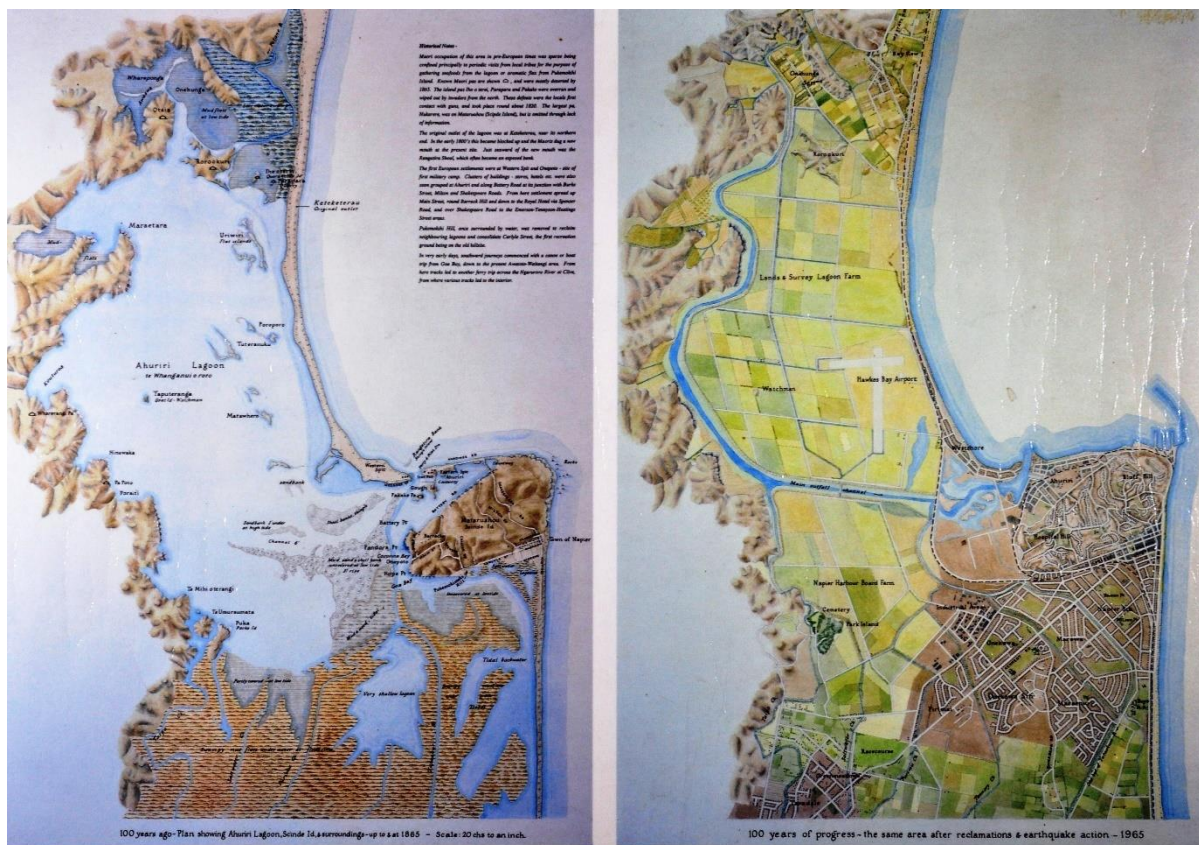


Figure 2.4: Ahuriri estuary forming a lagoon in 1865 (pre earthquake and development) and in 1965 (after the uplift and drainage for agriculture). Source: Napier — 100 Years of Progress' Map (1965). Hawkes Bay Digital Archives Trust, CC-BY-NC 4.0¹.

¹ Sourced from: <https://www.a-maverick.com/blog/from-te-kuri-to-te-mata-what-you-will-see-as-you-leave-gisborne-for-hawkes-bay>.

2.4 Vertical Land Movement

Vertical Land Movement (VLM) relates to changes in the land level associated with tectonics and other earth surface processes (such as subsiding alluvial material). If the land level at the coast is subsiding, there is a relative rise in sea level that can increase coastal hazards.

Past assessments of VLM for the Hawke's Bay region are summarised in existing coastal hazard reports (e.g. T+T, 2016; Komar and Harris, 2014). An important context for VLM in Hawke's Bay is the plate tectonic history and a major earthquake in 1931 that caused significant uplift between Tangoio and Awatoto (+1 to +2 m), and subsidence between Haumoana and Clifton (-0.5 to -1.0 m). The sudden change in vertical land level caused by the earthquake had a significant effect on the region's coastal geomorphology which has been described in previous reports (e.g. Komar and Harris, 2014). An important context for this study is that the uplifted areas effectively created new land for development close to the coast, in areas that were previously too low for development (Figure 2.4).

The gradual change in land level following the 1931 earthquake is less well understood. Periods of rapid tectonic uplift are often followed by periods of gradual subsidence (e.g. Komar and Harris, 2014). When considering short-term records of land level monitoring presented in Beavan and Litchfield (2012), Komar and Harris (2014) concluded that the Bay View and Haumoana littoral cells were likely subsiding at a rate of 0 to -1 mm/yr, with error values of a similar magnitude (Figure 2.5).

New information on VLM, specific to relative sea level rise has been assessed since previous coastal hazard studies were undertaken in Hawke Bay. These include the IPCC AR6 assessment and a New Zealand wide assessment of coastal VLM by the NZ SeaRise programme. The IPCC AR6 assessment considered VLM and provides values for total relative sea level rise. The rate of VLM adopted by the IPCC AR6 assessment at Napier was -0.5 mm/yr, based on tide gauge analysis methods (Kopp et al, 2014). This provides a reference point for comparing to the local site-specific data available through NZ SeaRise.

Site specific records of VLM around the New Zealand coast were assessed by the NZ SeaRise programme, which was released in a publicly available dataset in June 2022². The NZ SeaRise dataset provides site specific information on VLM and relative sea level rise at point locations spaced every 2 km along the NZ coast. The VLM assessment method used in the NZ SeaRise program is based on analysing Interferometric Synthetic Aperture Radar (InSAR) data from satellites (Levy et al., 2020; Hamling et al., 2022; Naish et al., 2022). The data were analysed for a period between 2003 – 2011 (8 years), which is a relatively short sampling period for adopting a long-term rate of change. The data represented in each point capture a radius of approximately 5 km. The high spatial resolution of locations assessed in the NZ SeaRise assessment results in approximately 35 points within the region from Clifton to Tangoio. The magnitude of VLM reported by NZ SeaRise in this region varies from -0.2 mm/yr to -4.73 mm/yr, with a site wide mean \pm standard deviation of -3.09 ± 1.15 mm/yr (Figure 2.5).

Data from NZ SeaRise shows a general south to north trend (as presented in Figure 2.5). VLM at the southern end of the site is close to zero, with the slightly negative means and error values that are significantly higher than the mean. Moderate rates of subsidence are present along the southern Haumoana Littoral Cell, increasing towards Awatoto. Note that the error value is close to the mean value for most of Haumoana, which provides significant uncertainty to the actual rate of VLM at this location. The average rate of subsidence across the Haumoana littoral Cell is -1.9 mm/yr. Higher rates of subsidence were observed in the Bay View Littoral Cell, with a mean rate of rates -3.8 mm/yr. The Hawke's Bay region is discussed specifically in Naish et al. (2022) as an example of how VLM can vary significantly within a regional management boundary or littoral cell. The rates of subsidence and spatial variation are explained in context of how the low-lying coast may still be

² <https://www.searise.nz/maps-2>.

settling after the 1931 uplift, with additional reasons being compaction of Holocene fluvial and estuarine sediments and extraction of ground water. This is in context of the higher rates of subsidence being associated with alluvial material that was uplifted in 1931 and lower rates of subsidence being associated with areas that were lowered in the 1931 earthquake.

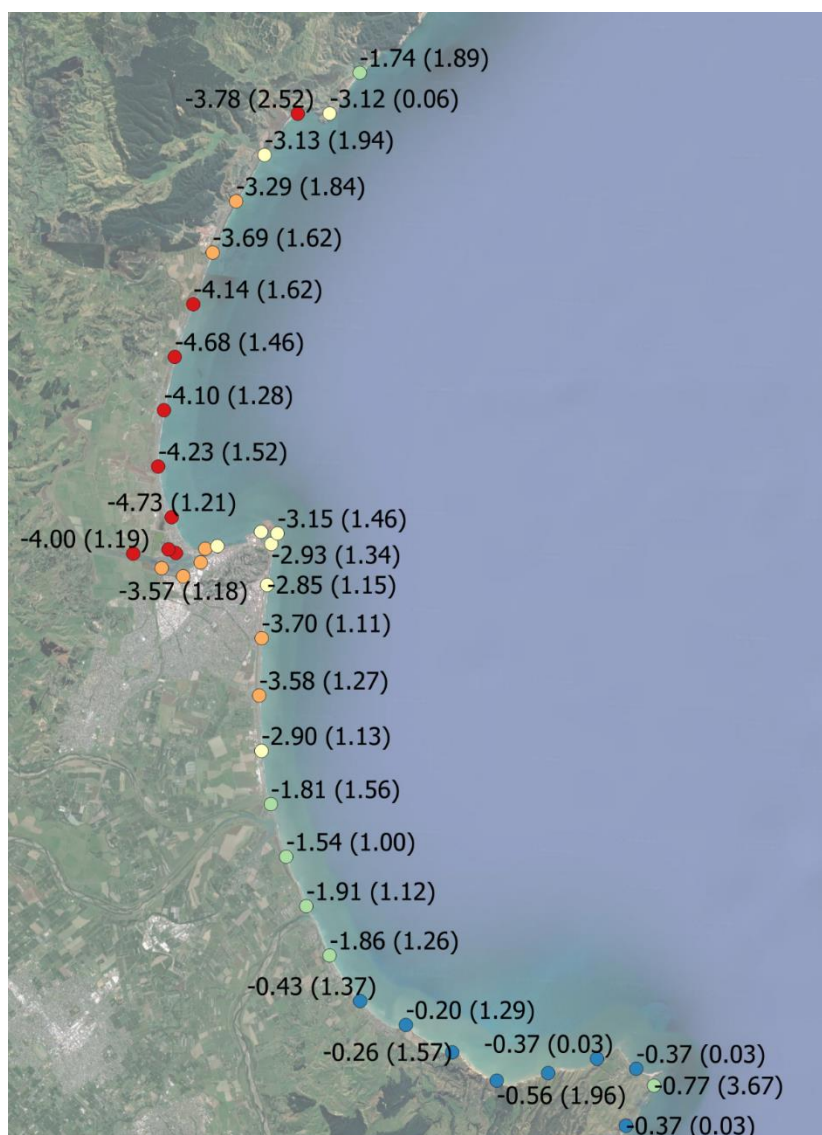


Figure 2.5: Value of VLM from NZ SeaRise showing the trend in mm/yr with associated error (+/-) in brackets.

2.5 Bathymetry

Bathymetry information for this project was provided by HBRC, based a composite bathymetry-topography elevation model compiled by GNS Science for a tsunami inundation hazard assessment. This bathymetry was established using multiple sources, including site specific bathymetry surveys, hydrographic charts and beach profile data that extend through the nearshore.

The regional bathymetry is presented in Figure 2.6, showing the general features of the Hawke Bay nearshore. In the Haumoana littoral cell, the nearshore contours indicate a flatter and shallower profile at the southern end between Clifton and Haumoana, where a series of contour bulges indicate a submarine ridge extended seaward of Te Awanga point. As the coast curves to face a more easterly direction, the bathymetry contours become closer together between Clive and Napier

Port. This results in an increasingly steep nearshore profile moving north along the Haumoana Cell with the 15 m depth contour becoming closer to the shoreline.

A network of submarine shoals located approximately 10 m below sea level, known as Pania Reef are located to the northeast of Bluff Hill along the Napier Fault line shown in Figure 2.2. The port has reclaimed land off the coast of Bluff Hill, and a dredged entrance channel is maintained for navigation. The nearshore contours between the port and Westshore indicate a shallow gradient, with some reefs present near the Ahuriri estuary entrance. The nearshore profile becomes gradually steeper between Westshore and Bay View, as the coast bends from a northeast orientation to an easterly orientation. The nearshore profile remains reasonably consistent between Bay View and Tangoio, except for a delta or bar system that builds seaward at the mouth of the Te Ngaru Stream.

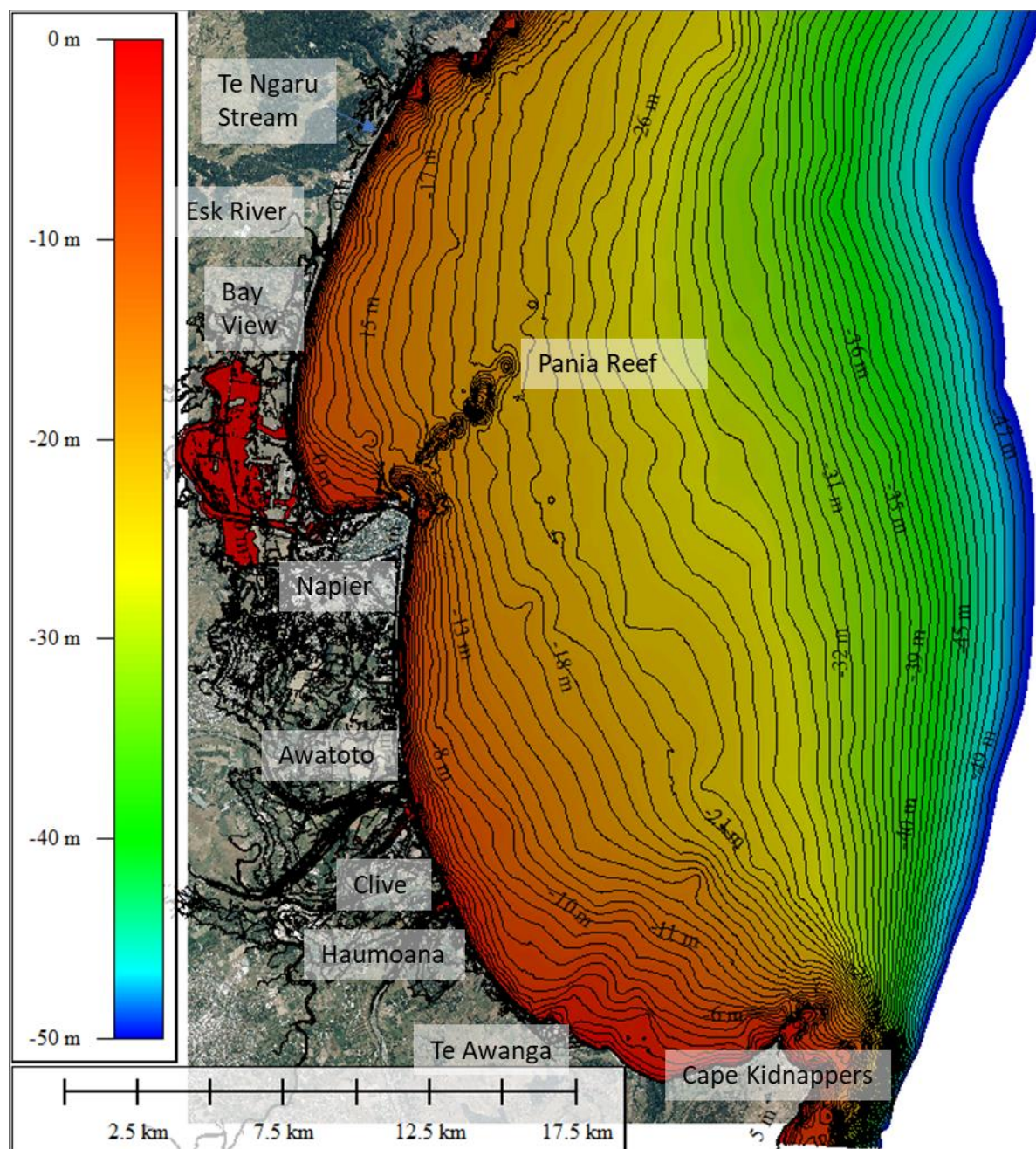


Figure 2.6: Hawke Bay Bathymetry, as processed by GNS Science.

2.6 Topography

The site is generally characterised as having a gravel barrier beach fronting the sea, with a raised crest and lower terrain landward of the beach. An important factor for coastal inundation is the beach crest level relative to the sea level and wave runup, with low elevation barrier crests likely more exposed to inundation hazards.

The barrier crest level varies along the site and is jointly influenced by historic uplift, contemporary coastal processes, and coastal management practises (e.g. the engineered bund at Westshore and the rebuilt crest at Haumoana following storm erosion). The lowest crest levels along the site are located at the southern end, at Clifton and Te Awanga (2 – 3 mRL), with a slight increase along Haumoana and Clive (4 mRL) (Figure 2.7). Crest level increases along Marine Parade, from 4 mRL at Awatoto to nearly 6 mRL near the port. Crest level at Westshore is defined by an engineered bund that is maintained each year using imported pebbles, with a crest level around 3.5 mRL. Crest levels at Bay View range between 5 – 6 mRL, before a significant increase in crest level occurs north of Bay View (6 - 10 mRL).

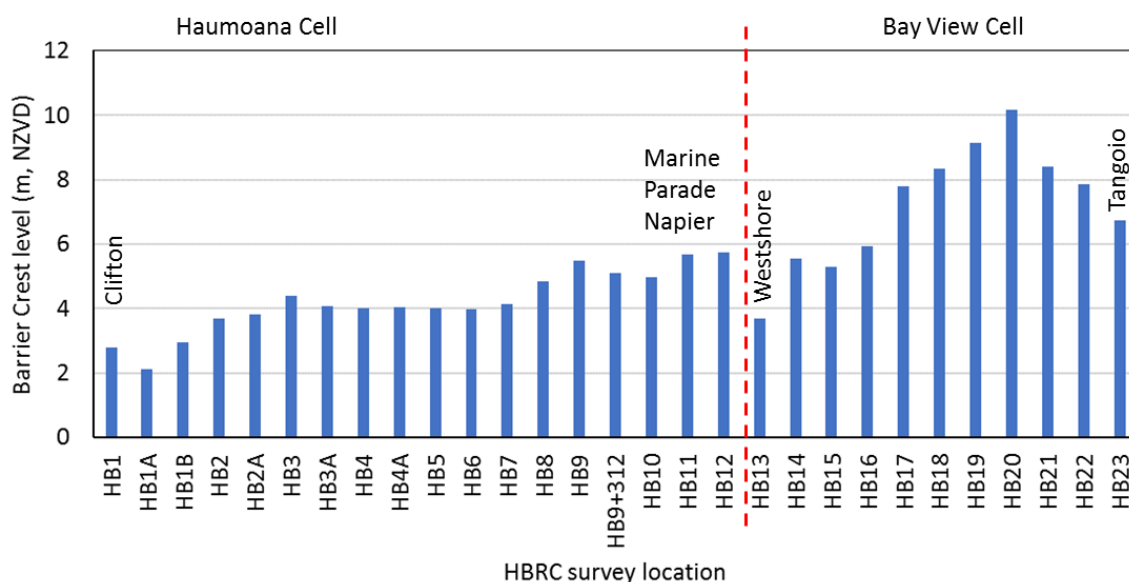


Figure 2.7: Barrier crest level at each beach profile monitoring location along the site, based on the most recent profile survey (2020 to 2022 depending on location).

A regional airborne LiDAR survey in 2020 provides up-to-date information on ground level for the full site extent at a resolution of 1 m horizontal, and vertical accuracy of 0.2 m (95% confidence interval). The LiDAR derived digital terrain model (DTM) was sourced from LINZ and is based on the removal of non-terrain points such as buildings, water, vehicles, and vegetation. An overview of the site elevation is presented in Figure 2.8, highlighting areas of the coastal barrier (typically in green) and a generally lower elevation terrain inland. Areas in light blue are very low (below 0 mRL) and outline the area where Ahuriri estuary previously extended before the 1931 uplift. Note that mean sea level is -0.15 m in the NZVD reference. Extended profile sections are presented for representative locations to show the terrain between the coastal barrier and landward backshore (Figure 2.9). These highlight the variation in crest level, crest width, and inland level along the site. The coastal barrier at Haumoana is notably low and narrow compared to most of the coast and is backed by low lying terrain.

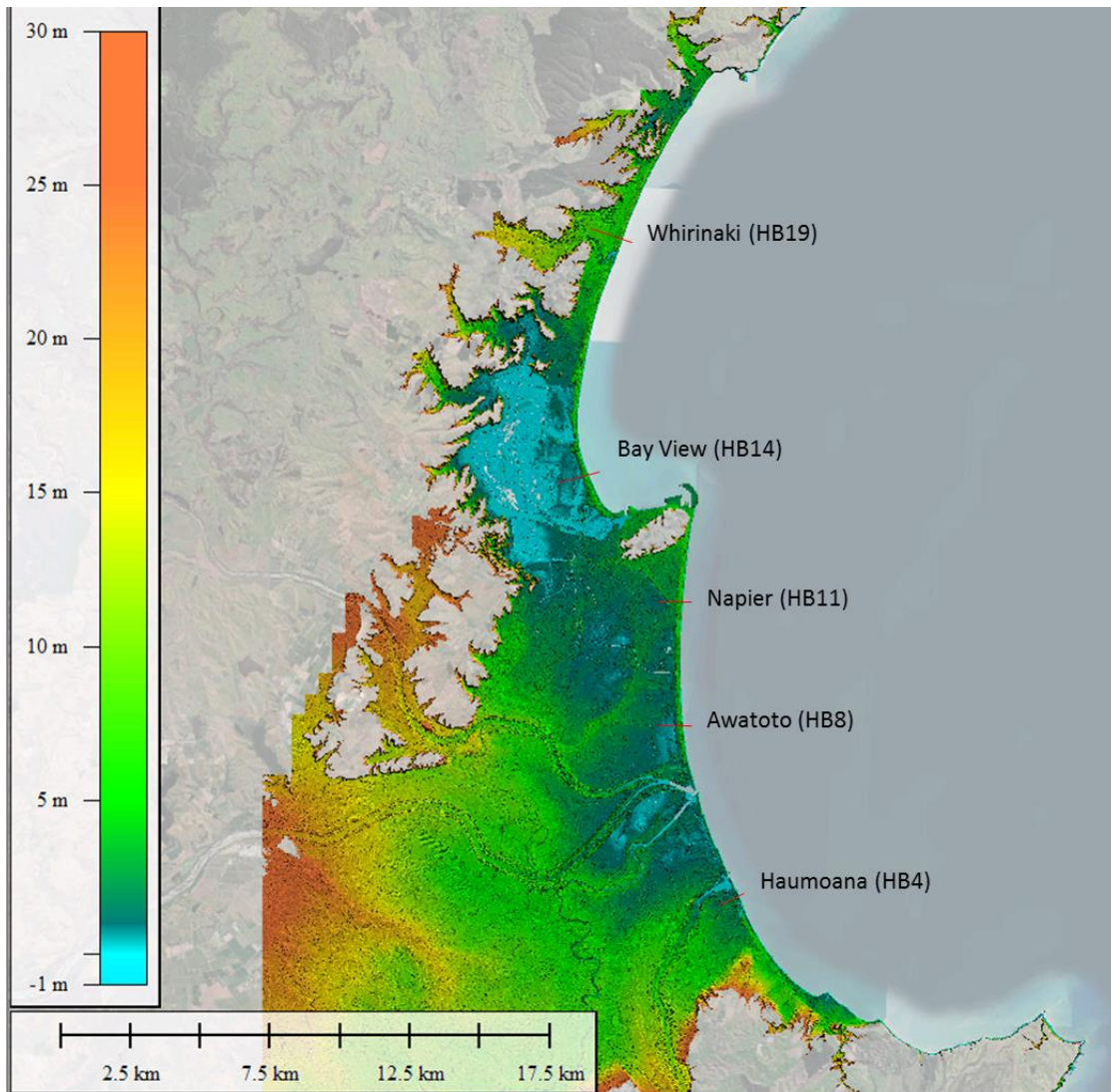


Figure 2.8: LiDAR map showing terrain elevation in NZVD2016 for the site, with elevations clipped between -1 m and 30 m to highlight important coastal features and low lying areas. Red lines show the location of extended coastal profiles in Figure 2.9.

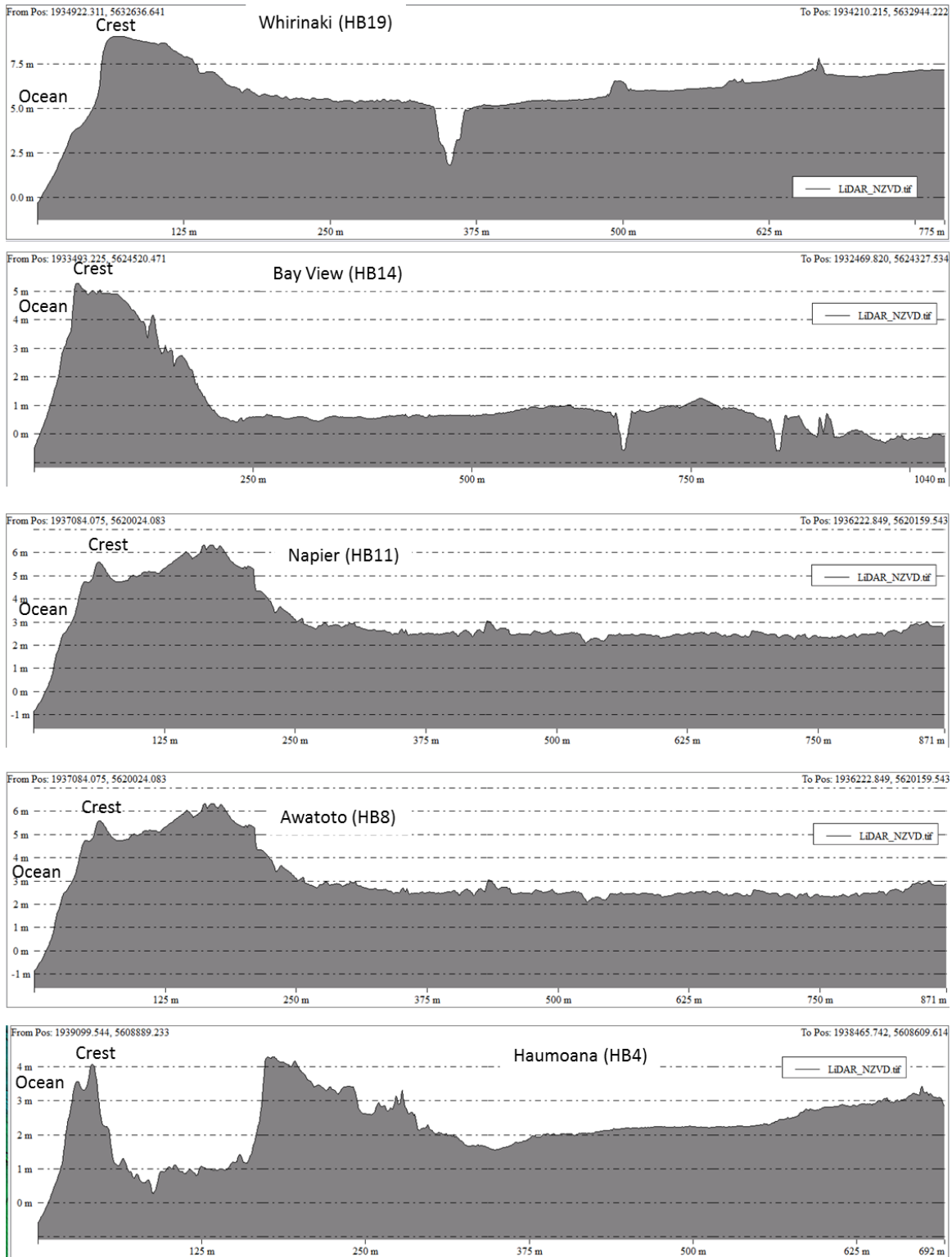


Figure 2.9: Extended coastal profiles at select HBRC monitoring locations based on 2020 LiDAR levels in NZVD 2016.

2.7 Coastal structures and management

The coastal edge along the site includes some discrete sites that have a historic and ongoing coastal management and modification, including:

- Stop banks have been constructed along all major river banks that discharge into the coast.
- Sea exclusion banks were constructed along Clive following a significant coastal inundation event in 1974.
- The Westshore bund, which is an artificial deposit of pebble and gravel size material that extends for 900 m along the coast of Westshore, providing protection to Westshore reserve. Approximately 10,000 – 30,000 m³ of material is deposited annually to shape the 4 m wide and 3.5 m high bund (personal comms Craig Goodier, 8 November 2022).
- Sections of armoured shoreline include:
 - Haumoana rock revetment.
 - Clifton rock revetment.
 - Private properties with ad-hoc coastal armouring at the property boundary along Haumoana beach (3 – 41 Clifton Road).
- Groynes have been constructed to manage coastal erosion at a few sites:
 - Haumoana (south bank of Tukituki River entrance).
 - Clive wastewater outlet.
 - North end of Marine Parade at Napier Port.
- Gravel extraction has occurred historically on the beach at Awatoto and only ceased operation in recent years.
- Beach crest reshaping has occurred after significant storms:
 - Haumoana crest was re-built following its destruction by waves in March 2015, associated with ex-tropical cyclone Pam.

2.8 Notable coastal inundation events

A summary of notable coastal inundation events is presented in Table 2.2. These events have been collated from the NIWA Extreme Weather Database³ and reports from HBRC.

Table 2.2: Summary of notable coastal inundation events along the site

Event description	Ocean conditions
<p>16 August 1974</p> <p>The event is described in the NIWA events catalogue⁴. Families were evacuated from Te Awanga and the Clifton Road was washed away.</p> <p>Seawater flooded Clive (300 Ha) turning the town into a salty lake that was 0.6 m deep in places.</p> <p>Waves were smashing into homes at Haumoana resulting in 4 of 5 homes being evacuated.</p> <p>Waves washed into the skating rink at Marine Parade, Napier.</p>	<p>Anecdotally, waves were in the order of 4.5 to 9 m high.</p> <p>Tide levels are unknown, but event lasted 2 days so would have coincided with at least 2 to 3 high tide stages.</p>

³ <https://hwe.niwa.co.nz/>.

⁴ https://hwe.niwa.co.nz/event/August_1974_Hawkes_Bay_Heavy_Seas.

Event description	Ocean conditions
<p>Shingle overwash deposits filled up the excavation site where the aquarium was being constructed. Beach level was lowered by up to 1.5 m.</p> <p>After the event a large sea exclusion bank was constructed in front of Clive, connected to river stop banks.</p>	
<p>29 March 2002</p> <p>Several homes along Haumoana were damaged by swell waves⁵. Waves were observed overtopping the gravel barrier at the northern end of Haumoana, washing gravel into the lagoon.</p>	<p>High tide and large swell. The port wave gauge recorded maximum waves of 4.7 m at a period of 15 seconds. Tide data is unknown.</p>
<p>30 July 2008</p> <p>Beach front properties damaged at Haumoana, with one partly submerged at high tide⁶</p> <p>Clifton road camp was eroded by waves a week earlier during storm conditions.</p>	<p>Napier Port Wave Buoy:</p> <ul style="list-style-type: none"> • $H_s = 4.7$ m. • $H_{max} = 7.8$ m. • $T_p = 11$ s. • No tide gauge data.
<p>5 March 2010</p> <p>A south easterly swell resulted in overtopping and property damage throughout Haumoana. Tide level at the port was 10 cm above MHWS.</p>	<p>Napier Port Wave Buoy:</p> <ul style="list-style-type: none"> • $H_s = 3.8$ m. • $H_{max} = 6.3$ m. • $T_p = 13$ s. • Max tide gauge level = 0.88 mRL.
<p>15 March 2015 TC Pam</p> <p>Well documented event with high runup and some overtopping and debris mapped by Goodier et al. (2015). Waves overtopped coastal barriers at:</p> <p>Bay View: minor overtopping</p> <p>Westshore: engineered bund wave overtopped and lowered by 1m.</p> <p>Clive: seaward barrier overtopped by waves causing flooding into wetland but not over sea exclusion bank.</p> <p>Haumoana: Gravel crest breached and lowered, pushing gravel into lagoon and channel. Several houses flooded.</p> <p>Te Awanga: Some flooding and overtopping</p> <p>Clifton: Damage to existing coastal protection, road and camps.</p>	<p>Napier Port Wave Buoy:</p> <ul style="list-style-type: none"> • $H_s = 4.5$ m. • $H_{max} = 8.3$ m. • $T_p = 15$ s. • Max tide gauge level = 0.93 mRL.
<p>4 July 2017</p> <p>Long period swell caused some overtopping, mostly focused on properties seaward of Clifton Road at Haumoana.</p>	<p>Napier Port Wave Buoy:</p> <ul style="list-style-type: none"> • $H_s = 2.5$ m. • $H_{max} = 4.0$ m. • $T_p = 15.5$ s. • Max water level = 0.61 mRL.
<p>28 May 2021</p> <p>Wave overtopping surged over / around the Westshore bund causing flooding to the reserve.</p>	<p>Napier Port Wave Buoy:</p> <ul style="list-style-type: none"> • $H_s = 2.8$ m. • $H_{max} = 4.5$ m. • $T_p = 12$ s. • Max water level = 0.95 mRL.

⁵ https://hwe.niwa.co.nz/event/March-April_2002_North_Island_and_Canterbury_High_Winds_and_Seas.

⁶ https://hwe.niwa.co.nz/event/July_2008_New_Zealand_Severe_Storm.

3 Water levels

3.1 Astronomical tide

Tide levels for Napier Port were obtained from LINZ (2021) Nautical Almanac, with reference to Chart Datum. Tide levels were converted to NVD-62 and NZVD-16 using the conversion values in Table 2.1.

Table 3.1: Tide levels for Napier based on LINZ (2021)

	Chart Datum (m)	NVD-62 (m)	NZVD 2016 (mRL)
HAT	2.00	1.08	0.88
MHWS	1.87	0.95	0.75
MHWN	1.46	0.54	0.34
MSL	0.97	0.05	-0.15
MLWN	0.45	-0.47	-0.67
MLWS	0.12	-0.80	-1.00
LAT	-0.02	-0.94	-1.14

3.2 Storm tide levels

This assessment specifically considers storm tide levels for the 1% AEP and 2% AEP event. The 1% AEP is equal to the 100 year ARI, and a 2% AEP is equal to a 50 year ARI. A review of existing storm tide levels was undertaken, and up-to-date tide gauge data were analysed to calculate storm tide level associated with the required return periods. This analysis is presented in Appendix A. A summary of storm tide level calculated for this assessment and previous reports are outlined in Table 3.2: . Details on the methods used in each assessment outlined in Table 3.2: are provided in Appendix A.

The updated extreme storm tide levels identified in this assessment are slightly lower than the values identified previously in T+T (2016), which is due to the longer dataset being assessed and peak events of similar magnitude, causing a plateau in the distribution.

The storm tide levels calculated for this study include the tidal and storm surge components of an extreme water level event. The 2% AEP storm tide of 2.31 m CD is 0.44 m above the MHWS level. Storm tide levels calculated here are close to MHWS + surge level from Beya and Asmat (2021) when the 5% contingency is removed (Table 3.2:).

Table 3.2: Comparison of current and previous extreme storm tide values

AEP	ARI	Current values (m, CD m)	T+T 2016 (m, CD m)	Beya and Asmat (2021) ¹	Beya and Asmat +5% (2021) ²
18%	5yr	2.25	2.21	2.26	2.28
10%	10yr	2.27	2.27	2.28	2.30
5%	20yr	2.29	2.32	2.31	2.33
2%	50yr	2.31	2.38	2.34	2.36
1%	100yr	2.33	2.40	2.37	2.39

¹Storm surge + MHWS.

²Storm surge+5% + MHWS.

Predicted storm tide levels from the various studies (current estimates, T+T 2016, and Beya & Asmat 2021) are all close to one another, with a maximum variation of 7 cm. The minimal variation between the three independent analyses gives confidence that the true storm tide levels lie within the range of values provided in Table 3.2: . With this, and in the context of inundation modelling for Building Code compliance, rationalised values have been adopted based on all the values in Table 3.2: (and that are appropriate for the model resolution). For this reason, proposed values of 2.35 m and 2.40 m CD are recommended for 2% and 1% AEP event respectively. With the repeatability between the independent analyses, these values are likely within 5 cm of the true 2% and 1% AEP storm tide levels. Converted to NZVD-2016, the adopted values for extreme water level in 2020 are 1.23 and 1.28 mRL for the 2% and 1% AEP event (Table 3.3).

Table 3.3: Present day (2020) storm tide levels adopted for this assessment

AEP	ARI	Storm tide (m NZVD)	Storm tide (m CD)
2%	50yr	1.23	2.35
1%	100yr	1.28	2.40

3.3 Sea level rise

Information on sea level rise for this assessment was sourced using the NZ Sea Rise portal⁷ for the Port of Napier. The SLR data used is consistent with the IPCC AR6 pathway SSP5 8.5M at 2100 (Rice Spier, 2021). Relative SLR includes the VLM contribution which produces different relative sea level rise for different section of the coast. Table 3.4 presents values for relative sea level rise for the SSP5 8.5M scenario at 2100 based on average rates of VLM along main section of the site. The resulting relative sea level rise varies along the site, from 0.8 m at Haumoana to 1.1 m at Whirinaki, indicating a significant spatial variation along the site.

Table 3.4: Magnitudes of relative sea level rise (m relative to MSL in 2020) at representative locations

SSP5 8.5M	Clifton to Tukituki	Clive	Napier South	Napier to Bay View	Whirinaki	Tangoio
VLM rate (mm/yr) ¹	-0.68	-2.04	-3.24	-3.62	-4.15	-3.39
2100	0.82	0.93	1.03	1.06	1.10	1.04

¹Based on the average VLM value along the section of coast.

⁷ <https://www.searise.nz/maps-2>.

Relative sea level rise is accounted for in this study by adjusting the model bathymetry according to the spatial trend in vertical land movement presented in Figure 2.5. The inclusion of VLM in the model bathymetry is further discussed in Section 5.3.

With VLM accounted for in the model bathymetry, the effect of absolute sea level rise (rise in ocean water level with no account for land movement) has been included by determining the absolute rise in sea level between 2100 and 2020. Under SSP5 8.5M, this absolute rise in sea level equates to 0.77 m. This increase in sea level has been added to the storm tide levels used for simulating present day coastal inundation.

4 Wave climate

4.1 Wave climate overview

This section presents an analysis of the Hawke Bay wave climate and details the wave boundary conditions for use in the Tangoio to Clifton coastal inundation simulations. A review of existing wave climate information is presented in Appendix B, including a new analysis of wave data from the Napier Port buoy and a regional hindcast model. The final section presents information on the extreme return period wave heights and periods for use at the offshore boundary of the inundation model.

The Hawke Bay wave climate is broadly influenced by its location on the North Island east coast, situated south of the East Cape and Mahia Peninsula (Figure 4.1). The region is generally sheltered from north-easterly waves, but is directly exposed to easterly waves, and south-easterly waves that refract around Cape Kidnappers. Therefore, the local wave climate within the Clifton to Tangoio section is variable and depends on the nearshore wave transformations from refraction, bottom friction, and shoaling. The dominant wave direction for the broader region is from the south to southeast, but the presence of refraction means there is substantial anti-clockwise rotation of the waves as they propagate into towards the coast. Shadowing from Cape Kidnappers and Bluff Hill (Figure 4.1) produce varying wave intensities throughout the region due to their sheltering effect on the areas northward of these promontories.



Figure 4.1 Hawke Bay Coastline.

4.2 Extreme events for inundation modelling

The XBeach-GPU modelling was done using five model domains that extend to at least to the -15 m contour (Figure 4.2). Extreme wave conditions were informed using an updated wave hindcast for the region, providing wave information offshore each model domain from 1980 – 2020 (Appendix B). The hindcast output points that are located closest to the seaward model boundary at the centre point of each domain were used to identify the extreme wave climate for simulating inundation. The

wave output point and model domains are presented in Figure 4.2, indicating the hindcast location is within a few hundred meters inside the model domain at typical depth of -17 m.

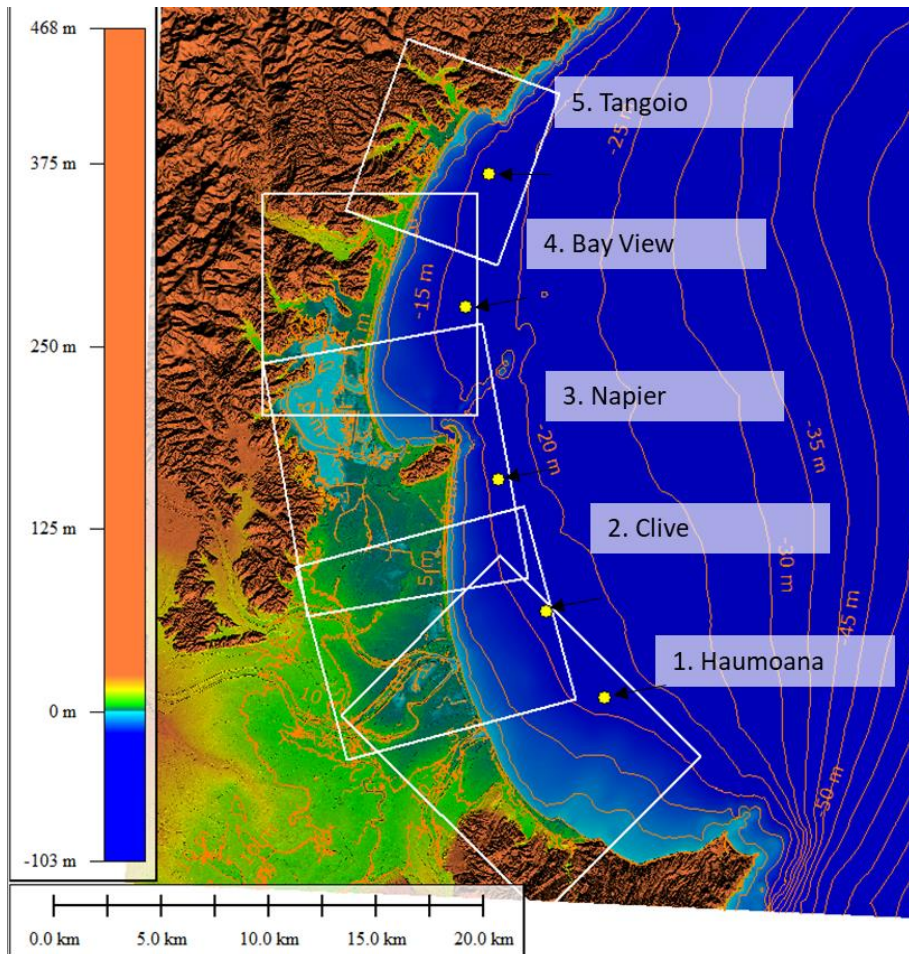


Figure 4.2: Model domains and wave hindcast locations overlain on bathymetry and topography.

The wave climate indicates that maximum wave heights are associated with mid-period storm events, with periods between 8 – 12 s, with longer period swell waves being associated with slightly lower heights (Figure 4.3). There is limited record of these mid-period events causing notable coastal inundation at present day sea level. However, the most well documented coastal inundation event was associated with swell waves at a period of 15 s generated by ex-tropical cyclone Pam in March 2015. Inundation from waves during the Pam event was documented at Clifton, Haumoana, along Marine Parade and at Westshore. Based on this, it is possible that coastal inundation is more likely to occur during a long period swell event, even if the wave height is lower than the wave height associated with a mid-period storm event.

Estimating the wave and water level conditions that contribute to an extreme inundation event proves challenging, particularly when the documented inundation is skewed towards longer wave period events as opposed to larger wave height events. The probability of a storm event that combines extreme wave heights, extreme water levels, and also large wave periods is rare and is far less likely than the AEP level that each of the individual constituents have been determined. With this, using extreme water levels and wave heights of the same AEP with a large wave period (e.g. the 15 s period experienced during the Pam event) will lead to a significant over prediction in the inundation that would realistically occur for the given AEP storm event.

Therefore, to ensure the appropriate wave boundary is being applied to the model, the 1% and 2% AEP wave height associated with a mid-period storm event, and a long period swell event were

calculated separately. The mid-period EVA was calculated using all wave data in the record, with the representative period being based on the relationship between wave height and period in Figure 4.3 indicating the maximum waves have a period below 12 s. The swell EVA was assessed by only including data points with a wave period above 14 s, before calculating the peak events and annual exceedance probability. By separating out wave data with periods above 14 s, a representative extreme swell event wave height is calculated for the desired 2% and 1% AEP event. The extreme wave heights associated with a mid-period storm and long period swell are presented in Table 4.1. The extreme swell wave height for the 1% and 2% AEP events were combined with the respective extreme water levels without considering the joint probability.

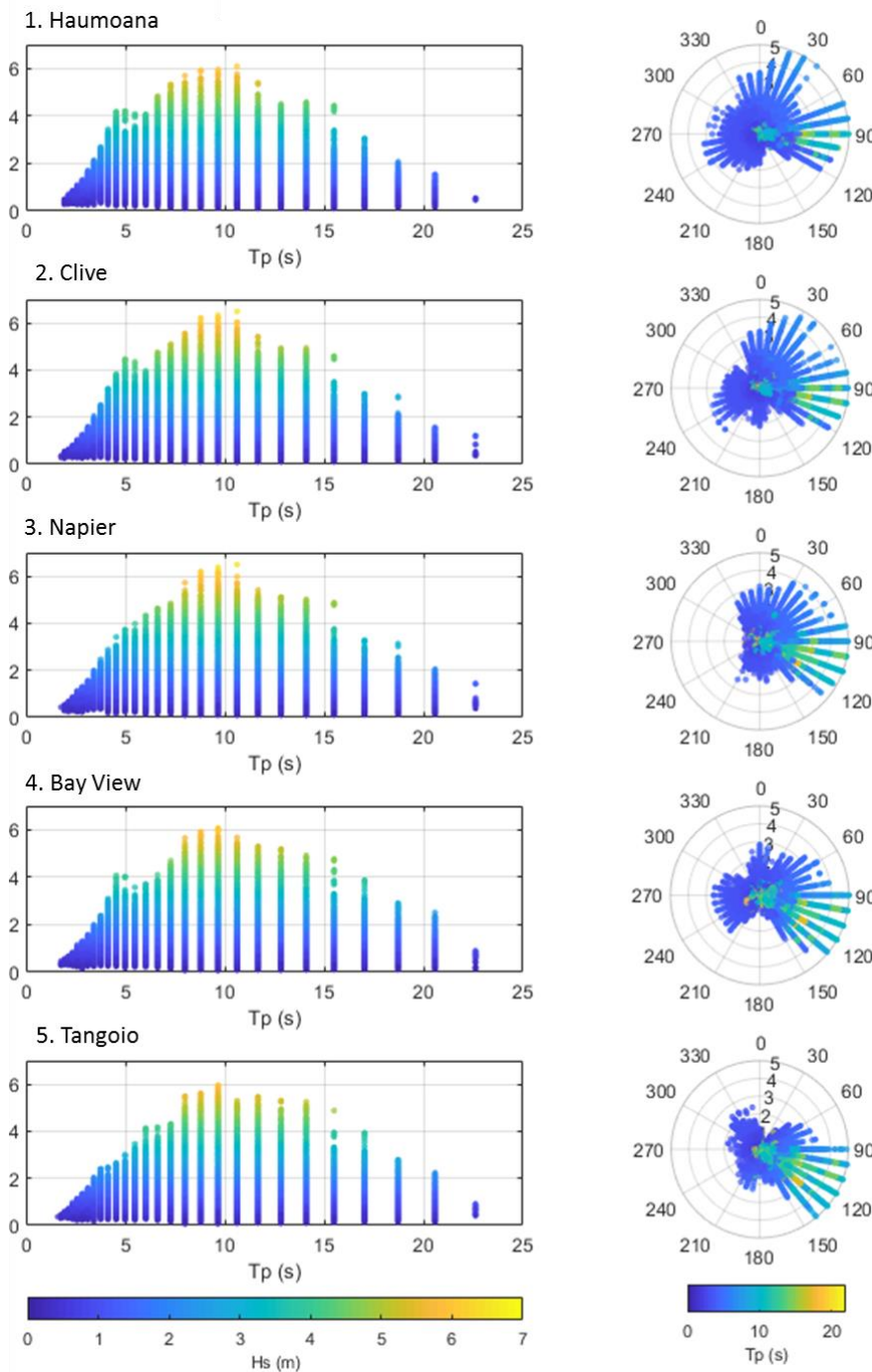


Figure 4.3: Relationship between wave height, wave period and wave direction at the each model boundary.

For the XBeach inundation modelling, sensitivity analysis during the model development phase indicated that inundation is more critical for a 2% AEP swell event compared to a 2% AEP event associated with a mid-period storm event (Section 5.6). Therefore, the 2% AEP swell condition is being used to simulate inundation with a representative wave period of 15 seconds is proposed for use in all inundation assessment simulations. Wave direction will be input normal to the model boundary which is aligned with -15 m offshore contour. This is appropriate based on the range of directions that extreme waves can approach from, based on Figure 4.3.

Table 4.1: Extreme significant wave heights (H_s) for storm and swell events

Domain	Mid-period storm event ($T_{rep} = 12s$)		Long period swell event ($T_{rep} = 15s$)	
	2% AEP	1% AEP	2% AEP	1% AEP
1. Haumoana	6.10	6.30	4.54	4.86
2. Clive	6.53	6.79	4.85	5.19
3. Napier	6.58	6.86	4.96	5.35
4. Bay View	6.24	6.44	4.97	5.36
5. Tangoio	6.07	6.24	5.16	5.64

T_{rep} is the representative wave period.

5 Inundation model development

5.1 Model description

Coastal inundation was simulated using XBeach-GPU (XBGPU), a tightly coupled wave-flow hydrodynamic model that is optimised for running on a graphics processing unit (GPU). Executing the model on a GPU provides a substantial speed up in computational time, allowing regional scale models to be resolved at high resolution for the timescale of multiple tide cycles. The GPU version of XBeach is a 'lightweight' implementation of the full XBeach model (Roelvink et al., 2009), and focuses on the fundamental wave, flow, sediment transport and morphodynamic components. A full description of the XBGPU model has been published (Bosserele, 2014; Bosserele, 2022) and the model has been comprehensively tested for accuracy and efficiency against the original XBeach model (Rautenbach et al., 2022). XBGPU has been used in a research capacity to study coastal inundation, and for applied projects to assess coastal inundation hazards at a regional level (Rautenbach et al., 2021; 2022).

XBGPU is a wave forced hydrodynamic model that resolves short waves using a spectral wave transformation model and long waves using the wave phase-averaged nonlinear shallow water equations. The free surface flow from surf-beat (infragravity waves with periods of 20 – 300 s) is therefore resolved dynamically in the nearshore, surf-zone and swash zone. The focus on surf-beat is appropriate for a coastal inundation model since the inner surf zone and swash zone show that a spectral shift occurs, where energy in the wind and swell frequency has dissipated by the shoreline, but energy in the infragravity frequency peaks at the inner surf zone and swash zone.

The resulting inundation simulated in the model accounts for:

- Refraction, shoaling and dissipation of short waves.
- Wave generated setup of the mean water level (including temporal and spatial dynamics of setup).
- Generation and propagation of surf-beat flow in the nearshore and surf zone.
- Overtopping and resulting overland flow at the wave group frequency.
- Time varying tidal level at the seaward boundary that can represent a measured or idealised storm tide signal.
- Feedbacks between waves, water level and flow.

5.2 Model limitations

The modelling approach has limitations, simplifications, and assumptions that are appropriate for the specific scope and brief of this project. These include:

- The model does not resolve water level dynamics from individual waves, as that requires a phase-resolving approach that is significantly more computationally expensive. The phase resolving approach is considered unfeasible at the regional scale and unnecessary for understanding the primary mechanics that cause a coastal inundation hazard.
- All ground in the model was considered impermeable, which means percolation into gravel, sand, and soil or ground water is not resolved.
- The inundation model is based on the underlying terrain, with objects such as trees, fences, and buildings removed, while recognising these features may locally alter inundation flow through impoundment or other processes.
- Drainage networks, including flood gates and pumps were not resolved in the model, unless they are part of the bathymetry.

- The model was implemented using a fixed bathymetry (no sediment transport or morphodynamic change).
- The model terrain is based on the LiDAR survey in 2020 but reduced to 5 m horizontal resolution which captures the general terrain but not highly complex features.
- The 2100 terrain model accounts for projections in vertical land movement but does not account for potential changes to the coast associated with erosion and barrier roll-over due to sea level rise. Further, the VLM data is based on the short-term past trend and is extrapolated 80 years into the future, which has an associated uncertainty.
- Coastal protection features around Napier Port are not resolved at a high enough resolution to assess coastal inundation at this location. The port is protected by a detached breakwater and channel that is not fully resolved in the model. Therefore, the port area is not included in this assessment.
- Coastal structures such as groynes and revetments were included as part of the bathymetry, but as impermeable slopes, not porous structures. Therefore, some dissipative features of the rock revetments may be underpredicted.
- River flow from a landward boundary was not represented in the simulations for this assessment.
- Model behaviour is calibrated using the best available data on observed wave inundation (ex TC Pam event) but has not been tested against multiple observed events.

5.3 Model bathymetry

The area was split into five model domains for running in XBGPU, with significant overlap between neighbouring model domains to check the behaviour and consistency (Figure 5.1). For each subdomain the model bathymetry extends just seaward of the -15 m contour, and landward to at least the 5 mRL contour. Most domains are in the order of 10 km wide from the seaward to landward boundary and the alongshore distance ranges from 8 – 15 km. The seaward edge of the model was aligned to the -15 m contour to allow wave generation at an alongshore consistent depth. The extent of each subdomain was based on the orientation of the -15 m contour and key bathymetry or shoreline features like river channels and headlands. The model grid resolution is a uniform 5x5 m DEM, resulting in 2.5 to 5.5 million grid nodes per domain.

An existing topography-bathymetry elevation model was provided for this work which was developed by GNS to undertake a tsunami hazard assessment. The GNS bathymetry was used as the primary terrain layer for establishing the model bathymetry and was adjusted to NZVD 2016 vertical for this purpose (Appendix A). Land areas were compared to the 1 m resolution LiDAR terrain model, which indicated some stop bank features were not properly resolved in the 5 m resolution model bathymetry. Stop banks levels were reviewed using the higher resolution 1 m LiDAR and updated in the 5x5 m model bathymetry accordingly to resolve the crest height and width of river stop banks and sea exclusion banks (Figure 5.2). Additional checks were made to compare the coastal barrier morphology in the 5 m resolution model bathymetry with beach profile surveys and 1 m resolution LiDAR.

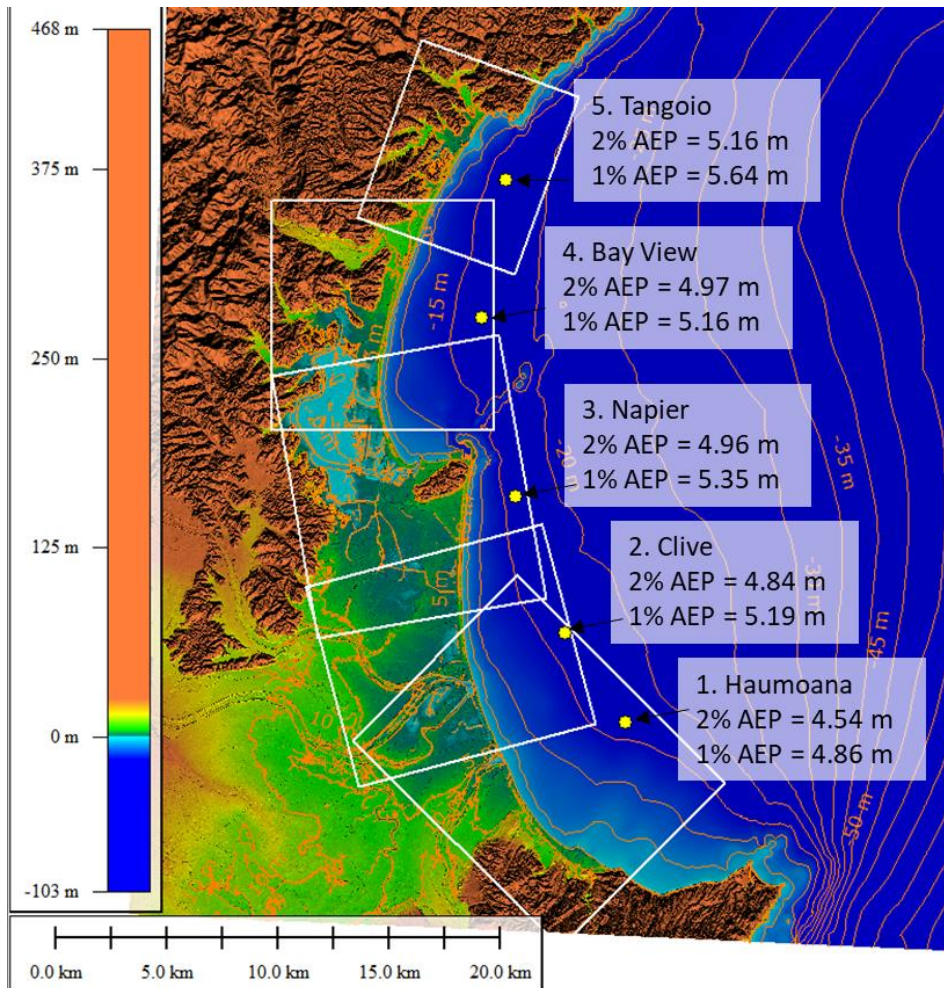


Figure 5.1: The five sub-domains including 1% and 2% AEP significant swell wave height at the model boundaries.

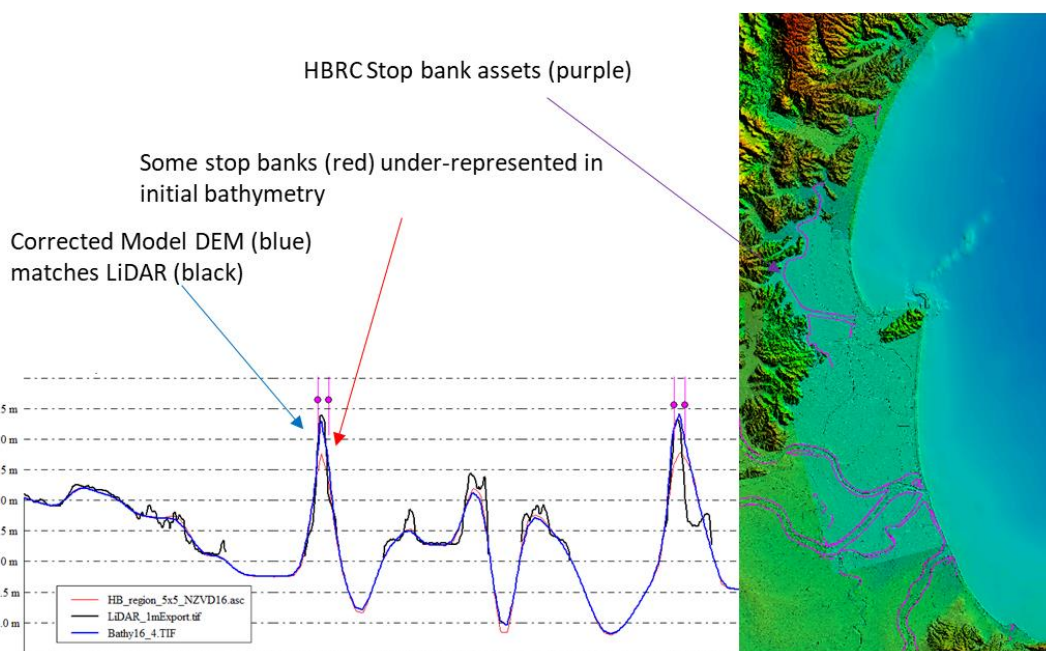


Figure 5.2: Location of stop banks based on the HBRC asset layer and correction of stop bank level in model bathymetry shown in an across channel profile section.

5.4 Model parameters

Model parameters were established based on existing published reports and papers (Rautenbach et al., 2022; NIWA, 2021) and a site-specific sensitivity analysis that was undertaken during the model calibration stage. Key parameters that were adopted in this assessment are summarised in Table 5.1.

Table 5.1: Key XBGPU parameters and values

Variable and values adopted	Notes
<p>Flow bottom friction (C_f) Spatially variable based on ground cover:</p> <ul style="list-style-type: none"> • Reef: 0.01 – 0.025 (local calibration dependent). • Coastal sediment: 0.01. • Wetland: 0.04. • Agriculture: 0.01. • Urban: 0.01. • Forest: 0.1. 	<p>Values based on land cover polygons from Land Care Research 2016 land use map. Marine areas default to coastal sediment, apart from specific reefs that are charted. Additional friction was only added to reefs in areas where initial model tests resulted in localised over-prediction of inundation during calibration.</p> <p>This approach and values are consistent with similar assessment on a similar coastal environment in Timaru (NIWA, 2021), and with the values used in Rautenbach et al., (2022).</p>
<p>Wave friction (W_f) Default of 0.001 for all areas except some reef areas:</p> <ul style="list-style-type: none"> • Te Awanga (Clive Hard) = 0.4 (calibrated). • Napier Reef and port revetment (0.35). 	<p>Additional friction was only added to reefs in areas where initial model tests resulted in localised over-prediction of inundation during calibration.</p> <p>Consistent with values used in Rautenbach et al., (2022).</p>
<p>Short wave direction 10 degree spacing between -90 to 90 degrees relative to the model boundary.</p>	<p>Wave direction was computed in bins at a resolution of 10 degrees, allowing refraction up to ± 90 degrees direction of the model boundary. This was appropriate for modelling refraction on reefs and sections of curved coastline around the port and Ahuriri.</p>
<p>Wave breaking (γ) Range tested: 0.5 – 0.9. Adopted: 0.75.</p>	<p>Sensitivity analysis shows best match to observed runup during TC Pam event. Lower values under predict, higher values are not physically sensible.</p> <p>Consistent with similar assessment on gravel coasts in Timaru (NIWA, 2021)</p>
Roller slope (β) = 0.1.	Default, discussed with HBRC and NIWA.
Roelvink slope (wave breaking) = 8.	Default, discussed with HBRC and NIWA.
Smagorinsky = Yes; coefficient = 0.3.	Default, discussed with HBRC and NIWA.
Minimum depth = 0.03 m.	Minimum depth considered at the moving shoreline.

5.5 Model calibration

A detailed model calibration process was undertaken to assess parameters and confirm the suitability of XBGPU for assessing coastal inundation for the Hawke's Bay region. Detailed reporting on the calibration event (ex-Tropical Cyclone Pam) and results is presented in Appendix C.

The overall model behaviour indicates that the wave generated coastal inundation from a high energy, long period swell event can be simulated with reasonable accuracy when compared to observed inundation between Bay View and Clifton. To summarise the comparison between model outputs and field measurements, the observed inundation level was compared to the modelled

inundation level at 13 locations along the site (Figure 5.3). This comparison shows a close fit between observed and modelled, with no bias and a mean absolute error of 0.20 m.

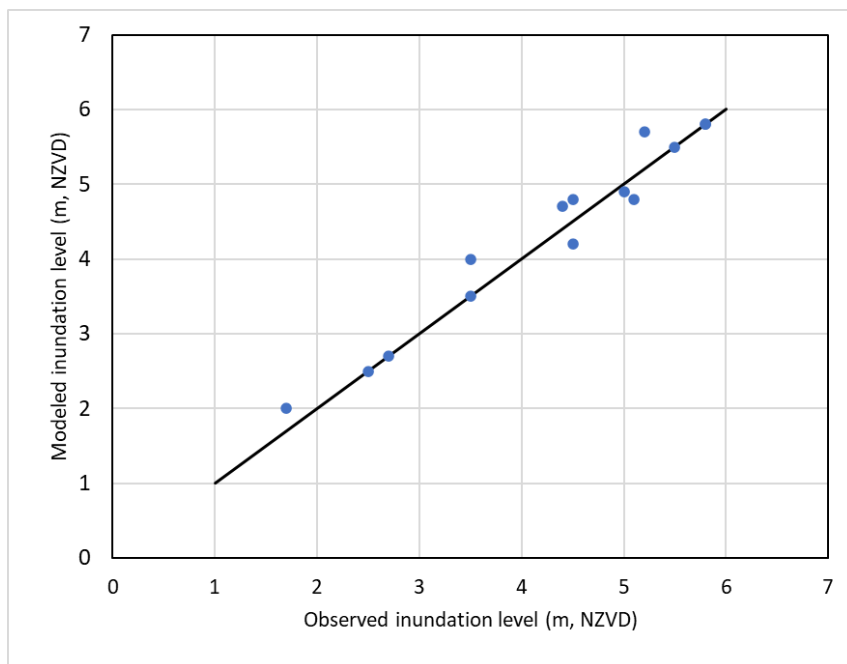


Figure 5.3: Comparison between observed inundation and modelled inundation level for the TC Pam event.

5.6 Sensitivity to a 50-year storm or swell event

The documented events that cause coastal inundation hazards along the Hawkes Bay are generally associated with long period swell events (14 – 16 s wave period). These swell waves have more power compared to storm waves that are generally associated with a mid-period (8-12 s wave period). The wave hindcast data show that the largest waves occur at the 8 – 12 second period (50 year ARI: $H_s = 6.0$ to 6.6 m), compared to slightly smaller waves at the swell period of 15 s (50 year ARI: $H_s = 4.5$ to 5.16 m).

To check that the appropriate 50 year and 100-year events were simulated in XBGPU, both scenarios were simulated using the 2100 terrain (adjusted for vertical land movement), and sea level rise. Results indicate that that the 50 year ARI swell event is the critical case for coastal inundation even though the wave height is lower than the 50 year ARI storm event with a mid-period (Figure 5.4). Therefore, the inundation scenarios produced for this assessment consider the 50-year swell event. This is also consistent with observed events (e.g. TC Pam) and the model calibration process.

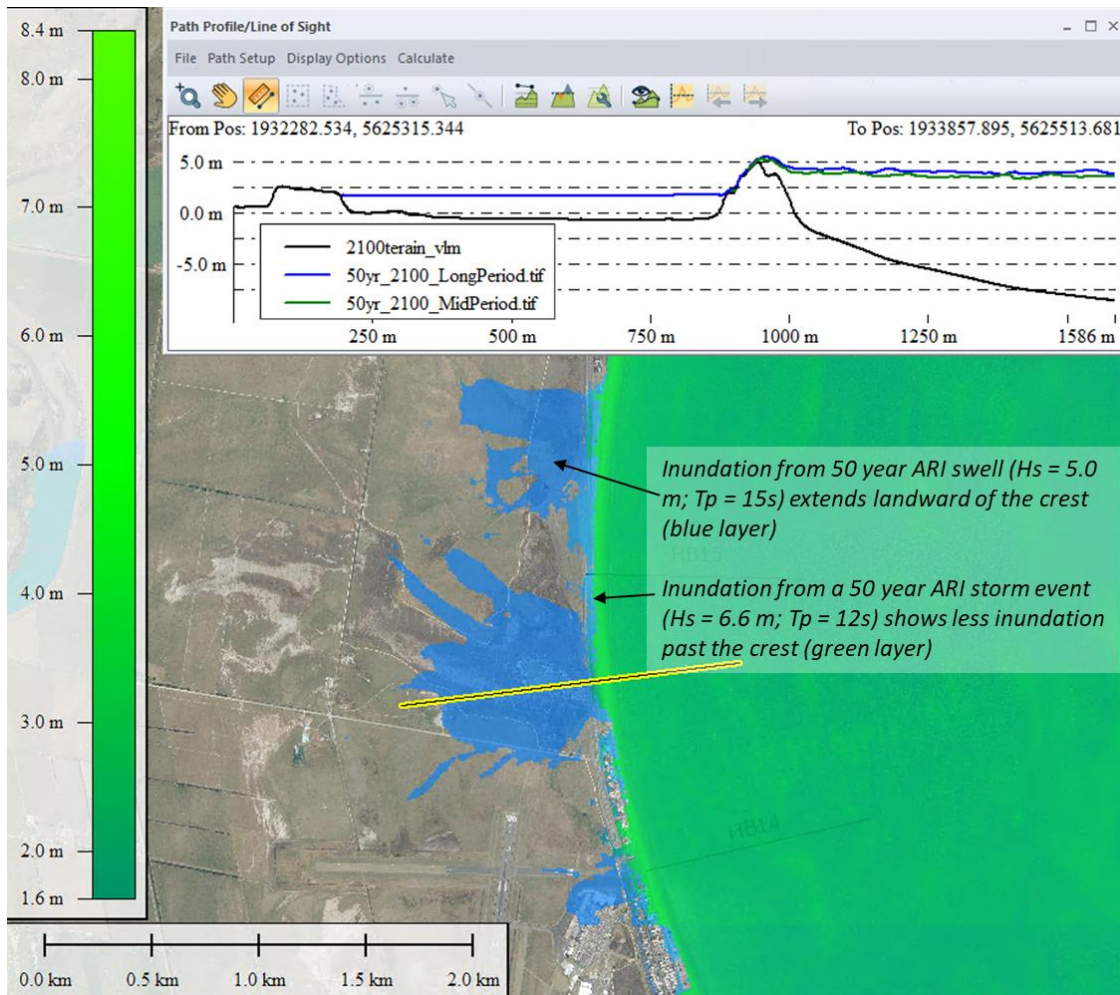


Figure 5.4: Comparison of inundation from a 50-year ARI swell event and 50 year ARI storm event.

5.7 Terrain changes since Cyclone Gabrielle

The coastal inundation model was based on the terrain surveyed by LiDAR in 2021, which is consistent across the extent, and combined with bathymetry surveys and river mouth profiles to seamlessly transition from subaerial terrain to underwater terrain (as detailed in Section 5.3). After the modelling was completed, ex-Tropical Cyclone Gabrielle impacted New Zealand on 12 - 16 February 2023 and caused significant changes to ground level in the lower catchments of the Esk Valley and the Heretaunga Plains, which are within the coastal inundation model extent.

Terrain mapping in response to catchment flooding and slips from Cyclone Gabrielle was undertaken by NIWA and the University of Canterbury over 3-5 March 2023. To understand the impact of terrain changes on the inundation model results, a review was undertaken to check the change in beach profile, berm level and areas of silt deposition in different locations in the inundation model, using provisional survey results provided by HBRC and NCC. Findings are described in Appendix E, which shows the extent of elevation changes in the lower Esk Valley and in the lower Heretaunga Plains. Results identify some changes to the beach level and changes around the morphology of river mouth bars. Some areas of silt deposition in Awatoto and Te Awa coincide with locations where inundation is modelled, and if the silt is not removed the inundation level should be re-defined based on the modelled depth above ground. However, in general the elevation of the coastal edge which controls wave overtopping was consistent between the 2021 LiDAR used in the model, and with the post-Gabrielle terrain. Therefore it was not considered necessary to update the model bathymetry to represent the post-Gabrielle terrain.

6 Coastal inundation hazards

6.1 Model inputs

Coastal inundation hazard simulations were undertaken for three scenarios:

- 2% AEP (50-year ARI) event at present day (2020).
- 2% AEP (50-year ARI) event at 2100.
- 1% AEP (100-year ARI) event at 2100.

The 2100 scenarios include the effects of vertical land movement (offsetting the grid spatially) and absolute sea level rise using SSP5 8.5M (0.77 m).

The sea level boundary was input to simulate the rising tide with a plateau at the peak storm tide level. The water level used at the initial timestep has some influence on the model behaviour because all areas with an elevation below the initial water level will be wet in the model, even if they are not connected to the sea. This means any overtopping flow across the barrier crest can plunge into already wet areas of the backshore if a high initial water level is used. Sensitivity runs were undertaken to start the simulation at mean sea level and mean high water spring (relative to 2020 or 2100). Results indicate that initiating the model at MSL is likely a more realistic way to represent the initially wet areas that are not connected to the sea (based on discussion with HBRC and NIWA). Therefore, the inundation scenarios were initiated at MSL relative to 2020 for the present day and MSL relative to 2100 (0.77 m SLR based on SSP5 8.5M) for the 2100 scenarios. The sea level signal used in the model is shown in Figure 6.1 for the 50 year ARI event at 2100. Note the storm tide levels for 2100 are 2.0 m and 2.05 m for the 2% AEP and 1% AEP event, respectively. The 2% AEP storm tide level at present day is 1.23 m.

Following the peak storm tide level, the water level recedes to allow drainage to occur. The total simulation time is 7 hours following this storm tide signal.

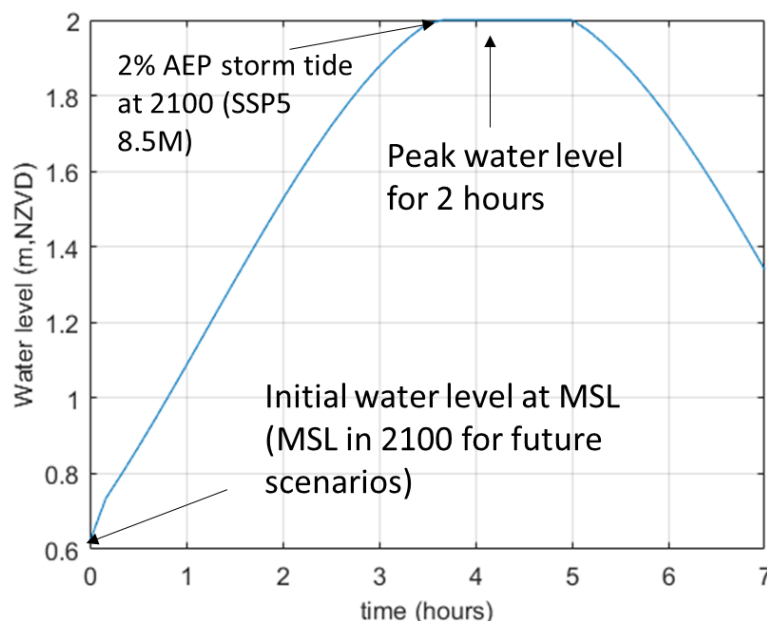


Figure 6.1: Water level timseries input at the seaward model boundary.

The wave condition was held constant for the 7-hour simulation using the 50 or 100 year ARI swell height associated with each model domain (Table 4.1), using a wave period of 15 seconds and

JONSWAP parameters $s=1000$ and $\gamma=5$ (Appendix C). These JONSWAP parameters were used as they are representative of long period swell conditions with a trapped fetch.

6.2 Model outputs

Model outputs were written to file every half hour during the simulation for maximum water level, mean water level, wave height, mean wave height and velocity (mean and maximum in x and y directions). The main output for this assessment is the maximum water level. To identify the coastal hazard extent, the maximum water level identified across all half hour outputs was identified. This approach captures the point in time during the simulation when maximum water level occurred due to wave exposure and water level.

Maximum water level during the 7 hour simulation was compared to water level at the initial timestep to identify the dynamic inundation area (directly influenced by wave surge). Areas of dynamic inundation were identified as having a maximum water level at least 0.03 m above the initial water level. A comparison is presented in Figure 6.2 showing the area of dynamic inundation compared to the initial water level (in this case MSL for 2100 based on SSP 5.8.5M).

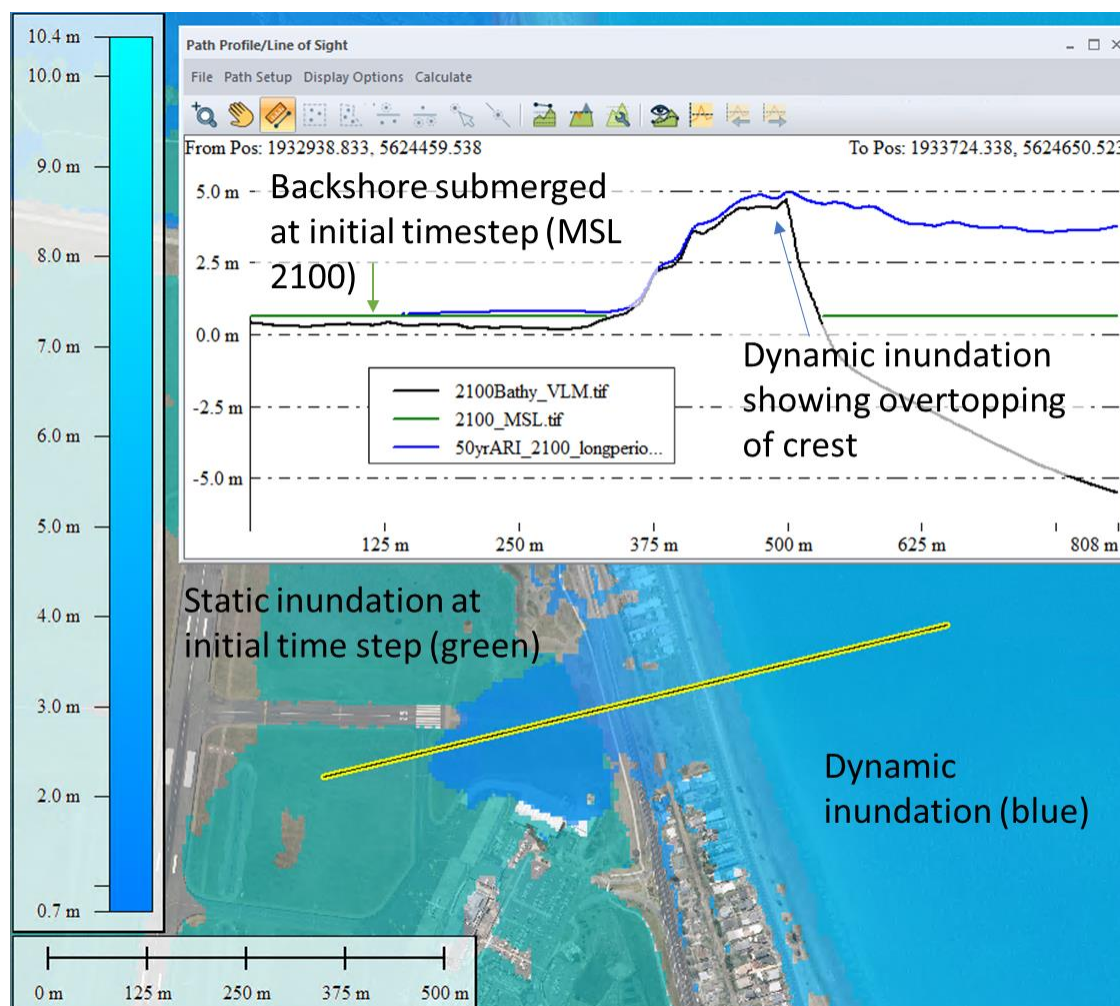


Figure 6.2: Example output showing how areas of dynamic inundation (from waves) are separated from areas of static inundation that may be disconnected from the sea.

Outputs from neighbouring and overlapping model domains were assessed to ensure overtopping flows at the crest or landward of the crest were not restricted by or influenced by the lateral model boundary. A generous overlap was used to ensure areas of inundation influence by a boundary in

one model were clipped out and that area was appropriately represented in another model domain with no potential boundary effects. Areas of overlap were also checked to ensure consistency between overlapping models and adjustments to the boundary position were made until all overlapping areas were resolved consistently. After clipping out areas with boundary influence, the remaining layers were combined to find the maximum level in areas of overlap. The Final output for each scenario is the maximum water level for dynamic inundation extending from Tangoio to Clifton, saved as a geotiff raster file at the model resolution of 5 m.

Inundation outputs are provided for the following scenarios:

- Dynamic inundation for 2100:
 - 2% AEP event (Building Code scenario).
 - 1% AEP event.
- Dynamic inundation for 2020:
 - 2% AEP event.
- Static inundation for 2100 (including areas disconnected from sea):
 - Mean sea level.
 - Mean high water spring.

6.3 Building Code scenario

The building code scenario modelled in this assessment is based on sea level rise of SSP5 RCP 8.5M at 2100 (0.77 m) with vertical land movement and a design event that combines a 2% AEP storm tide and a 2% AEP swell wave height. Outputs raster maps for inundation and depth are provided in digital format to HBRC, HDC and NCC. Example outputs for the maximum inundation level are summarised below for each township, highlighting areas where the coastal barrier is overtopped by waves. Key points to note in the outputs include:

- Coastal inundation exceeds the coastal barrier elevation at Clifton and maximum water level is generally 4 mRL at the coast, and tapers to 3.6 mRL at the landward extent which is up to 350 m from the coastal edge (Figure 6.3). The flood depth is generally less than 1 m relative to the ground level.
- Coastal inundation at Te Awanga extends up to 450 m landward of the coastal edge, at a maximum water level of approximately 3.6 mRL at the coast, tapering to 3.3 mRL at the landward extent (Figure 6.3). The landward limit is associated by an increase in terrain elevation. Waves pumping water over the barrier at Te Awanga results in an inundation area that overlaps with several properties. The flood depth is generally below 1 m relative to the ground level.
- Waves overtop the coastal barrier at Haumoana, resulting in inundation that extends up to 1,500 m from the shoreline, with flood depths generally below 1.5 m above the ground level (Figure 6.3). Maximum inundation level is approximately 4 mRL at the coast, which tapers to 3.5 m at the landward extent.
- Some overtopping of the sea exclusion bank is modelled for Clive, resulting in ponding of water on farmland and in the community at a maximum water level of 1 – 1.5 mRL (Figure 6.3). Flood depths landward of the sea exclusion bank were less than 1 m relative to ground level, and mostly shallower than 0.5 m. There is unresolved uncertainty regarding future coastal flooding at Clive. Most of the land is below the mean high water spring level predicted for 2100 (1.52 mRL). Therefore, the potential for flooding from groundwater intrusion and infiltration of the drainage network could compound the coastal hazard exposure in this location.

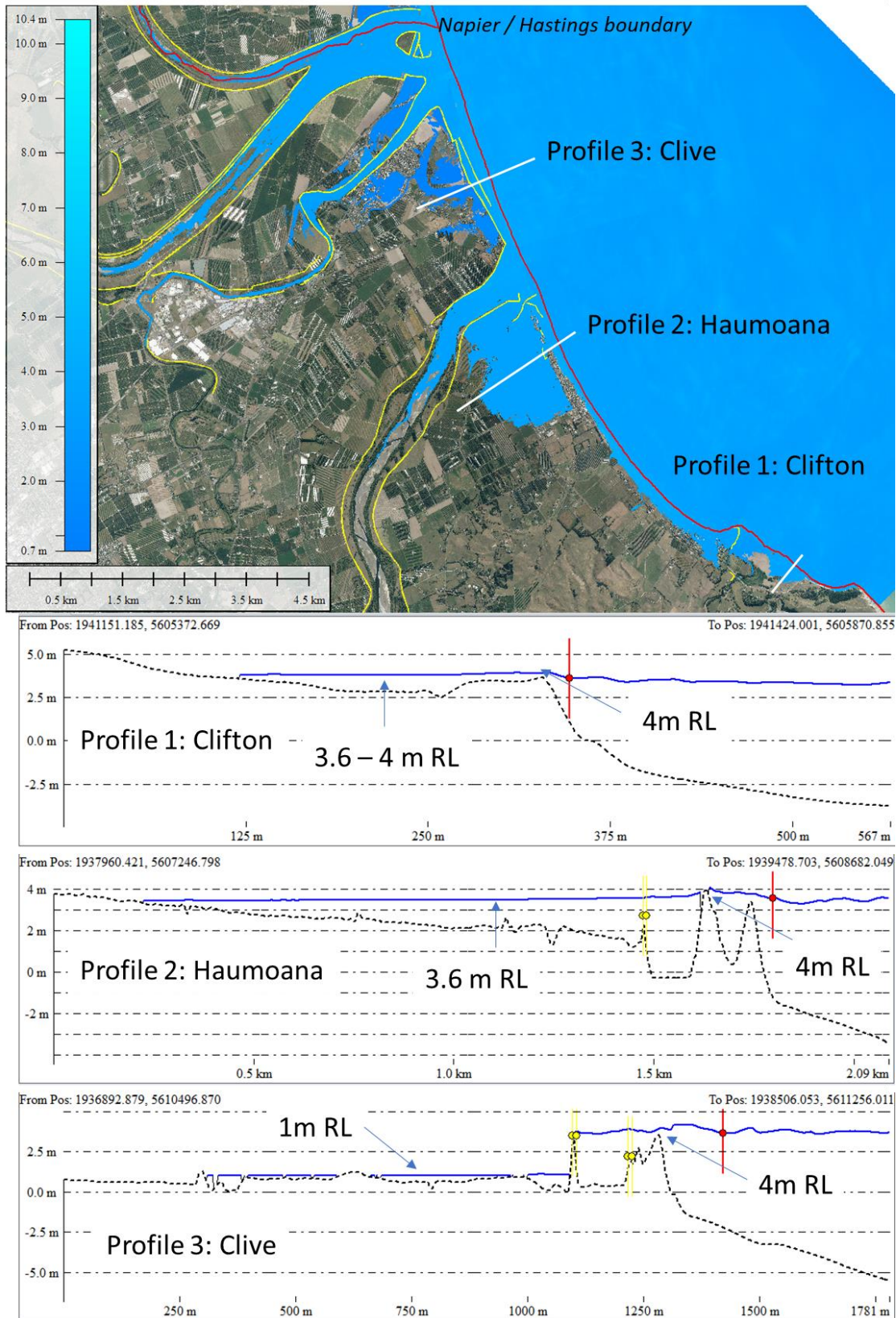


Figure 6.3: Inundation extent and level for Clifton to Clive for the design event with sea level rise to 2100 based on SSP5 8.5M and vertical land movement.

- Modelled inundation extents at the southern end of Napier show some waves surging over coastal barrier and to cause landward flooding between Awatoto and Te Awa (Figure 6.4). Coastal inundation levels associated with wave overtopping on the barrier reach a level up to 5.5 mRL (flow depth of 0.5 -1.5 m above barrier crest).
- The extent of flooding landward of the crest at Awatoto to Te Awa is associated with the low terrain level, and overland flow paths for wave overtopping flow to settle (Figure 6.4). The extent reaches up to 1,300 m inland of the shoreline, at a general maximum water level of 1.4 - 1.6 mRL. This results in an inundation depth less than 1 m relative to the ground level. Fine scale terrain and drainage features that are beyond the model resolution may mitigate some of the flood extents simulated in this model.
- Overtopping of the coastal barrier does not occur in the model for the section of coast north of the SH51 and Marine Parade intersection (Figure 6.4). The coastal barrier along Marine Parade is sufficient to accommodate runup levels and extents modelled for the 2100 design event. The modelled inundation extends onto and over the road at Marine Parade in some locations, but the inundation extent does not include the township or business area of Napier and Napier South. Inundation levels reach up to 6.5 mRL on the coastal barrier, with flood depths up to 1 m.
- Some overtopping is modelled along the shoreline at Ahuriri, with water level up to 4.3 mRL and shallow flow depth over the crest (<0.5 m). Some shallow ponding of the overland flow was modelled around properties between the reserve and rail line with depth below 0.5 m relative to ground (Figure 6.4).
- Coastal inundation flows were generally contained within the Ahuriri stop banks. However, some flow was modelled to extend to the southwest and inundate Lagoon Farm (Figure 6.4). The accuracy of modelled inundation in this area will depend on channel features and flood control systems that may not be fully resolved in the model bathymetry. Inundation at Lagoon Farm in the model is influenced by a narrow channel that slowly adds to the initial water level. The area is initially underwater at MSL in 2100, and additional water level due to dynamic inundation is less than 0.1 m.

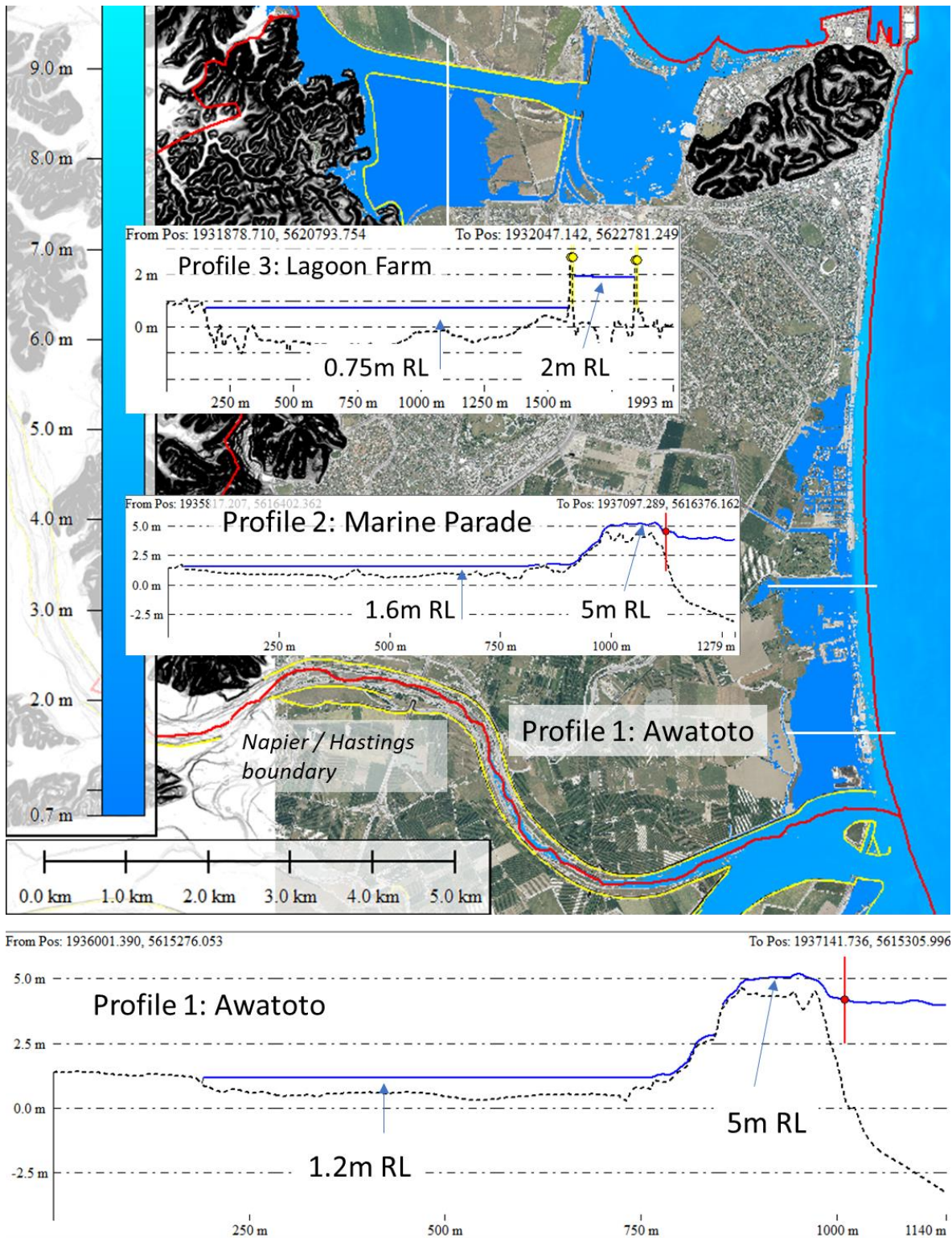


Figure 6.4: Inundation extent and level for southern Napier for the design event with sea level rise to 2100 based on SSP5 8.5M and vertical land movement.

- The industrial area at Pandora is located inside Ahuriri estuary and is characterised by low elevation terrain and drainage canals that are connected to the sea (Figure 6.5). Coastal inundation outputs show much of this area is exposed to inundation during the design event in 2100, with inundation levels of 2 – 2.2 mRL. Flood depths relative to ground vary along the site, between 0.5 - 1.5 m (depth is typically below 1 m).

- Wave overtopping is modelled to occur along Westshore, with inundation up to a level of 4.6 mRL. Inundation flows are modelled to surge over the Westshore barrier and flow into Ahuriri estuary in some location, but the coastal inundation surge is generally dissipated over the barrier crest. Inundation depth along Westshore is variable, but where properties are located is generally below 1 m.
- Wave overtopping of the coastal barrier is modelled for the Airport Gap at Westshore and further north in the undeveloped section between Westshore and Bay View, suggesting barrier crest levels below 5 mRL are susceptible to overtopping.
- Maximum water levels along Bay View are generally accommodated by the beach and barrier, with no significant overtopping of the road or properties. Some front yard sections may be washed by waves in this area.

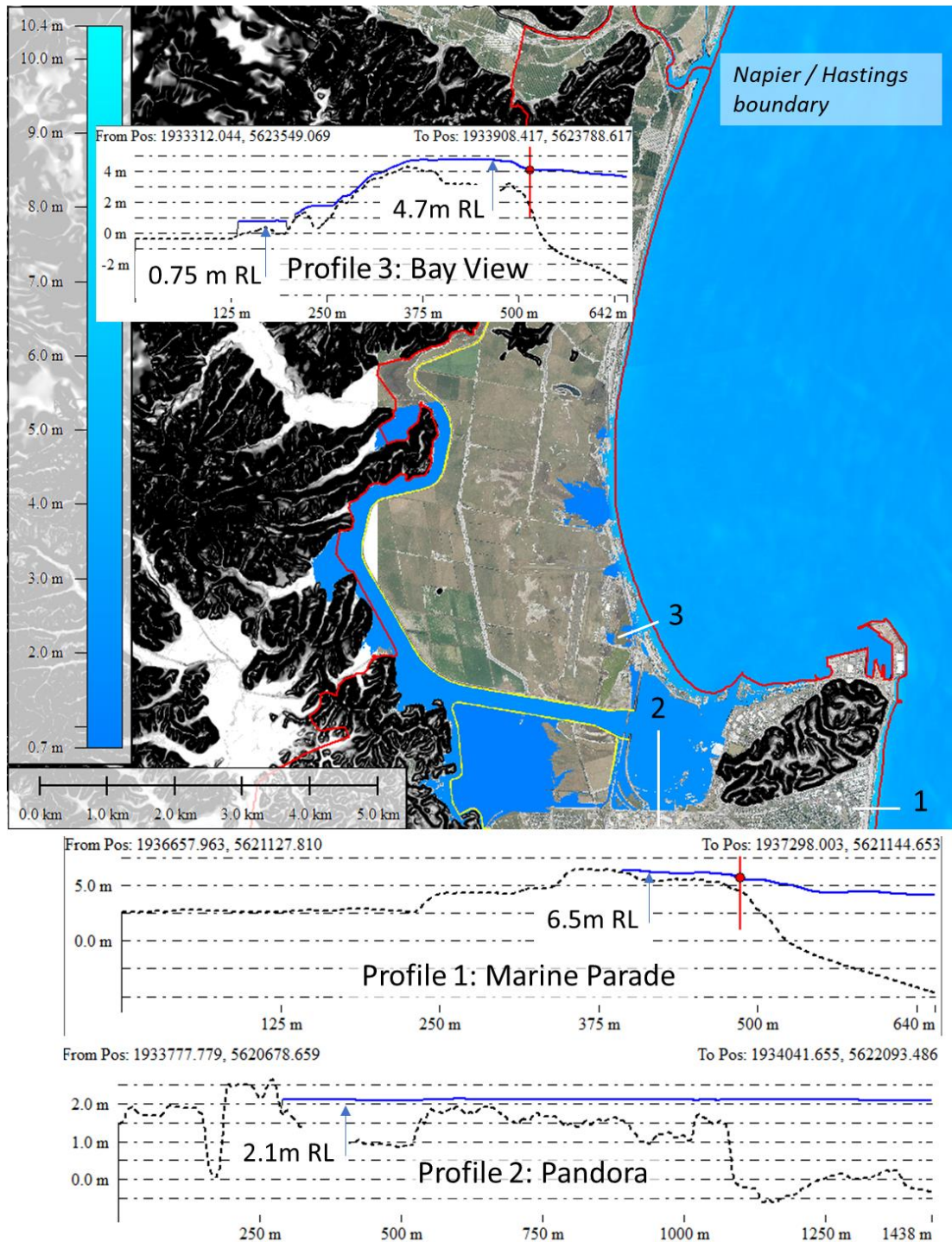


Figure 6.5: Inundation extent and level for northern Napier for the design event with sea level rise to 2100 based on SSP5 8.5M and vertical land movement.

- The coastal barrier north of the Esk River is elevated above 7 mRL and effectively prevents wave overtopping reaching properties and roads along most of Whirinaki and Tangoio (Figure 6.6).

- An area of coastal inundation does occur in the Pakuratahi Stream valley, where the coastal surge pushes into the river mouth and inundates a section of farmland between river channels (Figure 6.6).

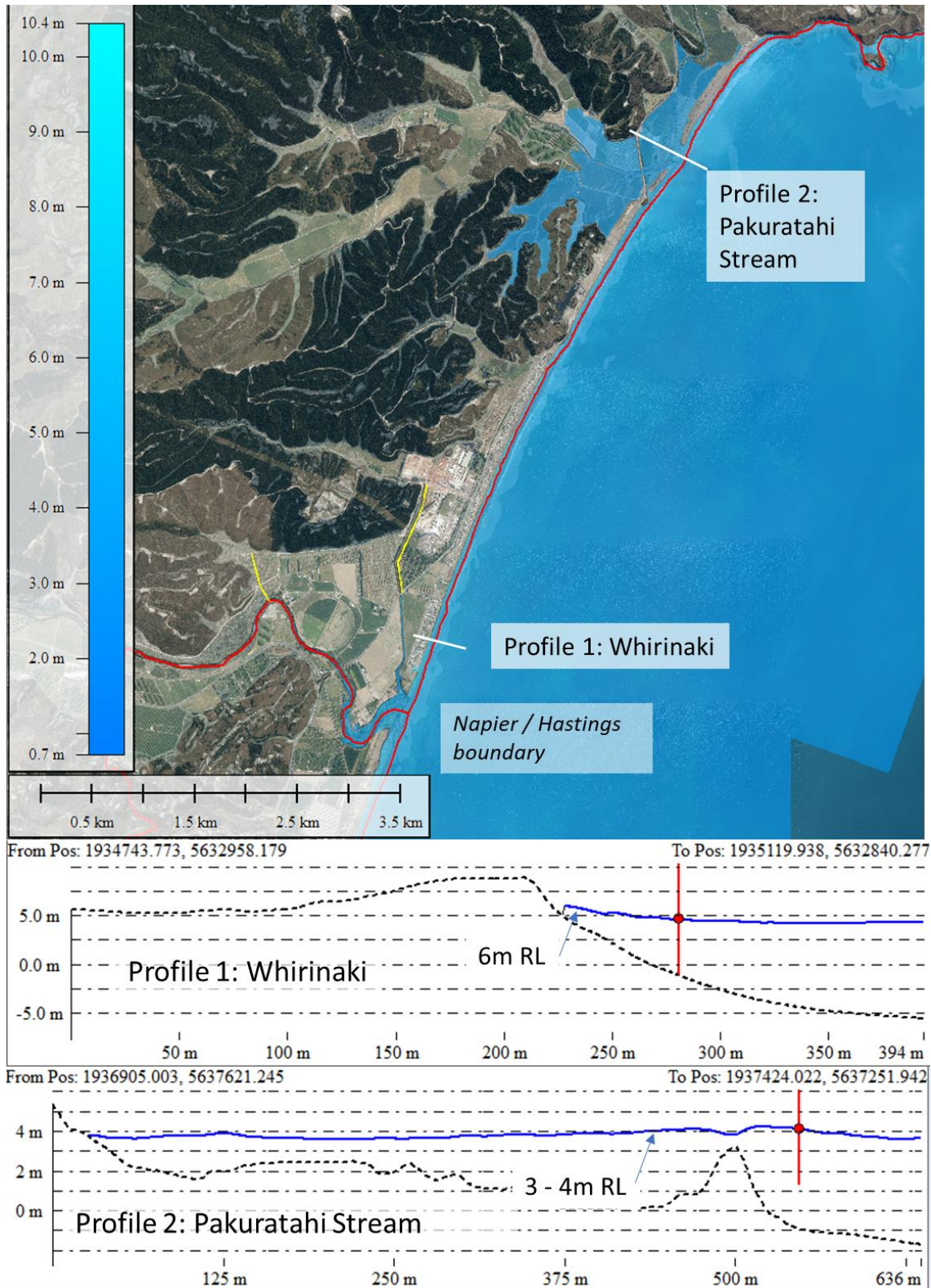


Figure 6.6: Inundation extent and level for Whirinaki to Tangoio for the design event with sea level rise to 2100 based on SSP5 8.5M and vertical land movement.

6.4 Areas potentially exposed to static inundation

This assessment focused on understanding coastal inundation hazards including the dynamic effects of waves. Results highlight the low-lying terrain between Clifton and Tangoio that exists landward of the coastal gravel barrier. To assist with management of the low-lying land, areas potentially exposed to flooding at mean sea level and mean high water spring in 2100 (based on SSP5 8.5M) were also mapped (Figure 6.7). The area where pre 1930s Ahuriri estuary formed a lagoon, is identified as being below the mean sea level (MSL) and mean high water spring (MHWS) level in 2100 (Figure 6.7). Some developed land withing Napier and Clive is also identified as being below the future MSL and MHWS level. These outputs include areas that may be disconnected to the coast, and therefore would require tidal flow to percolate through the ground or drainage networks to cause inundation. Development on land potentially exposed to tidal inundation up to 2100 should be considered when setting floor levels in areas outside the dynamic inundation zone.

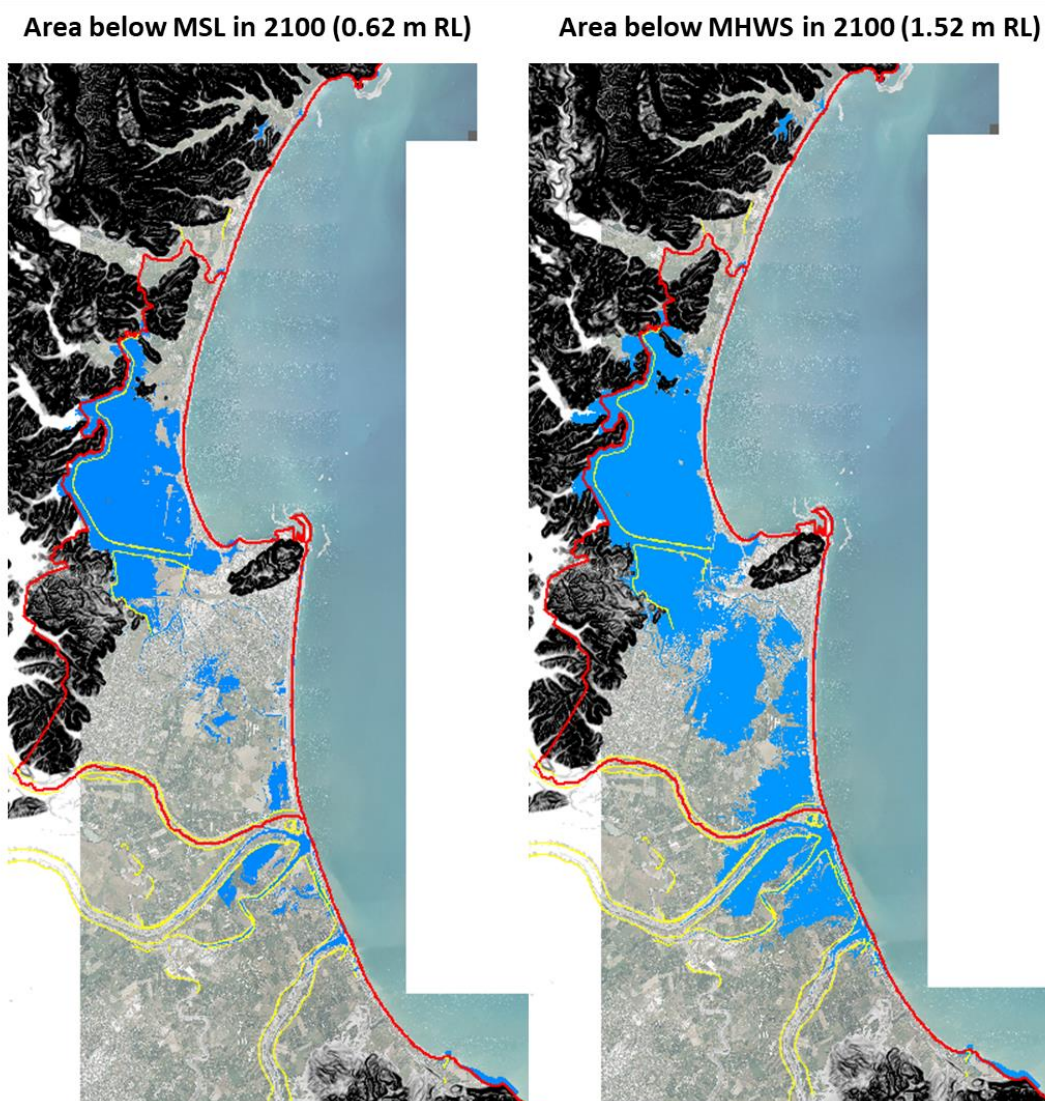


Figure 6.7: Extent of area below MSL and MHWS predicted for 2100 based on vertical land movement and sea level rise from SSP5 8.5M.

7 Summary

Three Hawkes Bay Councils (Hastings District, Napier City and Hawke's Bay Region) commissioned T+T to assess coastal inundation hazards between Tangoio and Clifton for the purpose of assess Building Consent applications.

The wave forced numerical model XBeach-GPU was used to simulate coastal inundation for the following scenarios:

- The 2% AEP event (50 year ARI) at present day sea level (used for sense checking).
- The 2% AEP event (50 year ARI) for 2100 using RCP 8.5M sea level rise (Building Code scenario).
- The 1% AEP event (100 year ARI) for 2100 using RCP 8.5M sea level rise (comparable to existing).

The model was comprehensively tested and calibrated using field observations of coastal inundation and overtopping from ex-Tropical Cyclone Pam in March 2015. The comparison between measured and modelled inundation level along the coast indicates a mean absolute error of 0.2 m. Inundation scenarios were simulated using a 5x5 m resolution model grid, with outputs showing the maximum inundation level during the simulation.

Scenarios associated with future sea level rise considered both the rising level of the sea and changes in land elevation due to subsidence. The absolute rise in sea level was informed by the IPCC AR6 assessment, indicating a 0.77 m increase in water level between 2020 and 2100 based on SSP5 8.5M. Subsidence was informed by high resolution outputs for vertical land movement generated by NZ SeaRise and show a spatially variable trend along the site. The resulting relative sea level rise ranges between 0.8 - 1.1 m along the site. The spatial variation in VLM was accounted for by adjusting the model bathymetry.

Model outputs for the Building Code design event (combined 2% AEP storm tide and 2% AEP swell wave height event in 2100) indicate that some areas of the coast along Clifton, Te Awanga, Clive and Awatoto are subject to overtopping, with overland flow extending inland. The section of barrier crest along Marine Parade is generally not subject to overtopping. Some wave induced surges were modelled to overtop the coast along Ahuriri, Pandora and Westshore. Overtopping of the coastal barrier did not occur in the model for developed areas of Bay View, Whirinaki and Tangoio. In addition to areas exposed to dynamic inundation from wave effects, areas below the level of MSL and MHWS in 2100 were mapped. These potential inundation areas highlight a vast area of land that could be subject to tidal inundation through drainage networks and ground water infiltration.

The resulting coastal inundation hazard was mapped as a raster layer (GeoTIFF) showing the inundation level and extent associated with dynamic coastal processes. Outputs for the coastal inundation level and depth are provided as digital files.

8 Applicability

This report has been prepared for the exclusive use of our clients Hawke's Bay Regional Council; Hastings District Council; Napier City Council, with respect to the particular brief given to us and it may not be relied upon in other contexts or for any other purpose, or by any person other than our client, without our prior written agreement.

We understand and agree that this report will be used by Hastings District Council, Napier City Council and Hawke's Bay Regional Council, in undertaking its regulatory functions in connection with assessing building consent applications with respect to coastal inundation.

Tonkin & Taylor Ltd
Environmental and Engineering Consultants

Report prepared by:



.....
Dr Eddie Beetham
Coastal Scientist

Holly Blakely
Coastal Engineer

Authorised for Tonkin & Taylor Ltd by:



.....
Richard Reinen-Hamill
Project Director

Report Reviewed by:

Patrick Knook

Richard Reinen-Hamill

\\ttgroup.local\files\aklprojects\1019664\workingmaterial\02 report\forfinalissue_nov_2023\2023_11_28_hb_inundation_final.docx

9 References

- Beya, Jose & Asmat, Cindy (2021). Short-term concept design and costing – Clifton to Tangoio 2120 Coastal hazards strategy – Stage 4 – Design workstream. Wave, shoreline evolution and gravel barrier response modelling – Groynes design and cost estimates. Hawke’s Bay Regional Council, Asset Management Group.
- Bosserelle, C., 2022. "XBeach GPU v1.0." Lightweight XBeach style model that runs on the GPU Retrieved 10/02/2022. from. https://cyprienbosserelle.github.io/xbeach_gpu/ .
- Bosserelle, C., Gallop, S.L., Haigh, I.D., Pattiaratchi, C.B., 2021. The influence of reef topography on storm-driven sand flux. *J. Mar. Sci. Eng.* 9 (3), 272.
- Beavan RJ, Litchfield NJ. 2012. Vertical land movement around the New Zealand coastline: Implications for sea-level rise. Lower Hutt: GNS Science.
- Cagigal L, Rueda A, Castanedo S, et al. Historical and future storm surge around New Zealand: From the 19th century to the end of the 21st century. *Int J Climatol.* 2019;1–14. <https://doi.org/10.1002/joc.6283>.
- Fox-Kemper, Bet al. Yu, 2021, Ocean, Cryosphere and Sea Level Change. In: *Climate Change 2021: The Physical Science Basis. Contribution of Working Group I to the Sixth Assessment Report of the Intergovernmental Panel on Climate Change* [Masson-Delmotte, V., et al (eds.)]. Cambridge University Press. In press.
- Goodier, Craig Ir. & Pearse, Lisa (2015). Storm Report: Cyclone Pam March 15-18,2015. HBRC Response to Cyclone Pam. Asset Management Group, Hawke’s Bay Regional Council. HBRC Report Number 4278, Plan number Am15/03.
- Hamling, I. J., Wright, T. J., Hreinsdóttir, S., & Wallace, L. M. (2022). A snapshot of New Zealand's dynamic deformation field from Envisat InSAR and GNSS observations between 2003 and 2011. *Geophysical Research Letters*, 49(2), e2021GL096465.
- Hull, A.G. (1990). Tectonics of the 1931 Hawke’s Bay Earthquake. *New Zealand Journal of Geology and Geophysics*, 29:75-82.
- Komar (2005). Hawke’s Bay: Environmental Change, Shoreline Erosion and Management Issues. Report for HBRC, NCC and Port of Napier.
- Komar, P. and Harris, E (2014). Hawke’s Bay New Zealand: Global Climate Change and Barrier Beach Response Processes. Report No. 14-02 for HBRC.
- Kopp, R. E., Horton, R. M., Little, C. M., Mitrovica, J. X., Oppenheimer, M., Rasmussen, D. J., ... & Tebaldi, C. (2014). Probabilistic 21st and 22nd century sea-level projections at a global network of tide-gauge sites. *Earth's future*, 2(8), 383-406.
- Levy, R., Naish, T., et al. (2020). *Te tai o Aotearoa – Future Sea level rise around New Zealand’s dynamic coastline*. in Coastal Systems & Sea Level Rise: What to look for in the future. Special Publication 4, December 2020. New Zealand Coastal Society, Wellington New Zealand.
- MetOcean (2011). Hawke’s Bay Wave Climate, Hindcast of wave conditions for the Hawke’s Bay and surrounding coastal region. Prepared for Hawke’s Bay Regional Council.
- MetOcean (2013). Hawke’s Bay Wave Climate: MetOcean Solution Ltd., New Plymouth, New Zealand.
- MfE (2017). Coastal Hazards and Climate Change, Guidance for Local Government. Lead Authors, Bell, R., J Lawrence., Allan, R., Blackett, P., and Stephens, S. <https://environment.govt.nz/publications/coastal-hazards-and-climate-change-guidance-for-local-government/>
- MfE (2022). Interim guidance on the use of new sea-level rise projections. Wellington: Ministry for the Environment.
- Naish, T., Levy, R., Hamling, I., Garner, G., Hreinsdóttir, S., Kopp, R., & Wallace, L. (2022). The significance of vertical land movements at convergent plate boundaries in probabilistic sea-level projections for AR6 scenarios: The New Zealand case. *Submitted to Earth’s Future*.
- LINZ (2021). New Zealand Nautical Almanac (NZ 204). 2021/2022 Edition.

- Rautenbach, C., Trenham, C., Benn, D., Hoeke, R., & Bosserelle, C. (2022). Computing efficiency of XBeach hydro-and wave dynamics on Graphics Processing Units (GPUs). *Environmental Modelling & Software*, 157, 105532.
- Rautenbach, C., Bosserelle, C., Arnold, J., Maltai, K., and Blackwood, P. (2021). Bay of Plenty Coastal Flood Modelling and Mapping. *Australasian Coasts & Ports 2021 Conference*.
- Rice Speir (2021). *Guidance on applying the Hawke's Bay Regional Council's Hazards Portal coastal inundation and flooding data to building consent applications*. Letter dated 13 October 2021.
- Roelvink, D., Reniers, A., van Dongeren, A., van Thiel de Vries, J., McCall, R., Lescinski, J., 2009. Modelling storm impacts on beaches, dunes and barrier islands. *Coast. Eng.* 56 (11), 1133–1152.
- T + T (2003). Hawke's Bay Nearshore Wave Climate. Unpublished report prepared for Hawke's Bay Regional Council. Tonkin + Taylor Reference: 20234.
- T+T (2016). Clifton to Tangoio Coastal Hazards Strategy: Coastal Hazards Assessment. Prepared for Hawke's Bay Councils (HBRC, NCC, HDC). May 2016. Reference 20514.005.CHA.v8.

Appendix A Water level analysis

A1 Model bathymetry adjustment to NZVD-16

The model topography/bathymetry digital elevation model (DEM) being used in this assessment was initially generated by GNS for tsunami inundation. The model bathymetry was generated in 2022 and has a vertical reference of MSL = 0. To confirm the offset between the provided bathymetry and NZVD-16, a comparison of levels was undertaken by using elevation difference grids between the 'MSL' model DEM and regional LiDAR in NZVD-16 (regional LiDAR data were collected over November – December 2020). Areas of bare ground at the coastal edge, on paddocks and along the runway were compared by creating difference grids at 1m spatial resolution throughout the domain and calculating the average difference. The difference between the model DEM and NZVD-16 LiDAR was consistent across the extent, and the average difference was -0.23 m (e.g. Figure Appendix A.1). Therefore, the model DEM is 0.23 m above NZVD-16, which is the recommended offset for converting the DEM to NZVD-16.

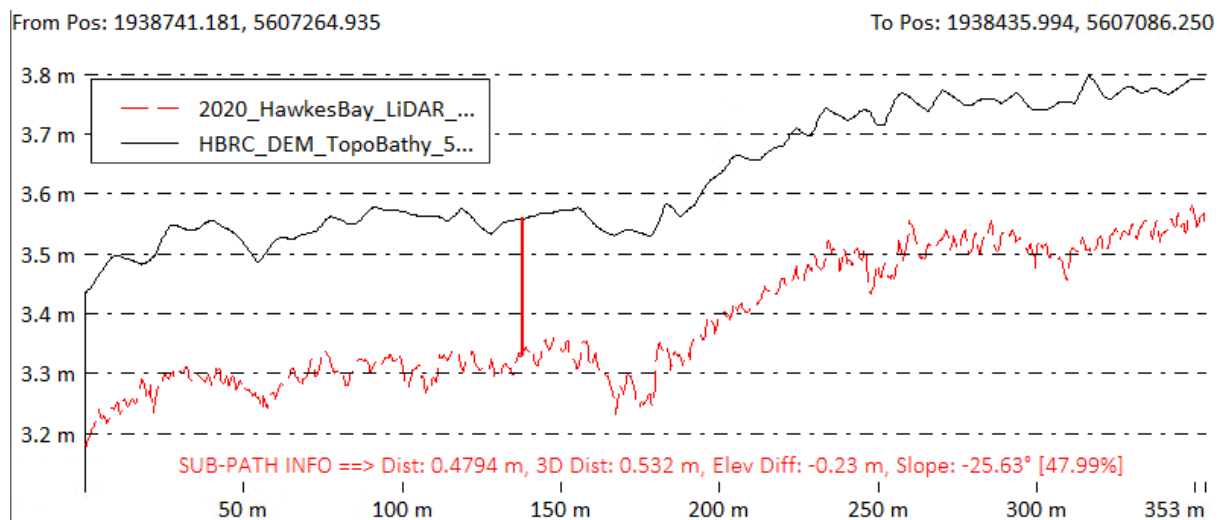


Figure Appendix A.1: Example of the elevation difference between the model DEM (MSL) and regional LiDAR (NZVD-2016) from a farm in Hastings.

A2 Previous assessments on extreme water levels

A previous assessment by T+T (2016) assessed storm tide levels for Hawke's Bay using tide gauge measurements from Napier Port between 1989 – 2014, with a 4 year gap resulting in 22 years of data. Storm tides were calculated using an extreme value analysis (Weibull distribution) and are presented in Appendix A Table 1. These have also been converted to NVD and NZVD for reference in this project. Note that the difference between the 50 year and 100 year event is only 0.02 m.

Appendix A Table 1: Storm tide levels assessed by T+T (2016)

AEP	ARI	CD (m)	NVD-62 (m)	NZVD-16 (m)
18%	5yr	2.21	1.29	1.09
10%	10yr	2.27	1.35	1.15
5%	20yr	2.32	1.40	1.20
2%	50yr	2.38	1.46	1.26
1%	100yr	2.40	1.48	1.28

Beya and Asmat (2021) calculated the storm surge component of extreme water level using calculations that account for wind induced setup and water level effects of atmospheric pressure. The resulting values for different extreme return periods are presented in Appendix A Table 2 and include a 5% increase due to future climate change over the design life. The values used by Beya and Asmat are consistent with T+T (2016) when MHWS is added to the surge component, with levels within 1-2 cm.

Appendix A Table 2: Design storm surge levels from Beya and Asmat (2021)

AEP (%)	Return Period (yr)	Storm surge (m)	Storm surge + 5% (m)	Surge+5% + MHWS (m, CD)
63%	2	0.35	0.37	2.24
18%	5	0.39	0.41	2.28
10%	10	0.41	0.43	2.30
5%	20	0.44	0.46	2.33
2%	50	0.47	0.49	2.36
1%	100	0.5	0.52	2.39

A3 Climate change projections of storm surge

Climate change is expected to result in altered weather patterns that could change storm surge levels. This was considered in Beya and Asmat (2021), where a 5% increase in the storm surge component was added due to climate change. Their assessment was based on New Zealand storm surge projections until 2100 from Cagigal et al. (2019). Although the addition of 5% was considered an appropriate contingency for designing coastal structures, the trends presented in Cagigal et al. (2019) is of stable or decreasing storm surge levels on the east coast of the North Island with RCP 8.5M. The main limitation of using Cagigal et al (2019) is that storm surge is modelled on a daily time step and therefore is not likely appropriate for capturing the peak height of individual storms, which is especially true for ex-tropical cyclones that impact the Hawke Bay during summer. Based on the trend of consistent or negative changes in storm surge on the North Island east coast, we consider the 5% contingency is not required for the Building Code assessment purpose.

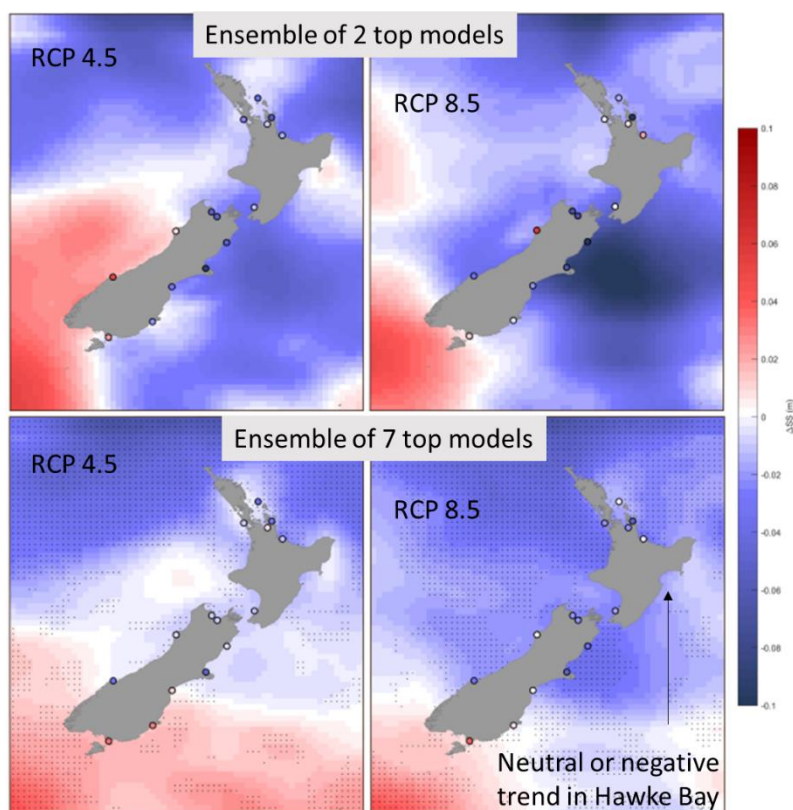


Figure Appendix A.2: Changes in the 2% AEP storm tide level between historic (1975 - 2004) and future projections (2070 - 2100) using different model ensembles and RCPs. Adapted from Cagigal et al (2019).

A4 Reanalysis of storm tide level

Napier Port tide gauge data is available from 1989 – 2020 from the University of Hawaii. This provides 27 years of available data with respect to Chart Datum (not including the 4 year gap). Hourly data has been assured as ‘research quality’ (<http://uhslc.soest.hawaii.edu/data/?rq#uh668a>). Analysis of tide gauge data for assessing extreme water levels incorporates interannual oscillations in mean sea level (e.g. ENSO signal) and localised storm surge events associated with onshore wind and low atmospheric pressure.

Analysis of tide gauge data used the following steps:

First, the mean monthly sea level was assessed to identify the rate of long-term sea-level rise for the full dataset (3.48 mm/yr), and between 2000 and 2020 (5.41 mm/yr).

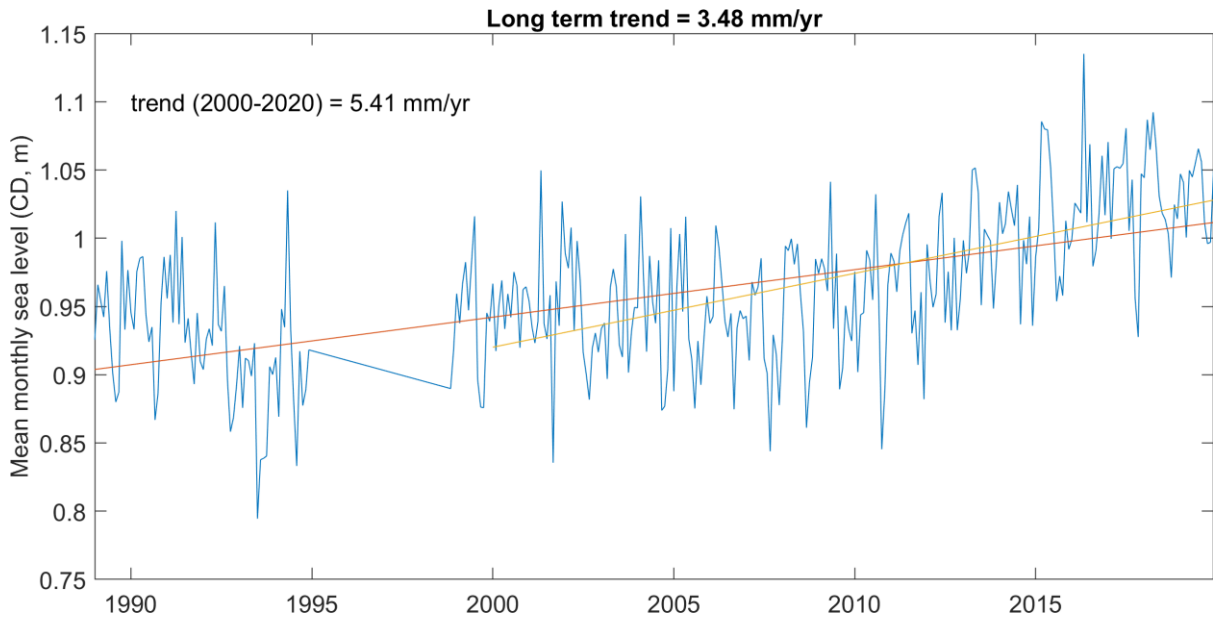


Figure Appendix A.3: Mean monthly sea level at Napier Port using raw data.

Second, the long-term sea-level rise trend was removed from the raw data to get a 'detrended' signal. This is done to prevent skewing storm tide levels to favour recent events when mean sea level is higher. The 'detrended' data was centred around a 20 year mean sea level baseline at 2010 (mean between 2000 and 2020), which is 0.974 m above chart datum.

Third, the 'peaks over threshold' method was used to identify the maximum storm tide events that correspond to the years of data available (27 years), resulting in a threshold of 2.141 m. A notable cluster of peaks is evident in 2017, when mean sea level was relatively high and likely being influenced by inter-annual climate patterns (Figure Appendix A.4).

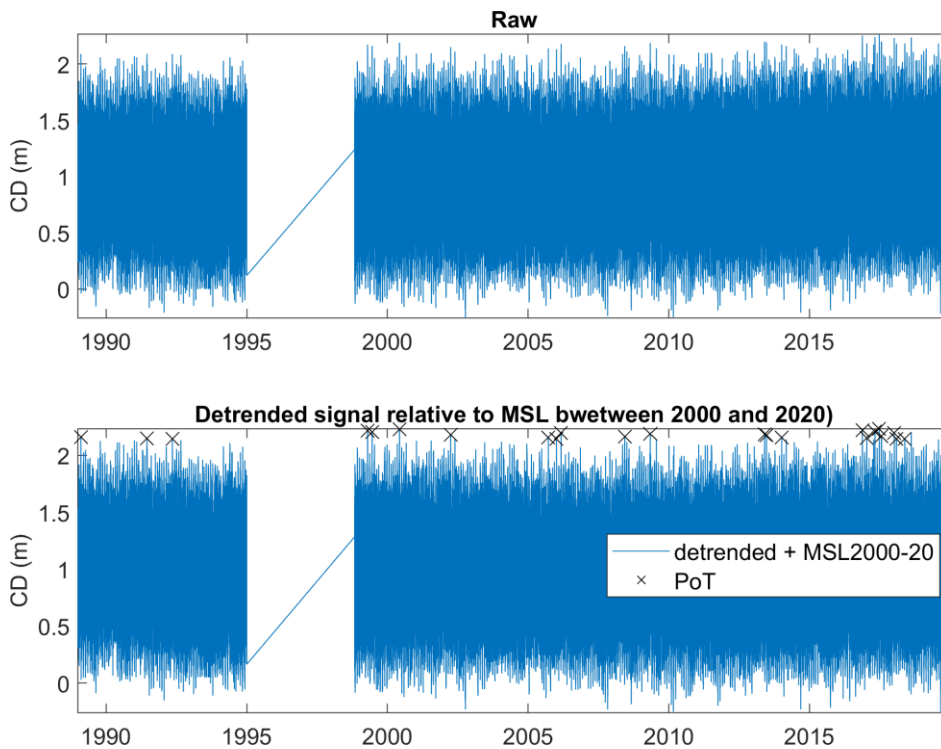


Figure Appendix A.4: Hourly water level data showing the raw signal in chart datum, and the detrended data centred on mean sea level in 2010.

Forth, different extreme value distributions were considered when assessing the extreme return periods. The Generalised Extreme Value (GEV) distribution, Gumbel distribution, and Weibull Distribution were tested, and all have a relatively close fit when visualised against the peaks (Figure Appendix A.5). The GEV distribution was identified as being the more conservative approximation for extreme storm tide level, using the ‘Probability Weighted Moments’ method. Based on the curve in Figure Appendix A.5, the GEV distribution provides slightly higher levels compared to both the Gumbel and Weibull distribution for a 1% and 2% AEP event, which is considered suitable for the relatively short data set (Appendix A Table 3).

Appendix A Table 3: Extreme storm tide level for different return periods based on different distributions, relative to MSL in 2010

AEP	ARI	GEV (m, CD)	Gumbel (m, CD)	Weibull (m, CD)
18%	5yr	2.20	2.20	2.21
10%	10yr	2.22	2.21	2.22
5%	20yr	2.24	2.23	2.22
2%	50yr	2.26	2.25	2.23
1%	100yr	2.28	2.27	2.24

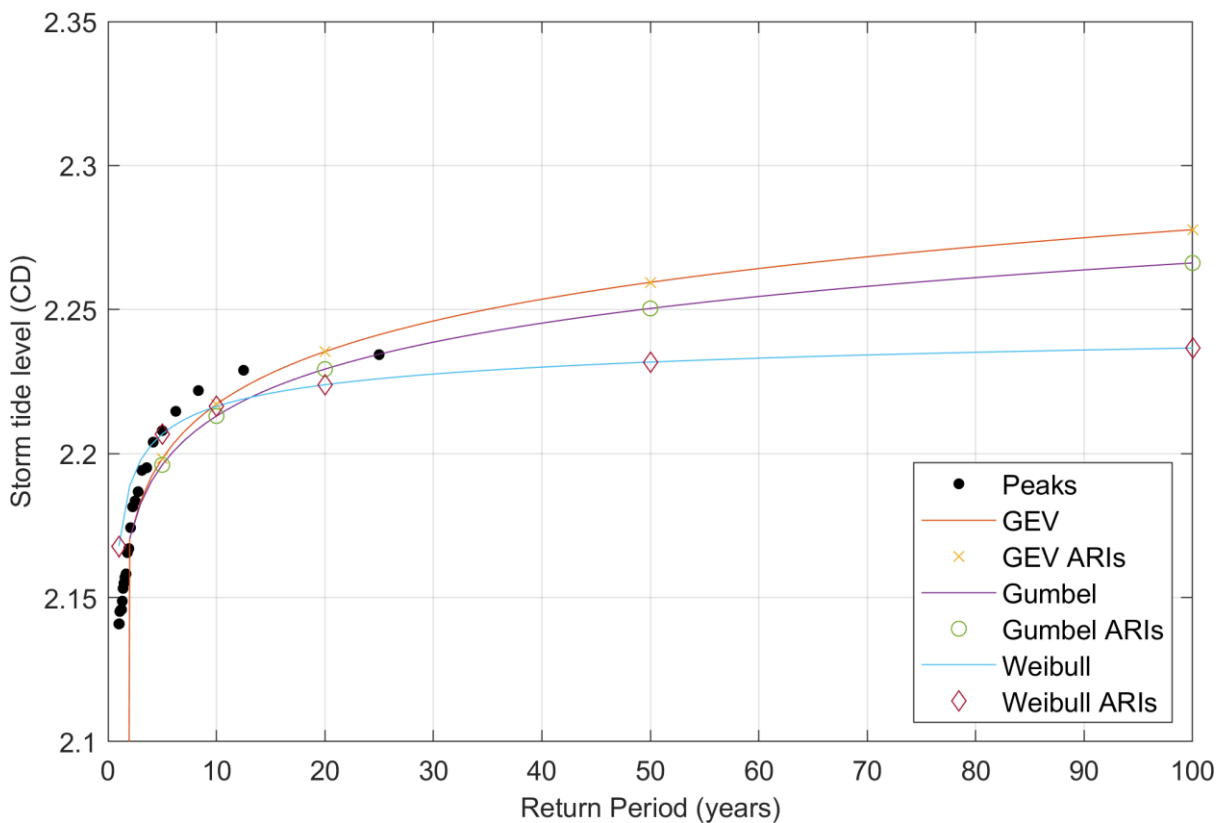


Figure Appendix A.5: Extreme value distributions for fitting peak water level measurements.

Fifth, storm tide levels were then converted to a 2020 mean sea level baseline using the measured rate of sea level rise between 2000 and 2020 (10 years at 5.41 mm/yr = 0.0541 m) and converted to NVD and NZVD (Appendix A Table 4).

Appendix A Table 4: Extreme storm tides relative to MSL in 2020 based on the GEV distribution

AEP	ARI	CD (m)	NVD (m)	NZVD (m)
18%	5yr	2.25	1.33	1.14
10%	10yr	2.27	1.35	1.15
5%	20yr	2.29	1.37	1.17
2%	50yr	2.31	1.39	1.20
1%	100yr	2.33	1.41	1.21

A5 Sea level rise

The sea level rise scenario recommended for this assessment is SSP5 8.5M at 2100 (Rice Spier, 2021). The latest data on climate change induced sea level rise (SLR) was considered in this assessment, based on the IPCC AR6 report released in 2021 (Fox-Kemper et al., 2021). AR6 values of sea level rise were sourced for Napier Port from a global portal⁸ and from a New Zealand specific platform NZ SeaRise⁹. Both sources provide information on absolute sea level rise (not including VLM) and relative sea level rise including VLM. Values presented in AR6 and NZ SeaRise for absolute sea level rise at Napier Port are the same. However, there are differences in VLM between the global assessment (AR6) and the national NZ SeaRise data.

Values of absolute sea level rise are presented in Appendix A Table 5 for select shared socioeconomic pathways (SSPs), that are consistent with the previous AR5 Representative Concentration Pathways (RCPs). These levels are consistent across the IPCC AR6 data portal and NZ SeaRise data when VLM is removed. Magnitudes of absolute SLR were adjusted to a 2020 baseline of zero to be consistent with storm tide analysis. This was done by subtracting the change in sea level between the 2005 baseline and 2020 (which is 0.06 m for the 8.5M scenario).

Appendix A Table 5: Projections of sea level rise from IPCC AR6 (excluding vertical land movement) for Napier relative to a 2020 baseline

Year	SSP2 4.5 median (m)	SSP5 8.5 median (m)	SSP5 8.5 high (m)
2020	0.00	0.00	0.00
2030	0.05	0.05	0.05
2040	0.09	0.11	0.13
2050	0.16	0.19	0.23
2060	0.21	0.27	0.34
2070	0.29	0.38	0.48
2080	0.36	0.49	0.64
2090	0.43	0.62	0.81
2100	0.51	0.77*	1.00
2110	0.60	0.88	1.20
2120	0.67	1.02	1.39
2130	0.75	1.15	1.58

*Value adopted for this assessment

⁸ https://sealevel.nasa.gov/data_tools/17

⁹ <https://www.searise.nz/maps-2>

Relative sea level rise includes the rate of vertical land movement and the magnitude of absolute sea level change. Information on relative sea level rise including VLM was sourced from the NZ SeaRise database along the site, using averaged rates of VLM for discrete sections of coast. Appendix A Table 6 presents values for relative sea level rise for the SSP5 8.5M scenario and highlights the 2100 line for use in this assessment.

Appendix A Table 6: Magnitudes of relative sea level rise (m relative to MSL in 2020) at representative locations

SSP5 8.5M	Clifton to Tukituki	Clive	Napier South	Napier to Bay View	Whirinaki	Tangoio
VLM rate (mm/yr)¹	-0.68	-2.04	-3.24	-3.62	-4.15	-3.39
2020	0.00	0.00	0.00	0.00	0.00	0.00
2030	0.06	0.07	0.08	0.09	0.09	0.08
2040	0.12	0.15	0.17	0.18	0.19	0.18
2050	0.21	0.25	0.29	0.30	0.31	0.29
2060	0.30	0.35	0.40	0.41	0.44	0.41
2070	0.41	0.48	0.54	0.56	0.59	0.55
2080	0.53	0.61	0.68	0.71	0.74	0.69
2090	0.67	0.76	0.85	0.87	0.91	0.86
2100	0.82	0.93	1.03	1.06	1.10	1.04
2110	0.94	1.06	1.17	1.21	1.25	1.19
2120	1.09	1.22	1.34	1.38	1.43	1.36
2130	1.23	1.37	1.51	1.55	1.61	1.52

¹Based on the average VLM value along the section of coast.

Appendix B Wave climate analysis

B1 Wave climate review

Previous investigations have modelled the nearshore wave climate models within Hawke Bay. Studies conducted by T+T (2003) and MetOcean (2011; 2013) used the numerical model SWAN to transform offshore wave hindcasts into the nearshore region. These studies focused on outputting wave statistics at the 5 and 10 m depth contours. Maximum significant wave heights varied from 2.1 m to 4.4 m. Wave heights in these investigations peaked at different areas. T+T (2003) found maximum nearshore wave heights at the northern end of the Bay View Littoral Cell (close to Tangoio) while MetOcean (2011; 2013) found peak waves close to Napier (northern end of Haumoana Littoral cell).

Following these two studies, investigations focused on the Port of Napier wave buoy data (installed in 2000) as well as developing refined wave hindcasts. Komar (2014) used wave data measured directly from the Port of Napier wave buoy. This data were transformed twice; first into the deep-water environment by comparison with T+T (2003) wave values and second into the breakpoint using empirical shoaling equations.

More recent assessments conducted by T+T (2016) and Beya and Asmat (2021), used extended nearshore SWAN model hindcasts that were calibrated against the recorded wave buoy data. The T+T (2016) study used a MetOcean hindcast covering a 34 year period. Beya and Asmat (2021) developed a 37 year SWAN hindcast. T+T (2016) outputted wave statistics at the 5 and 10 m depth contours (HBRC datum) at 12 locations throughout the study area (Appendix B Table 1).

Appendix B Table 1: Significant wave heights at the 5 m and 10 m depth contours from the T+T (2016) assessment.

Site	Return period (years)					
	1	5	10	25	50	100
Bay View 5 m	2.6	3	3.15	3.25	3.4	3.48
Bay View 10 m	2.62	3.05	3.20	3.38	3.50	3.61
West Shore 5 m	2	2.13	2.2	2.26	2.32	2.37
West Shore 10 m	2.57	3.03	3.20	3.39	3.53	3.65
Napier 5 m	2.65	2.85	2.9	2.95	3.02	3.05
Napier 10 m	2.82	3.28	3.45	3.65	3.79	3.91
Haumoana 5 m	2.2	2.35	2.4	2.46	2.53	2.58
Haumoana 10 m	2.62	3.12	3.30	3.53	3.69	3.84
Te Awanga 5 m	2.02	2.04	2.05	2.07	2.09	2.1
Te Awanga 10 m	2.76	3.25	3.43	3.66	3.81	3.95
Clifton 5 m	1.95	1.97	1.98	2	2.02	2.03
Clifton 10 m	2.94	3.49	3.70	3.95	4.13	4.30

Beya and Asmat (2021) outputted wave hindcast data at points located 500 m seaward of the shoreline for each of the 23 HBRC beach profile locations. An extreme value analysis (EVA) was conducted at these locations (Figure Appendix B.1). Spatial variability of the Beya and Asmat (2021) assessment indicates the trend of increasing wave height moving northward within each of the two littoral cells. With the lowest wave heights experienced at Westshore (HB13) and Te Awanga (HB1).

This trend is correlated to the sheltering effect of Bluff Hill and Cape Kidnappers (Figure Appendix B.1) respectively.

The modelled wave hindcast at the wave buoy location was also compared to Port of Napier Wave Buoy recordings with regards to understanding the extreme wave climate (Appendix B Table 2). Results indicate that the wave hindcast, which extends for an extra 20 years is associated with larger extreme waves compared to the wave buoy measurements.

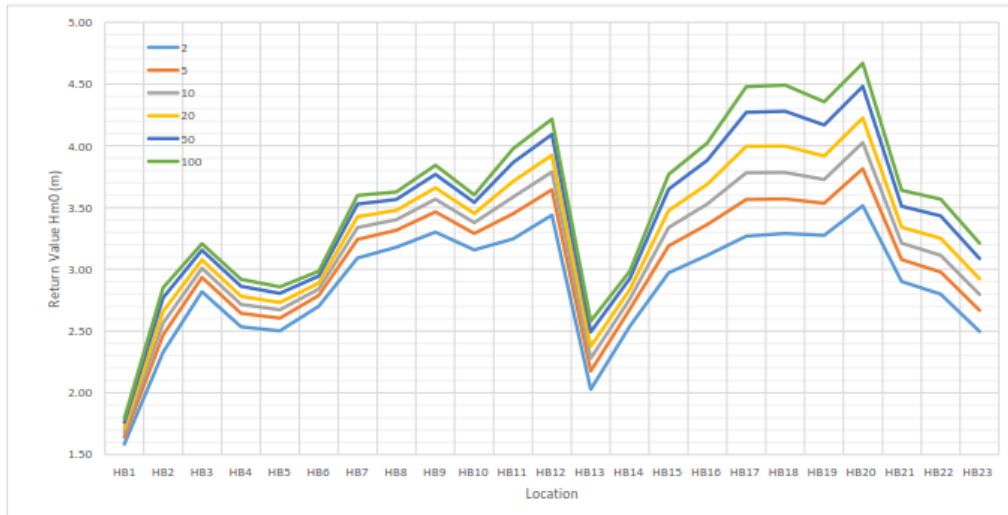


Figure Appendix B.1: Significant wave heights at points 500 m offshore of beach profile locations (Beya and Asmat, 2021).

Appendix B Table 2: Significant wave heights determined from analysis of port buoy measurements (Beya and Asmat, 2021)

Return period (years)	Port buoy measurement return value (H_{m0})	Port buoy measurement upper level 95% confidence band (H_{m0})	Port buoy hindcast return value (H_{m0})
2	3.89	4.10	4.46
5	4.20	4.52	4.77
10	4.39	4.86	5.25
20	4.55	5.23	5.60
50	4.75	5.73	5.96
100	4.88	6.11	6.43

B2 Wave climate analysis

The wave climate analysis presented in this report will follow a similar procedure to that conducted by Beya and Asmat (2021). Updated timeframes for both Port of Napier wave buoy recordings and HBRC SWAN hindcast data were used in analysis.

B2.1 Napier Port wave buoy

Port of Napier wave buoy data are now available from Jan 2000 – December 2021. The relationship between peak wave direction, peak period and significant wave height is presented in Figure Appendix B.2. Directional analysis of wave data collected at the Port of Napier wave buoy shows a

strong clustering of waves from the easterly direction (between 60° (ENE) and 90° (E)). Longer wave period events appear to be primarily reaching the wave buoy from true east. The lack of south-easterly waves indicates that significant refraction has occurred before waves reach the Napier wave buoy location, at a depth of approximately 15 m. Refraction at this location may be associated with Cape Kidnappers, a network of offshore shoals and Pania Reef.

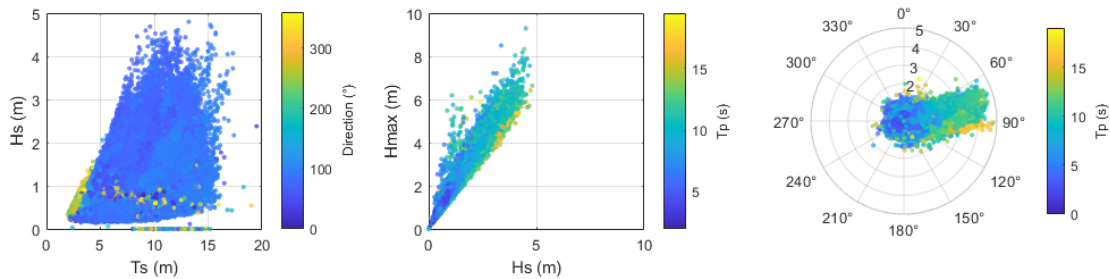


Figure Appendix B.2: Summary figures from the Port of Napier Wave Buoy.

Different extreme value distributions have been tested against the wave buoy data (Figure Appendix B.3 and Appendix B Table 3). A Generalised Extreme Value (GEV), Gumbel, and Weibull distributions were tested. Of these distributions the Weibull distribution showed the closest fit to the measured wave buoy peaks (Figure Appendix B.3). A peaks-over-threshold method was used to filter input values for each extreme value distribution. An iterative method was developed to identify the peak threshold associated with an average of 1 storm event per year in the dataset. The Weibull EVA tends to underpredict peaks for low return periods (less than 5 years) but shows a close fit for the larger return period events (Figure Appendix B.3). Other distributions showed over predictions of the larger return period events, which could result in greater inundation extents than are likely. The Weibull distribution also resulted in extreme wave heights close to the values identified in Beya and Asmat (2021), as previously presented in Appendix B Table 3.

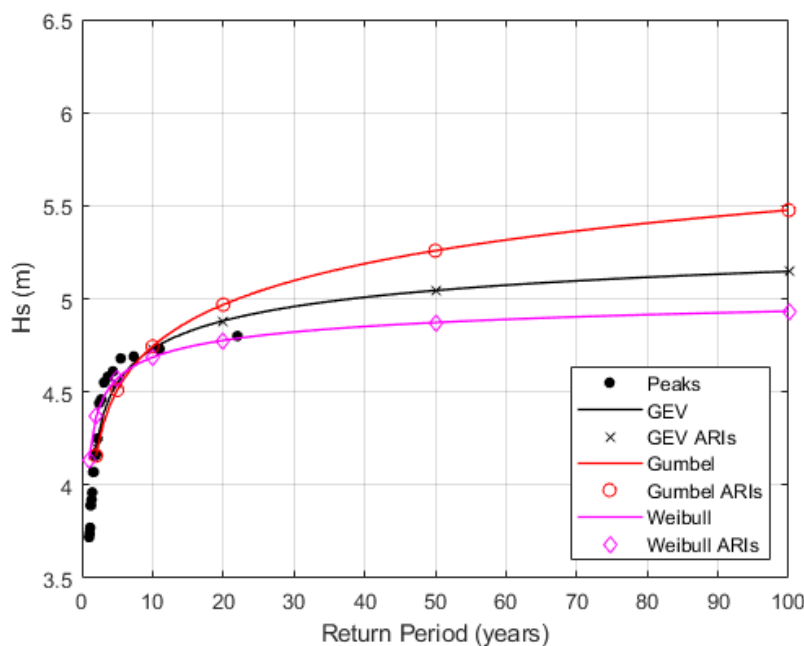


Figure Appendix B.3: Extreme value distributions fitted to peak wave buoy measurements.

Appendix B Table 3: Extreme significant wave heights based on the different distributions

AEP	ARI	GEV (m)	Gumbel (m)	Weibull (m)	Beya and Asmat (2021)
18%	5yr	4.55	4.51	4.57	4.20
10%	10yr	4.73	4.74	4.69	4.39
5%	20yr	4.88	4.97	4.78	4.55
2%	50yr	5.04	5.26	4.87	4.75
1%	100yr	5.14	5.48	4.93	4.88

B2.2 HBRC hindcast model

The regional SWAN hindcast presented in Beya and Asmat (2021) was extended to 2020 by HBRC for use in this assessment, resulting in a 40 year dataset. HBRC provided the updated hindcast from 1980 to the end of 2019, with hourly data at 400 locations within the site of interest. These points were spaced in regular intervals of 250 m along the HBRC beach profile transects and extend from -5 m to -15 m CD.

An output location close the Napier Wave Buoy was compared with the wave buoy data for comparison (Figure Appendix B.4). A comprehensive presentation of the hindcast model calibration and comparison to observations is presented in Beya and Asmat (2021), indicating a mean absolute error of 0.25 m for wave height. The general trend in wave height observed at the buoy matches the hindcast, but some peak events are higher in the numerical hindcast model.

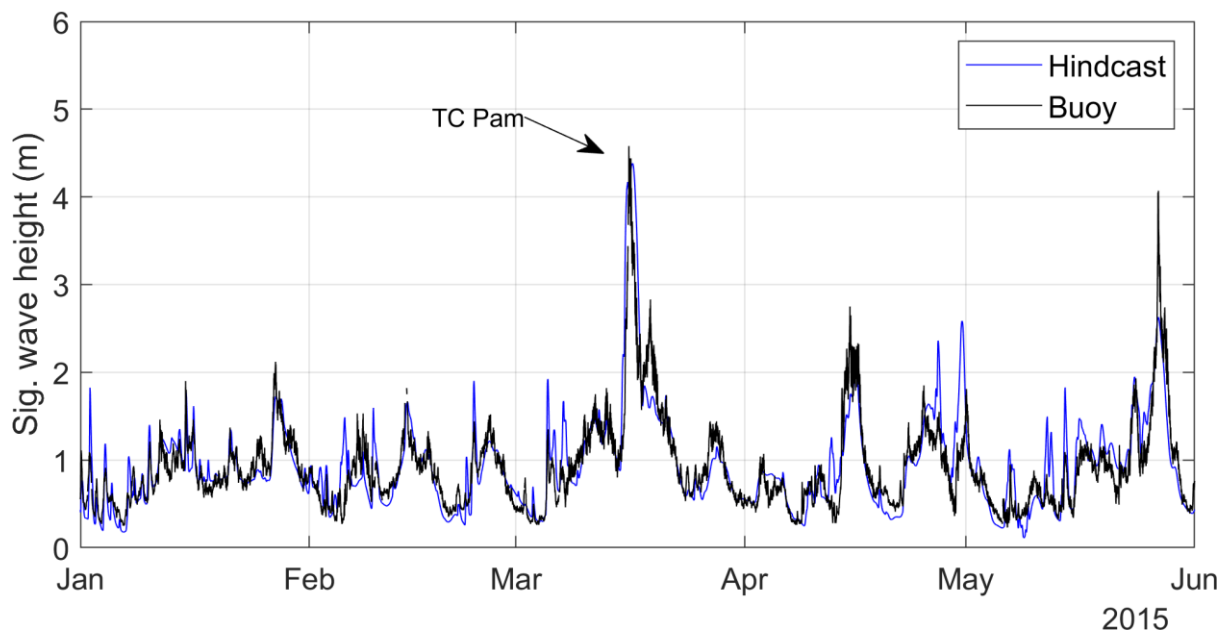
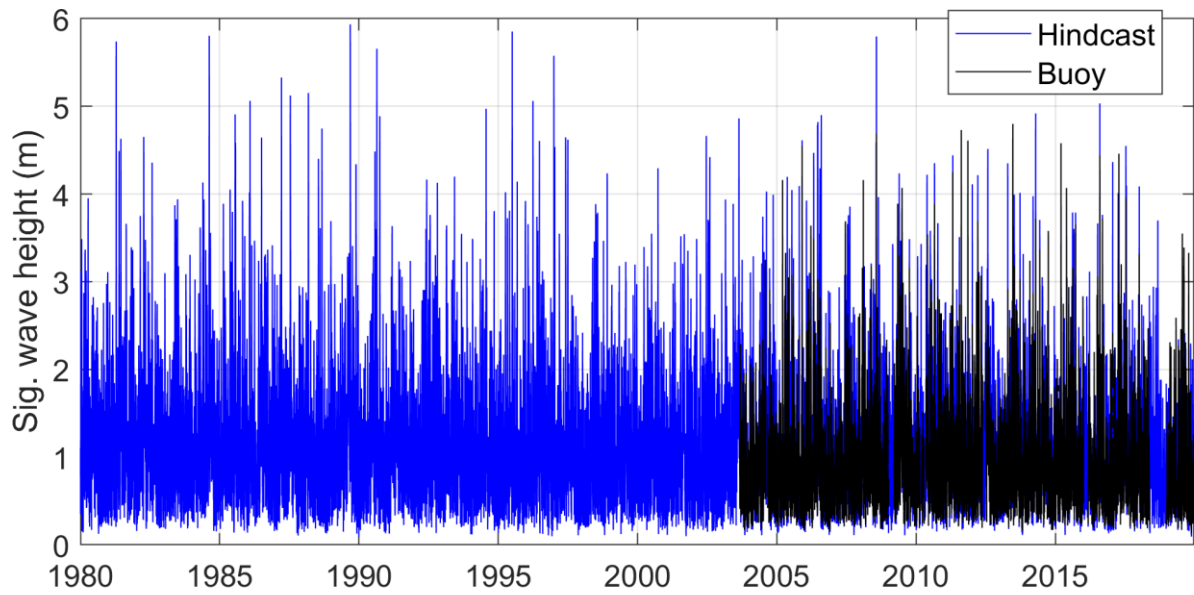


Figure Appendix B.4: Comparison between wave buoy and hindcast for all data available (top), and for the first half of 2015 when a few inundation events occurred.

An extreme value analysis (EVA) was undertaken on the 400 hindcast output points to understand general exposure to waves within the site. Similarly, to the Napier Port wave buoy data, various distributions were tested for fit against the hindcast data (Figure Appendix B.5). The Weibull distribution was identified as the closest representation of peak wave events, particularly for the larger extreme events.

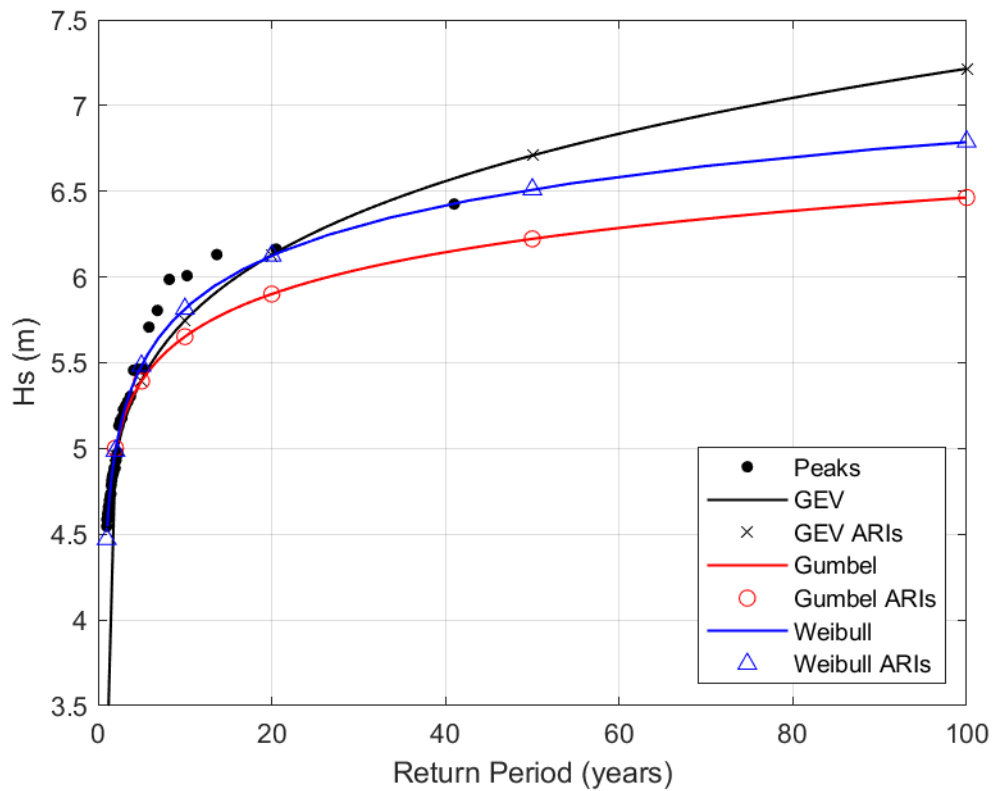


Figure Appendix B.5: Example of the extreme value distributions fitted to peak wave hindcast data at HBRC Beach Profile 10 (near the middle of Model Domain 3).

Wave EVA statistics for 5 year, 10 year, 20 year, 50 year, and 100 year events were outputted for each of the 400 points (Figure Appendix B.6). Extreme wave heights were largest offshore of Awatoto and Marine Parade, with a reduction towards Cape Kidnappers due to the presence of sheltering. Bluff Hill also provides some sheltering of nearshore waves at the southern end of Westshore. The effect of this sheltering quickly diminishes moving northwards, with less spatial variation in wave height present.

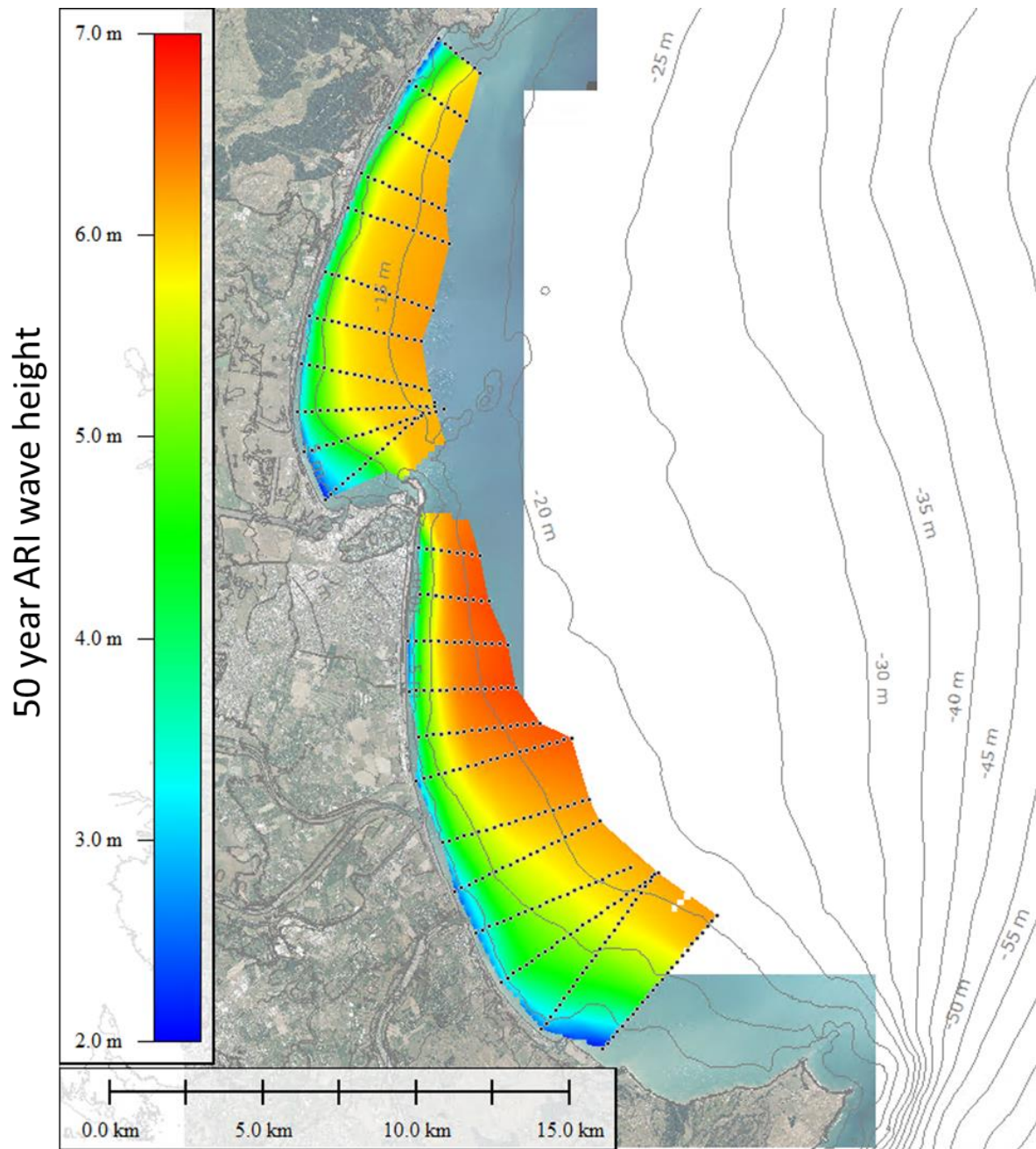


Figure Appendix B.6: 50 year ARI wave heights across the Hawke's Bay, based on gridding the 400 hindcast points.

Extreme wave conditions at the points closest to the -15 m depth contour (NZVD16) were specifically assessed for all HBRC beach profile locations (Figure Appendix B.7). From these locations, HBRC profiles 3, 6, 10, 14, 18, and 22 have been identified as being close to the middle of each of the respective 6 model domain boundaries (moving northwards) and have been used to give representative wave boundary conditions along the site.

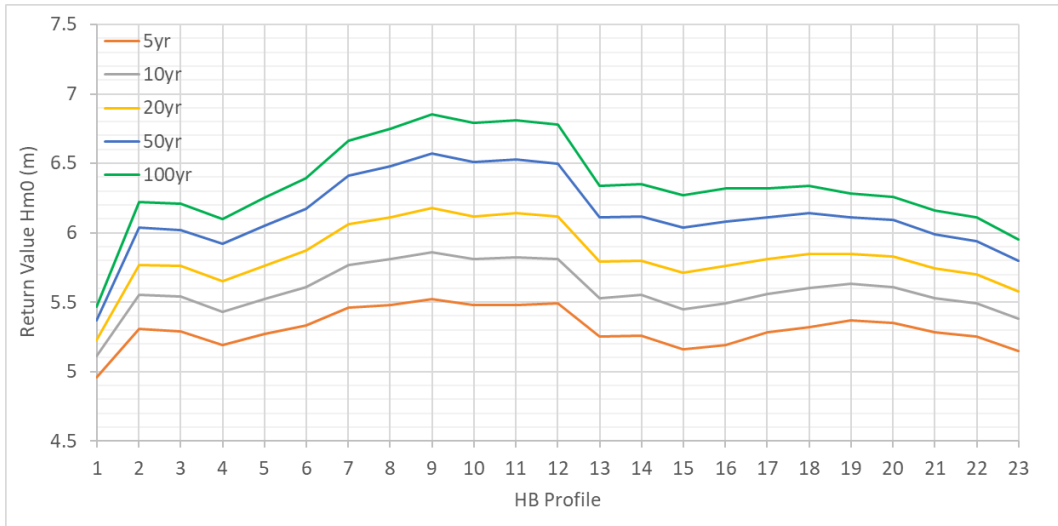


Figure Appendix B.7: Extreme significant wave heights at the 15 m depth contour for each of the HBRC beach profile sites.

Extreme significant wave heights determined from the SWAN hindcast are larger than from the Port of Napier wave buoy data. This has been attributed to the longer time that is covered by the hindcast data. Analysis of hindcast data close to the wave buoy found that 90% of the largest peak events occurred before the buoy was installed in 2000.



Appendix C Model calibration

C1 Observed wave inundation during TC Pam

Observations of wave runup and overtopping associated with ex-tropical cyclone Pam (TC Pam) in March 2015 provide a useful dataset to test the model’s capability to represent high runup and inundation associated with a high energy swell event.

Documentation of wave washed debris and direct observations of inundation extent were captured during and after the event, with clear reporting of the inundation extent in reports, maps, and photos (e.g. Goodier et al., 2015). Observed wave inundation was captured along most of the site, including Clifton, Te Awanga, Haumoana, Clive, Awatoto, Marine Parade, Westshore, and Bay View. An overview of the observed inundation is presented below. Lines on the inset images show the inundation or debris line. Traffic light colours indicate different levels of confidence in the inundation extent (green = high, orange = medium, red = low). Blue lines indicate the debris line.

Appendix C Table 1: Reported coastal inundation from TC Pam swell waves

Location	Description
<p>Clifton</p> 	<ul style="list-style-type: none"> • Waves washed across road between campgrounds, depositing some gravel material. • Minor damage to block wall at motor camp 2. • Minor damage to road at camp 1. • Inundation and debris levels mapped at 2.7 mRL. • Lines on the image to the left show the inundation or debris line.
<p>Te Awanga</p> 	<ul style="list-style-type: none"> • Debris washed up creek onto road at Wellwood Terrace. • Wave overwash reached Clifton Road in gaps between properties. • There is no record of waves washing through the motor camp at Te Awanga. • Inundation and debris levels mapped at 2.5 mRL.

Haumoana



- Waves washed into beach front houses on Clifton Road.
- Properties at 63A – 65 Beach Road were inundated by flood water in the lagoon, which filled up due to waves overtopping the gravel barrier.
- Gravel filled up the lagoon drainage network causing a blockage.
- Locals indicate that the gravel barrier was breached, causing the crest to lower in height significantly which exacerbated overtopping.
- Drainage was managed using pumps.
- The crest was rebuilt using excavators following the event.
- Inundation and debris levels mapped at 3.5 mRL (crest level).

Clive



- Waves washed over the eastern gravel barrier and into the wetland that sits between the barrier and sea exclusion banks.
- Waves did not wash over the sea exclusion bank or stop banks.
- Inundation and debris levels reached the ocean side of sea exclusion bank.

Awatoto



- Wave runup washed over beach crest and into shingle extraction plan area.
- Inundation and debris levels mapped at 4.2 mRL.

Marine Parade



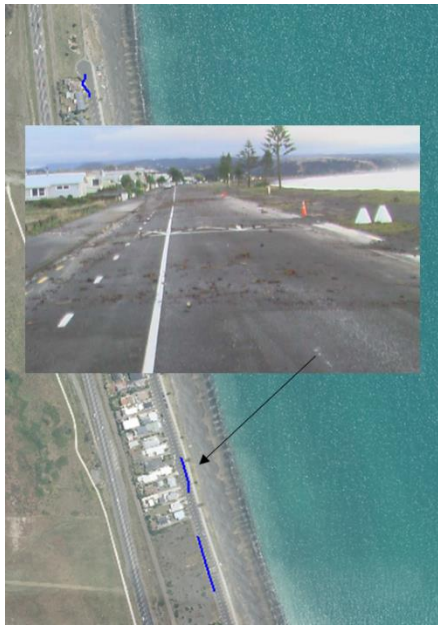
- Waves were documented washing over the beach crest, across the bike path and into reserve space, carparks.
- Gravel material deposited on reserve, path, and carparks along the Marine Parade stretch, with mapped inundation or debris lines at seven locations.
- Inundation and debris levels mapped at 4.5 – 5.5 mRL, increasing in elevation northward.

Westshore



- Waves were observed overtopping and breaching the Westshore bund, resulting in water ponding between the bund and road.
- The crest level on the bund reduced by approximately 1m during the event.
- Waves washed across the crest and over the carpark near the surf club.
- Inundation and debris levels mapped at up to 3.5 mRL (crest level of bund).

Bay View



- Some wave washed debris were recorded on The Esplanade in a few places, including the airport gap.
- Inundation and debris levels mapped up to 5.5 mRL.

C2 XBGPU model of TC Pam

Observed wave and tide conditions associated with TC Pam were used to calibrate XBGPU and check that the model can replicate the processes causing coastal inundation during a significant swell event.

Model boundary conditions were informed using the SWAN hindcast point at the model boundary for each grid location. Wave heights at the model boundary (Appendix C Table 2) are slightly higher than recorded at the Napier wave buoy (4.5 m at 15.5 s) because of the deeper and more seaward location. Wave period in the SWAN model (14.5 s) was slightly lower than the buoy (15.5 s), so the wave buoy measure period was used at all locations. Wave conditions in XBGPU were generated using a directional JONSWAP spectrum, and tests were undertaken to use the appropriate values for directional spread and spectral peak (γ), which are further discussed below. The peak tide level during TC Pam was 0.93 mRL, which was used as a static water level in the model boundary. Model calibration simulations were undertaken at a stable sea level for 3 hours, allowing time for the sea state to develop and potentially cause inundation at the shoreline. Model outputs were extracted every 30 minutes, with the maximum water level during the full 3 hour simulation used to map inundation.

Appendix C Table 2: Wave conditions each model boundary during Cyclone Pam

Location	H _s (m)	T _p (s)
1. Haumoana	4.35	15.5
2. Clive	4.60	15.5
3. Napier	4.80	15.5
4. Bay View	4.50	15.5
5. Tangoio	4.55	15.5

C2.1 Model sensitivity

The model was sensitive to key variables including wave spectrum parameters, bed friction, wave friction, wave breaking ratio and the seaward boundary location. Model parameters were adjusted until the simulated runup extent was a close match to the observed runup at most locations between Clifton and Bay View, keeping all variables within realistic bounds.

Initial simulations tended to under-predict the observed runup extent when using mostly default settings in XBGPU and spatially uniform friction for waves and flow. The wave boundary was assessed initially to make sure the wave spectrum generated in XBGPU was representative of long period swell conditions. The peak enhancement factor in the JONSWAP spectrum (γ), and directional spreading were adjusted in XBGPU to better represent long period swell condition. A γ value of 5.0, and a low directional spread ($s=1000^{10}$; $\sigma=2.5^\circ$) was identified as being most representative of the long period swell conditions. Wave breaking is another sensitive parameter, with runup level increasing proportional to the breaking ratio between wave height and water depth. A ratio of 0.75 was found to give the best fit with observations, using the swell parameters in the JONWASP spectrum. This is consistent with the breaking ratio used in NWIA (2020) for Timaru, where the gravel beach profile is comparable to Hawke's Bay.

Model sensitivity to wave height and period was also tested. Increasing the offshore wave height by 5 to 15% made only a minor difference to the modelled inundation. Increasing the period was found to be more sensitive, with significantly more inundation with a 16 s period compared to a 12s period, using the same wave height. This model behaviour is physically sensible, based on the steep nearshore profile along most of the site and the raised gravel crest.

C2.2 Comparison to observed inundation

The calibrated XBGPU model shows a good match to the observed inundation (or debris) line from surveyed after TC Pam. A series of figures are presented below, comparing the modelled inundation extent and level to the observed inundation and level.

Along The Esplanade at Bay View, the modelled inundation is generally level with the beach crest, with only a few minor locations showing flooding onto the road (Figure Appendix C.1). The modelled inundation level is consistent with observed level, but the observations show some waves did cross the road. This minor underprediction in the extent is explained by the observed debris likely being deposited by one large waves, without a multi wave surge crossing the road. Modelled inundation at the Westshore reserve carpark and bund shows a close fit with the observed inundation extent and level (Figure Appendix C.1). The modelled inundation overtops the beach barrier, and artificial bund causing flooding to a significant area of reserve space, which is consist with observations (Figure Appendix C.1).

¹⁰ https://xbeach.readthedocs.io/en/latest/xbeach_manual.html?highlight=jonswap#jonswap-wave-spectra.

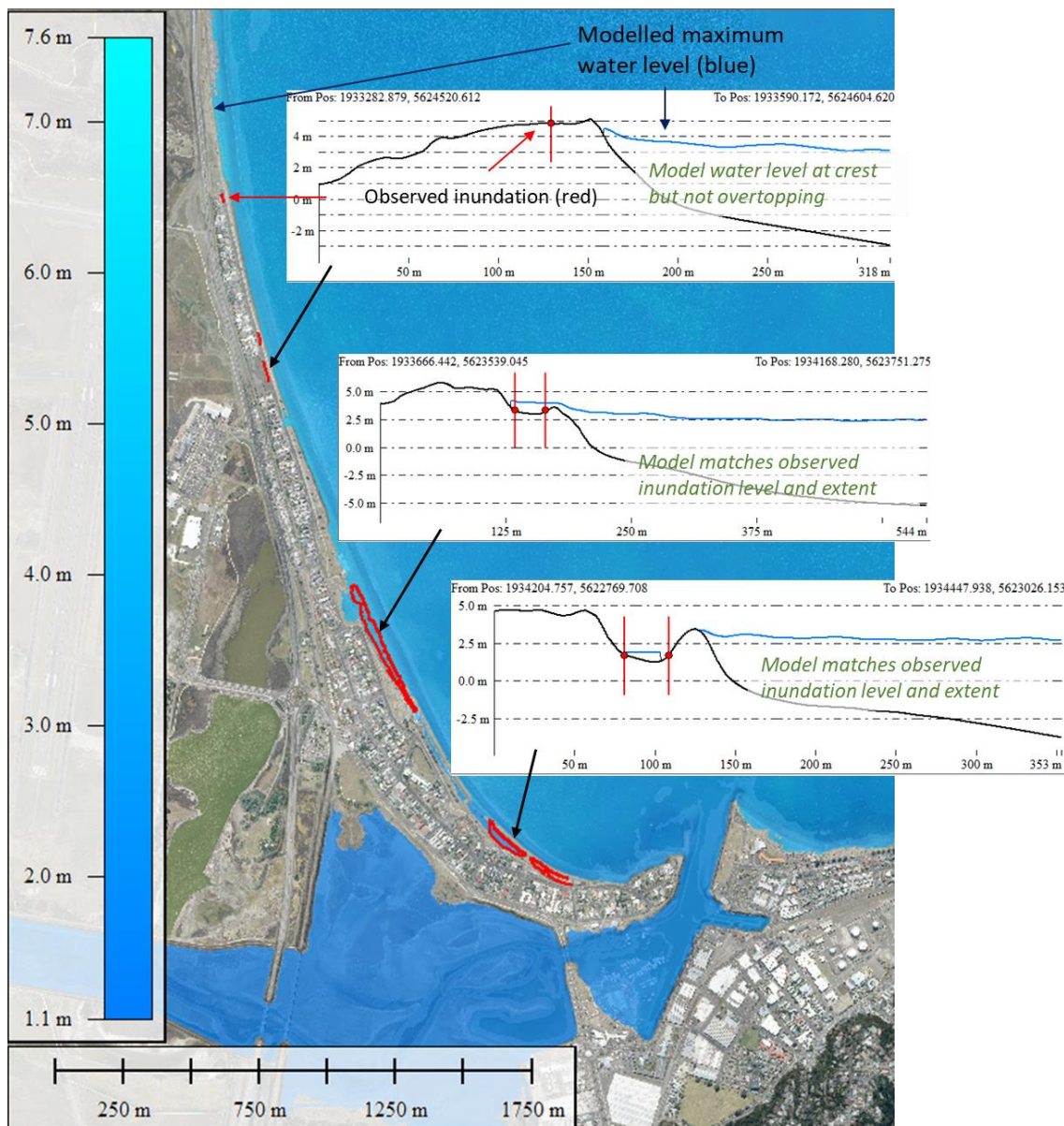


Figure Appendix C.1: Comparison between modelled inundation from TC Pam and observations along Bay View and Westshore. Mapped inundation is in red and the blue shade indicates the modelled inundation extent.

Modelled inundation extents and levels along Marine Parade generally show a close match with observations (Figure Appendix C.2). In a couple of the observed locations, the model output shows the maximum water level reaches the crest but does not cause an overland surge that would be required to deposit the mapped debris line. However, the modelled inundation level is very close to the observed level. This difference is balanced by modelled inundation showing similar extents and locations adjacent to the observations. An important context for this comparison is that five years of coastal change has occurred since the observations were made and the LiDAR informed model bathymetry was surveyed. Therefore, some accretion of the crest measured in recent years (HBRC, 2020) explains the minor under prediction in some locations. The model also does not resolve how the crest level can be flattened by overtopping surges, which may have occurred during the event. Despite these minor differences in some locations, most of the comparisons show a near exact match between the modelled inundation extent and the observed (Figure Appendix C.2).

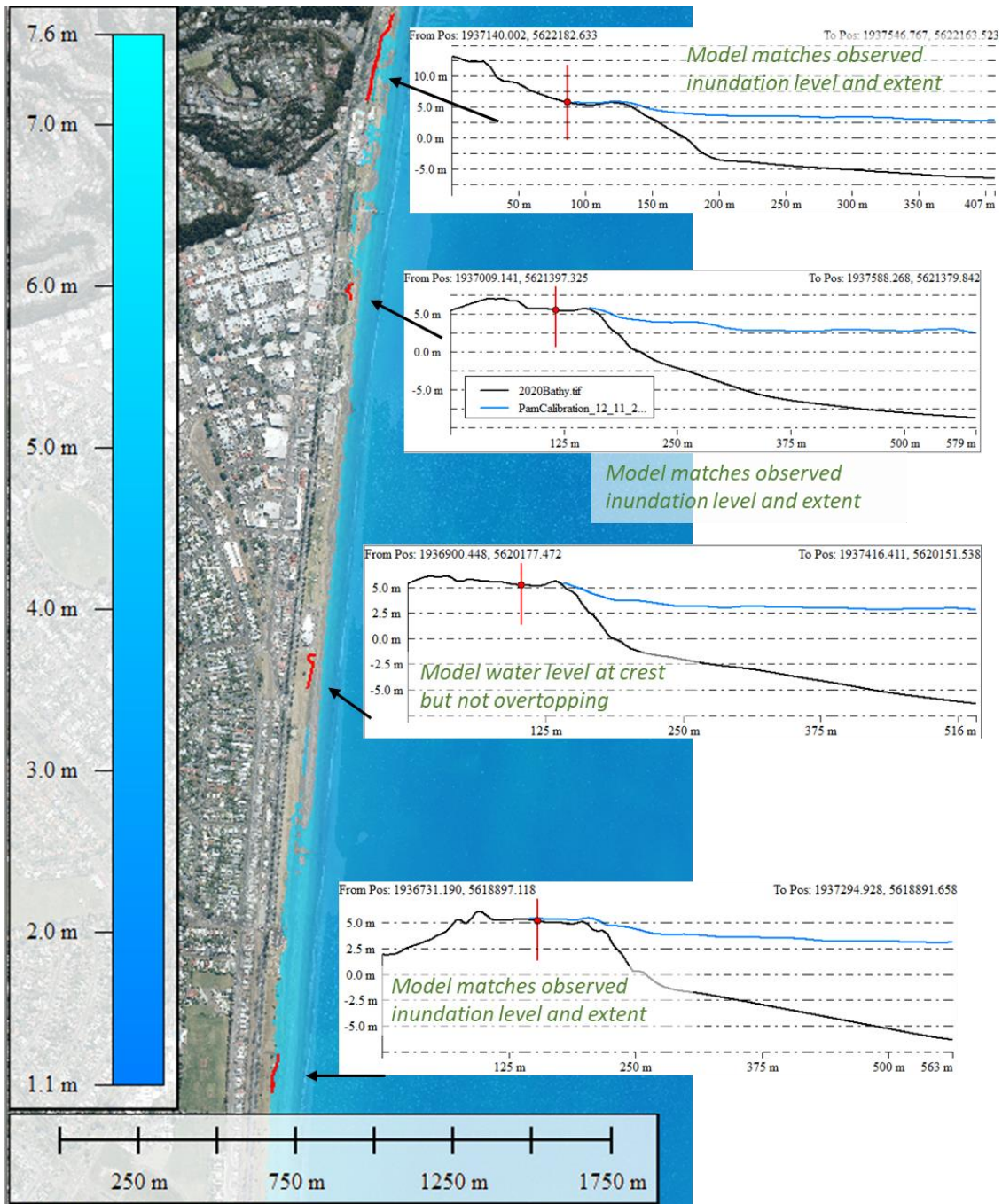


Figure Appendix C.2: Comparison between modelled inundation from TC Pam and observations along Marine Parade. Mapped inundation is in red and the blue shade indicates the modelled inundation extent.

The southern end of Marine Parade shows similar behaviour, with a close match to the observed inundation extent and level (Figure Appendix C.3). Modelled inundation at Awatoto was at the crest level, but showing no overland flow, which under-predicts the observations. Beach profiles at this location have likely adjusted in recent years (since TC Pam) now that shingle extraction operations on the beach have stopped. However, the modelled inundation is still close to the observed level. Modelled inundation at Clive shows waves washing over the gravel barrier crest and ponding in the wetland area that have developed between the gravel spit and the sea exclusion bank. This is consistent with aerial photos of the event, although no mapped line is used to show the observed extent (Figure Appendix C.3).

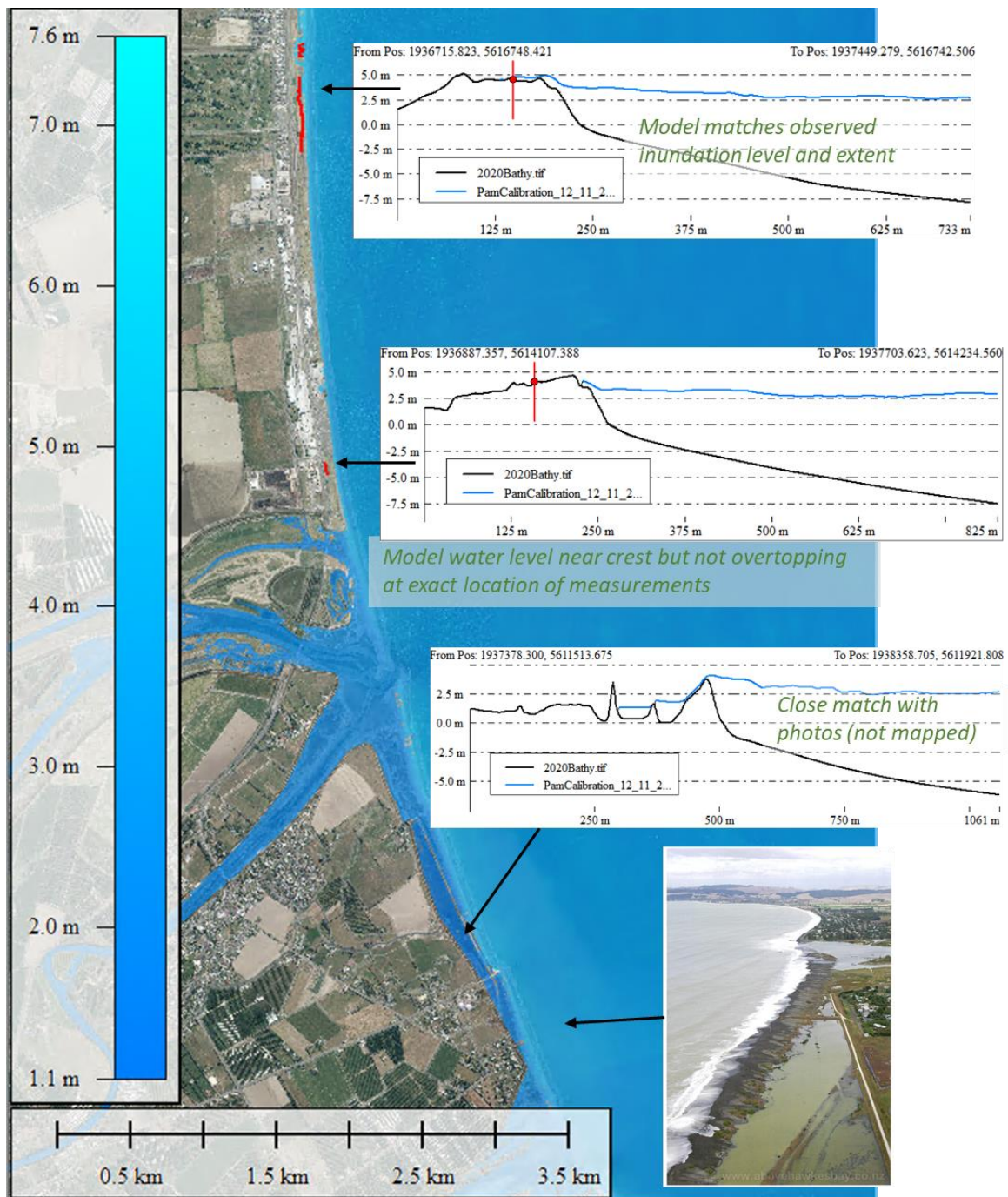


Figure Appendix C.3: Comparison between modelled inundation from TC Pam and observations from southern Marine Parade to Clive. Mapped inundation is in red and the blue shade indicates the modelled inundation extent. Inset photo from Goodier et al., 2015.

The extent of inundation at Haumoana during extreme events are not well mapped, but photos and discussions with the local community indicate that the gravel barrier was overtopped at the northern end, with waves washing into the lagoon and creek, causing some flooding to properties (personal comms Ann Redstone 5 November 2022). This is consistent with modelled inundation extents in XBGPU (Figure Appendix C.4).

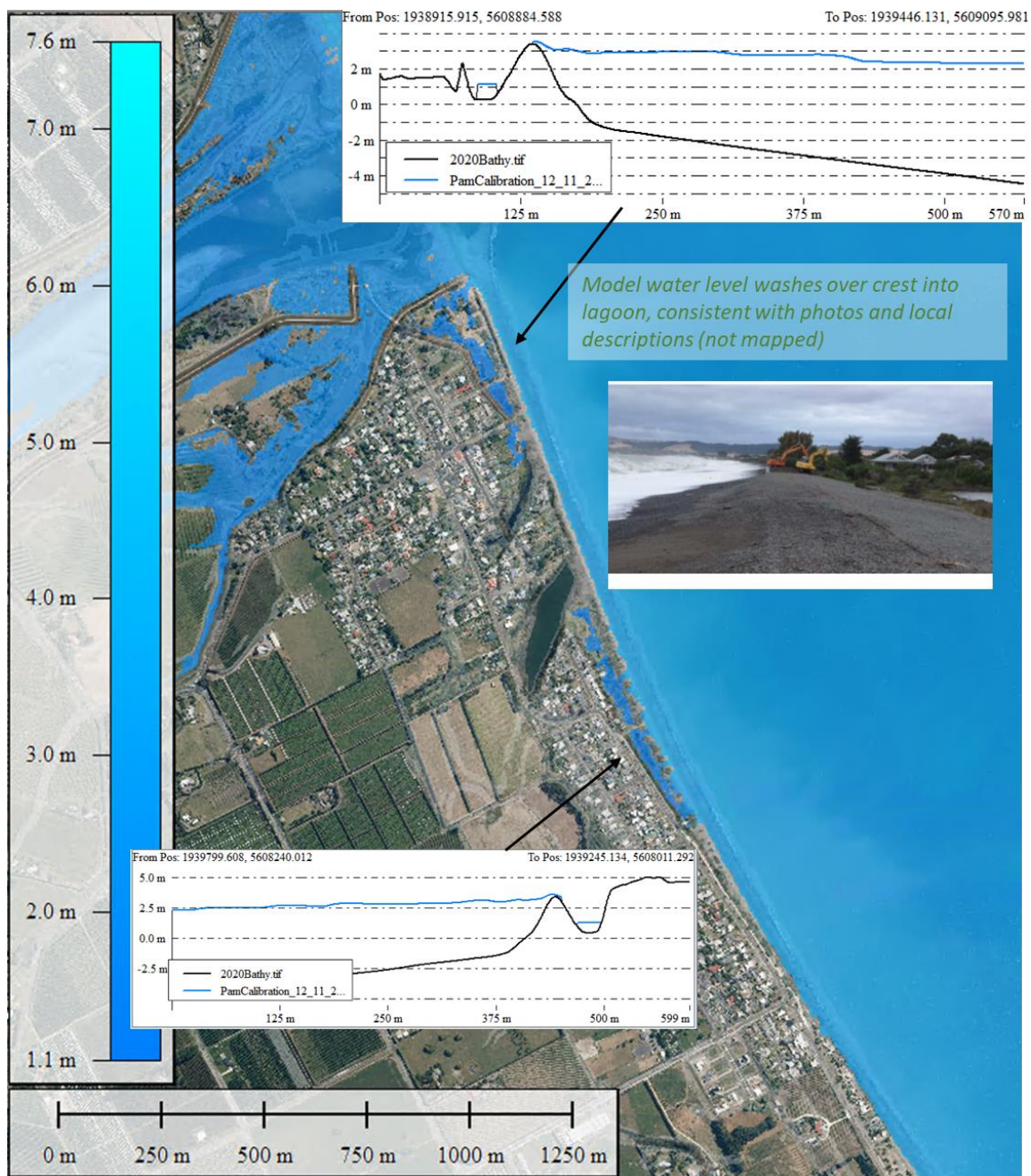


Figure Appendix C.4: Comparison between modelled inundation from TC Pam and observations at Haumana. Blue shade indicates the modelled inundation extent. Inset photo from Goodier et al., 2015.

There was a balance of minor over and under prediction at Te Awanga initially and localised calibration was undertaken to match the observed inundation. The default model tended to overpredict inundation at Te Awanga in initial simulations, with water flooding the campground, across the road and into some properties. TC Pam inundation debris were documented on Wellwood Terrace due to the flow channelling up the creek, but there is no clear record of flooding in private property or in the campground. At first the model behaviour appears to be sensible because the crest level is very low along Te Awanga with a freeboard of only 1 m above the peak tide level during TC Pam. Further investigation indicates two localised features that explain the over-prediction at Te Awanga. First, the wave height reaching the coast that was documented in photos does not look as high as the rest of the coast. This indicates a localised bathymetry feature could be causing some dissipation due to roughness. A ridge is present in the seaward contours extends off Te Awanga, and

a series of reefs are known to exist in the area, including mussel beds (Haggitt and Wade, 2016). Side-scan sonar mapping of the Clive Hard, indicates the areas surrounding Te Awanga is characterised by rock reef (MetOcean, 2011). Additional roughness was added to the nearshore off Te Awanga to represent roughness of a reef feature, resulting in slightly reduced wave energy approaching the coast. A wave friction value of 0.4, and a flow friction of 0.025 was found to give a better fit with the observations, resulting in inundation contained to the lagoon and motor camp. The second reason flooding is potentially over predicted at Te Awanga motor camp is that the 5 m bathymetry resolution does not fully resolve the creek and wooden fence that separates the camp from the beach. Based on discussions with long-time camp residents on site, it appears that waves regularly overtop the beach crest but are absorbed into the creek without causing flooding to the camp. The small-scale complexity of this process is not fully captured in the model and therefore the calibrated model still shows some inundation to the campground during TC Pam.

The calibrated model shows a reasonably close fit with observations at Te Awanga, with waves washing into the lagoon and creek (Figure Appendix C.5). The modelled inundation of the motor camp is due to the localised drainage network not being fully captured at the model resolution. A minor under prediction of inundation north of the camp is likely due to changes in crest level during the event, and in the years since 2015, although the modelled inundation level is consistent with observations (Figure Appendix C.5).

Modelled inundation extents and levels are generally consistent with observations at Clifton, although some high-resolution terrain features and coastal defence implementations are not fully resolved in the model resolution (Figure Appendix C.5). The Clifton Road rock revetment was constructed after TC Pam.

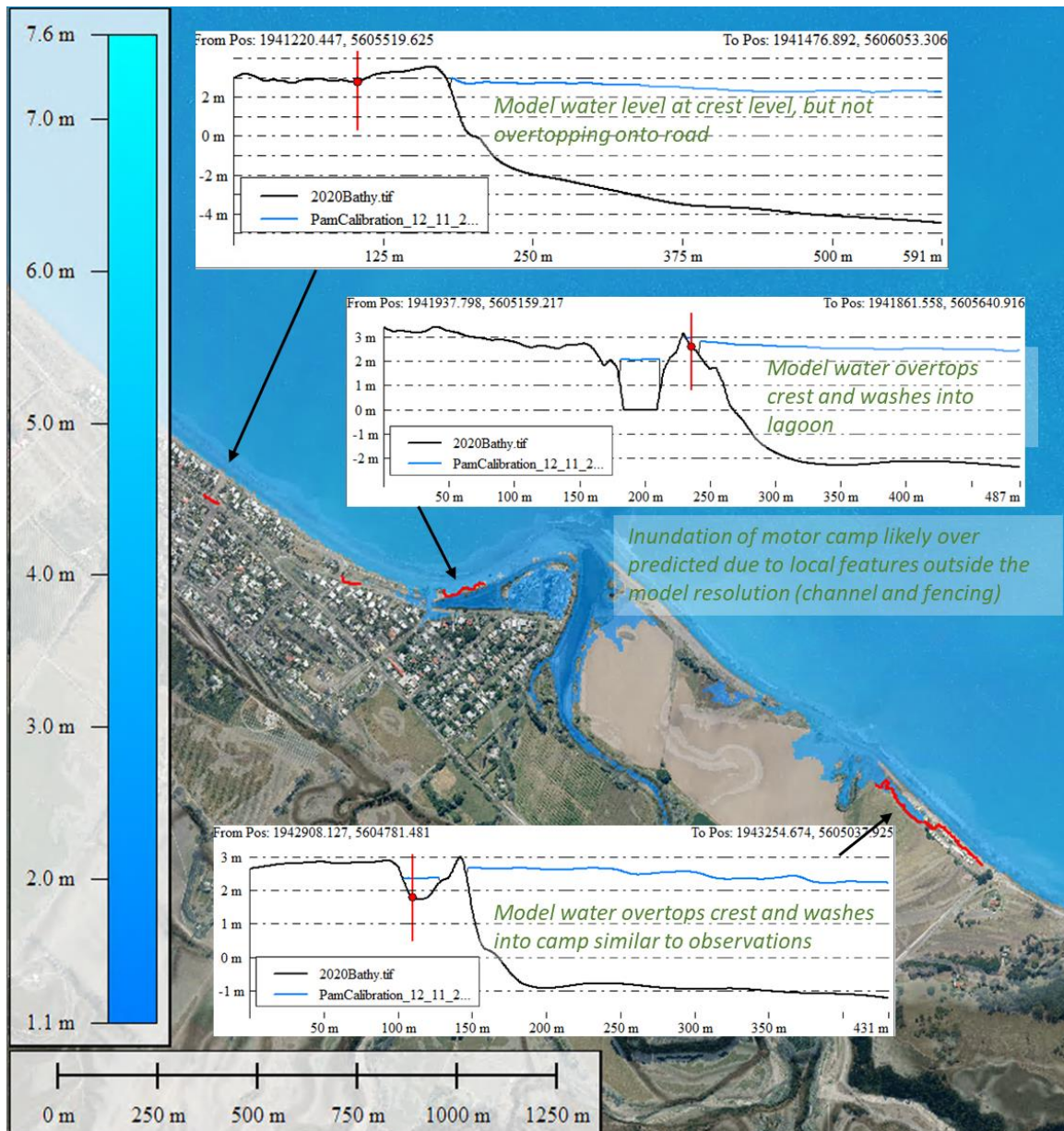


Figure Appendix C.5: Comparison between modelled inundation from TC Pam and observations at Te Awanga to Clifton. Mapped inundation is shown in red and blue shade indicates the modelled inundation extent.

Appendix D Peer Review Letter



28 April 2023

Yvonne Moorcock
Hastings District Council
Private Bag 90002,
Hastings 4156,
New Zealand

Dear Yvonne,

RE: Peer Review of Coastal Inundation Assessment: Tangoio to Clifton.

NIWA was engaged by Hastings District Council to undertake a peer-review of the Coastal Inundation Assessment: Tangoio to Clifton, report delivered by Tonkin+Taylor to Hawke's Bay Regional Council, Hasting District Council, and Napier City Council in 2022. The Tonkin+Taylor Coastal Inundation Assessment: Tangoio to Clifton (2022) (hereafter T+T (2022)) evaluates coastal inundation hazard (extent, level and depth) associated with a 50-year ARI event for present and 2100 climate outlooks in the area between Tangoio to Clifton using a high-resolution process-based model, XBeach_GPU. The outputs will be used to assess building consent applications and building code compliance in this region.

This report provides a peer-review of the numerical modelling method, model input and forcing, model parameters, the resulting inundation maps including any post-processing applied to the model output.

Numerical modelling method

T+T (2022) used the XBeach_GPU model for simulating the 50-year ARI inundation extent. This model is especially suitable for this type of analysis because it simulates the transformation of waves in the surf zone, as well as the generation and amplification of infra-gravity waves that are responsible for most of the coastal inundation in the study area.

Model input and forcing

Coastal inundation simulations are often only as good as the topography and bathymetry used. Bathymetry and topography used in this analysis is a combination of HBRC and LINZ datasets. The bathymetry vertical datum has been verified for each data source. The model was setup with a resolution of 5 m. This allows the model to capture small topographic features while maintaining a realistic model run time. Topography was enhanced where coastal or flood management structures are present to remove any aliasing/smoothing of these features.

The topography is further corrected to account for expected future Vertical Land Movement (VLM) consistent with the 2100 horizon using the recently released NZ

SeaRise project results. The VLM is further discussed in the context of the post-seismic land movement from the 1931 earthquake.

Sea level rise for the 2100 outlook is used in modelling future scenarios consistent with the RCP8.5 recommended by HBRC to T+T for building code assessment.

Other forcings to the numerical model includes storm-tide and waves. Storm-tide is a combination of storm surge and tide and is derived from an up-to-present extreme analysis of the Napier tide gauge. The updated results are consistent with previous assessments. The comparison with other assessments provides a qualitative confidence interval on the analysis performed and confirms that the selected values are adequate for coastal inundation assessment. For these reasons it is reasonable to assume the storm-tide analysis is valid from Tangoio to Clifton.

For simulation of the waves, wave hindcasts are used to estimate extreme waves near the model boundary. Because XBeach_GPU is computationally demanding, the study area was split in five domains and an extreme wave height forcing was calculated for each domain. The T+T analysis correctly identifies that extreme inundation is associated with long period waves and present an extreme analysis of wave heights for long wave periods. These types of extreme events are often associated with an ex-tropical cyclone reaching the east coast of NZ.

The probability of occurrence of extreme wave and storm tide from ex-tropical cyclones reaching a particular region is very complex to evaluate because of their rarity. Hence, combining the extreme storm-tide analysis with wave forcings obtained from an independent extreme analysis of long period waves is likely the most rational methodology to capture the effect of such event in Hawke's Bay; as was presented in the T+T analysis.

Model parameters

XBeach_GPU requires parametrisation of some of the physical processes captured. Values recommended by developers of the model are used for most parameters. A range of values was tested for the wave breaking parameter for which the model is sensitive to. The value of 0.75 was retained because it compares best with ex-TC Pam inundation. This value is within the recommended range and consistent with other studies in NZ.

For flow roughness on land, a map of roughness was constructed based on the land cover map. Similarly, a roughness map for wave dissipation was used to account for the reefs in Hawkes Bay. These methods are consistent with similar studies carried out in NZ.

Model post-processing

Results from each computational domain were combined to produce seamless maps of inundation extent, water elevation and depth. The inundation maps were further post-processed to distinguish between static inundation where land elevation is below the relative mean sea level, and inundation from the wave event. The post-processing methodology required rotating and reprojecting the model results, which does not compromise the results.

Inundation results

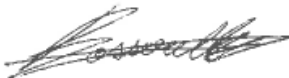
Inundation maps and cross-sections presented by T+T (2022) show how the inundation reaches the backshore and explains the flow pathway and inundation extent. Results are consistent with the presented methodology.

Summary

The T+T (2022) assessment presents an assessment of the coastal inundation hazard designed for use in building consent processes and building code assessment. The method uses modern modelling tools, up-to-date analysis and current best practice for producing the maps. The analysis provides useful maps for assessing coastal inundation hazard for each of the design events assessed. Based on the methodologies and assumptions employed in the study, the modelling results are adequate for the intended information use purposes. As with any assessment, there are uncertainties associated with every step of the analysis which are identified in the report and needs to be considered when using the results.

Yours sincerely

Cyprien Bosserelle
Hydrodynamics Scientist



**Appendix E Comparison of 2020 and 2023 LIDAR in
context of the 2022 Clifton to Tangoio
Coastal inundation assessment**

Memo

Napier City Council (NCC)

To: Hawke's Bay Regional Council (HBRC) **Job No:** 1019664
Hastings District Council (HDC)

Eddie Beetham

From: Richard Reinen-Hamill **Date:** 28 November 2023
Lovleen Acharya-Chowdhury

cc: Heather Bosselmann (NCC)

Subject: Comparison of 2020 and 2023 LIDAR in context of the 2022 Clifton to Tangoio Coastal inundation assessment

1 Introduction

Tonkin & Taylor Ltd (T+T) undertook a coastal inundation assessment for the Clifton to Tangoio area of the Hawke's Bay in 2022. This work was commissioned jointly by Hastings District Council, Napier City Council and Hawke's Bay Regional Council (HB Councils), for the purpose of assessing building consents. The modelling work was completed in 2022 and was informed by terrain information from a regional LiDAR survey from 2021.

Ex-tropical Cyclone Gabrielle impacted New Zealand on 12th – 16th February 2023 and caused significant changes to ground level in the lower catchments of the Esk Valley and the Heretaunga Plains, which are within the extent of area assessed for coastal inundation.

In a Joint Council workshop on 12th May 2023, Napier City Council requested that T+T review the changes in ground level following Cyclone Gabrielle and comment on the implications for the modelled inundation levels and depths.

This memo sets out the differences in ground level, as captured by a LiDAR survey in 2021 (from LINZ) and a post Cyclone Gabrielle LiDAR survey in 2023 (collected by the University of Canterbury and NIWA).

2 Available data

2.1 Pre Gabrielle (used to inform the model)

The following datasets were used to inform the inundation model and provide a reference for changes that have occurred following Cyclone Gabrielle:

- Digital terrain model from a regional LiDAR survey captured from 11th November 2020 to 24th January 2021 (referred to as 2021 LiDAR). Data sourced from LINZ as a gridded terrain model at 1 m resolution in Figure 2.1.

- A combined topographic and bathymetric digital terrain model created by GNS and HBRC for tsunami inundation modelling. This includes nearshore bathymetry and details around river mouths and channels that are not captured in the 2021 LiDAR due to water.
- Aerial imagery surveys by LINZ in 2019 and 2022.

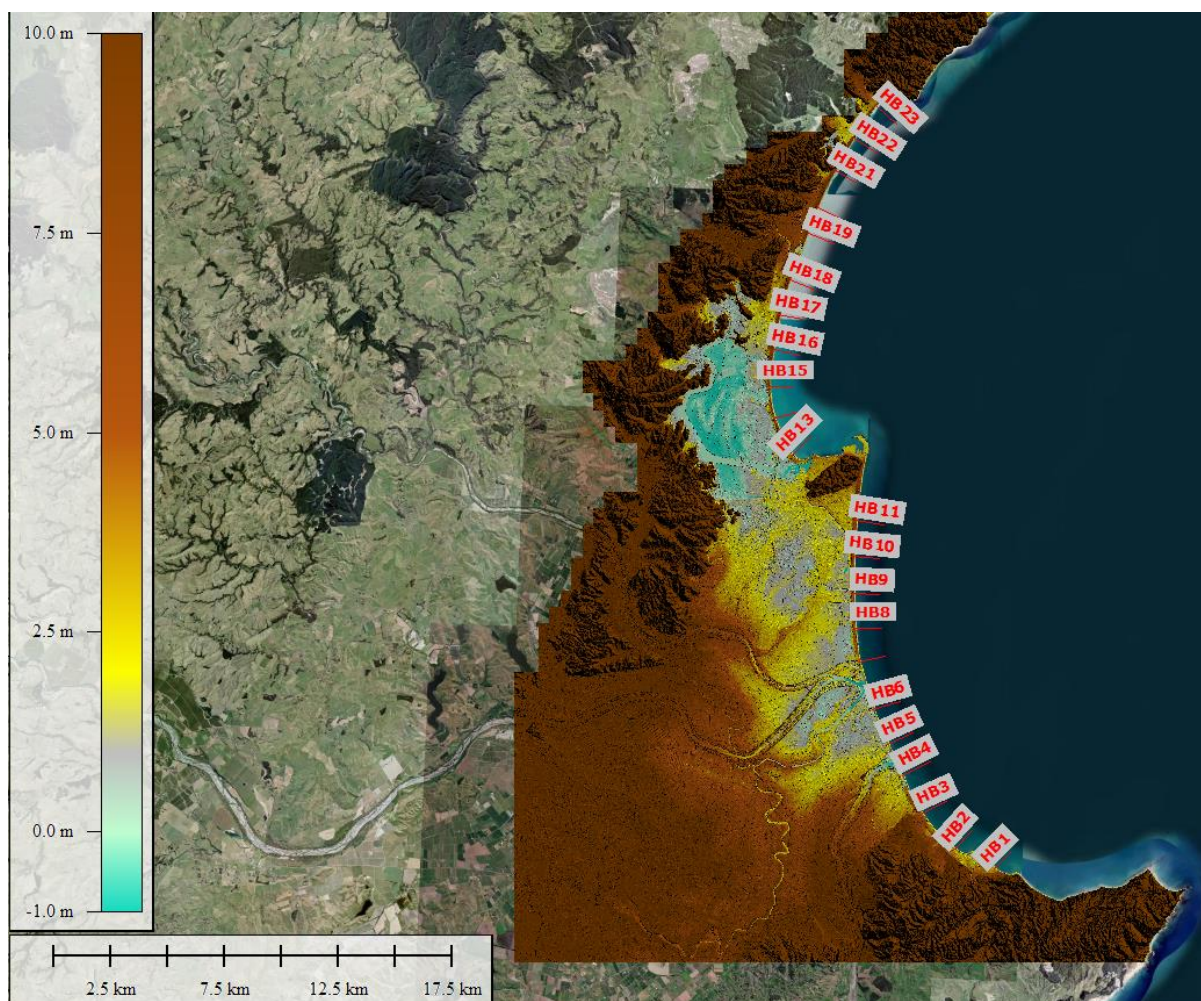


Figure 2.1: LiDAR from 2021 covers the full Hawkes Bay Region. Colour scale clipped to +10 m NZVD.

2.2 Post Gabrielle

The following datasets were collected in response to Cyclone Gabrielle:

- A post event LiDAR survey collected by University of Canterbury and NIWA over 3rd - 5th March 2023. This was provided to T+T by NCC and HBRC in preliminary format. The gridded digital elevation model format at 1 m resolution was used for this comparison in Figure 2.2.
- A post event aerial image survey from LINZ captured on 19th - 20th February 2023. Aerial images provide important context for interpreting LiDAR data from 2023 in areas influence by silt deposition, ponding water, bank erosion, and driftwood debris.

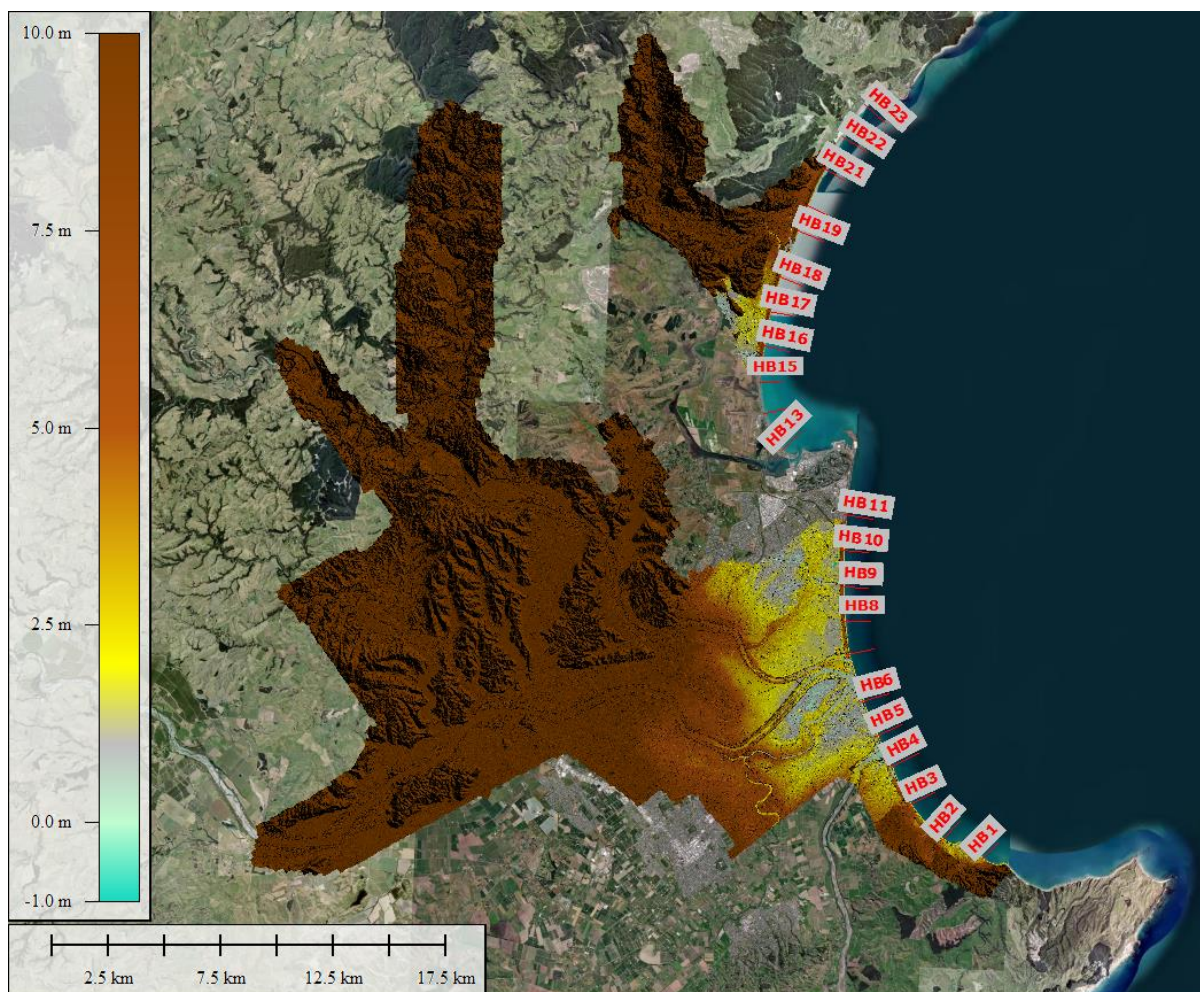


Figure 2.2: LiDAR from 2023 covers specific catchments at the Esk Valley and Heretaunga Plains. Colour scale clipped to +10 m NZVD.

3 Limitations

We understand that the gridded data from 2023 is still being processed and is provisional. To understand the limitations of comparing the 2023 and 2021 LiDAR data, a comparison was made in urban areas where no real change from earth surface processes was expected. Most of the coast was reasonably consistent, except between Te Awa and Awatoto, where up to 0.2 m difference in elevation was identified on a carpark area (Figure 3.1). This elevation difference of 0.2 m is used as a reference for considering the implication of changes to areas mobile terrain on the gravel beach crest.

A summary of limitations that were considered when interpreting the significance of differences in terrain level between 2021 and 2023 include:

- Potential offset error of up to 0.20 m near Awatoto.
- Dynamic change around beaches and river mouths is ephemeral when considered over decadal timescales considered in the inundation model.
- Ponding water may influence elevation levels in 2023 dataset. It is unknown how this has influenced LiDAR levels showing a ~ 0.6 m increase in ground level inland of Awatoto.
- LiDAR does not show terrain details under water, so some areas in river channels and river mouths cannot be properly compared.

- Drift-wood debris in 2023 complicates detection of morphological change on upper beach.
- Object removal in 2023 DEM is still provisional and shows some non-ground features in the terrain model.
- Recovery work on stop banks and silt laden land may alter terrain since the 2023 LiDAR survey.
- If silt deposits are un-removed, dynamic settlement of silt layers may still alter land in near future.

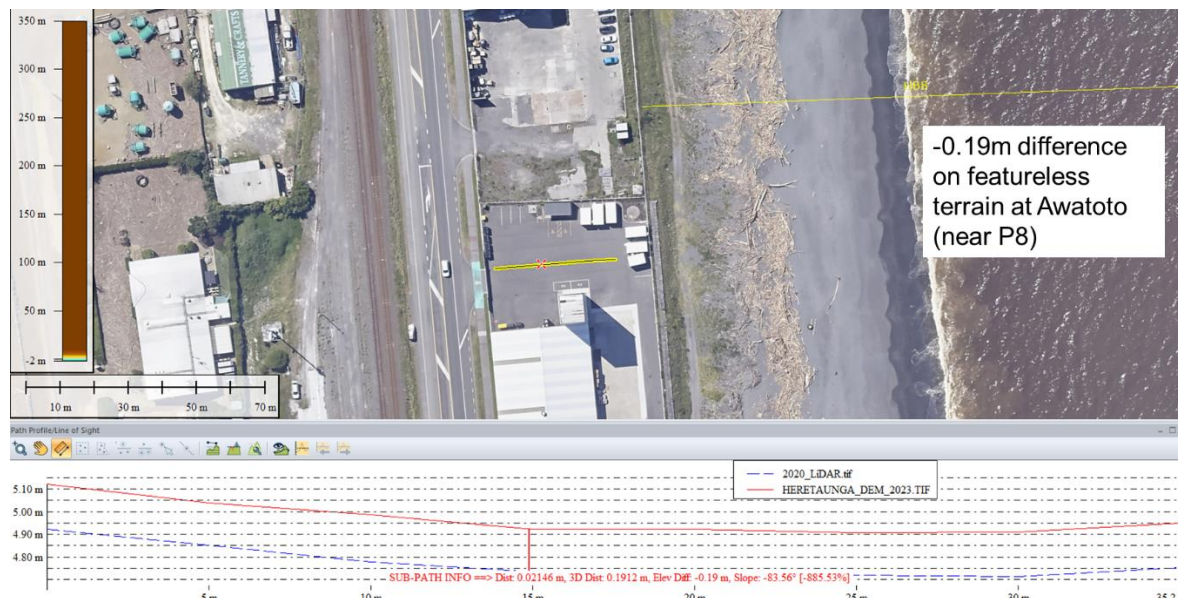


Figure 3.1: Example of the difference (error) between 2021 and 2023 gridded LiDAR datasets at an urban carpark in Awatoto.

4 Comparison of ground levels in the lower Esk Valley

4.1 Overview

A difference plot (2023 minus 2021) for the full extent of the 2023 Esk survey is presented in Figure 4.1, with a close up of the Esk River mouth in Figure 4.1. This figure shows the large area of silt deposition on the lower Esk Valley flood plain in blue. The red areas indicate erosion and are mainly where the coastal berm across the river mouth was eroded, or where the riverbank has eroded near the mouth. Some erosion and lowering of the dynamic gravel beach face is also evident.

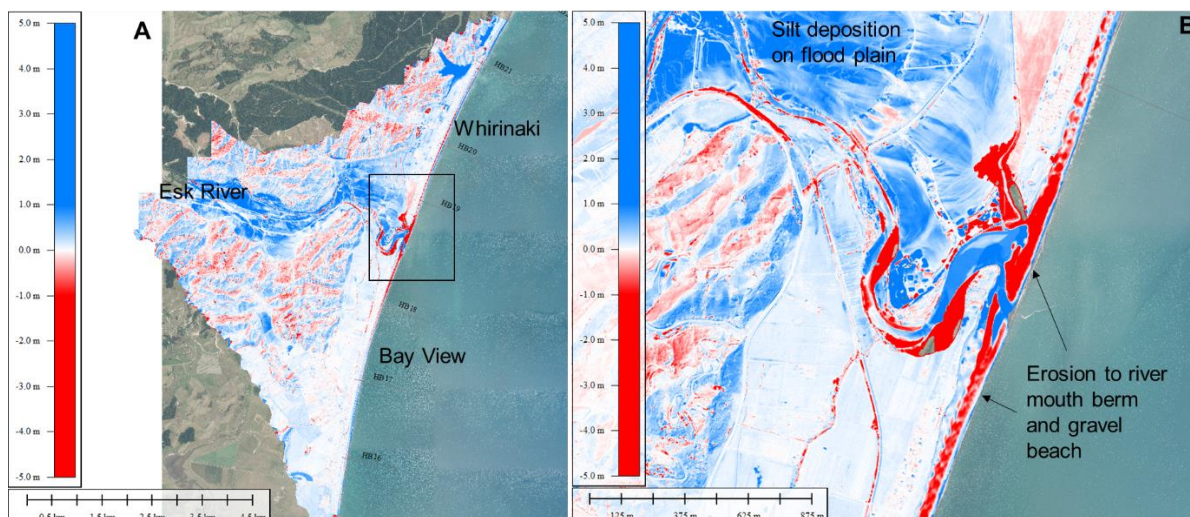


Figure 4.1: Difference plot showing the change in terrain level (2023 minus 2021) with erosion in red and accretion in blue. Colour scale truncated at ± 5 m.

The sections below summarise the ground level changes for different coastal communities covered in the Esk Valley LiDAR comparison. This was informed by reviewing cross sections of the terrain profile and the modelled inundation levels at each of the HBRC beach profile locations. These profile figures are presented in Appendix A.

4.2 Whirinaki

- Changes to ground level in Whirinaki were significant in the lower reach of the Esk Valley, with silt deposition on flood plains and erosion of riverbanks.
- Erosion to the Whirinaki Drain was considerable, with a sink hole forming.
- Some erosion occurred to the gravel beach along North Shore Road, with the upper beach moving back by 5 m at profile HB19.
- The carpark at the south end of North Shore Road has new rock protection at the coastal edge (installed post Cyclone Gabrielle), because overland flow during the storm (from land to sea) caused scour erosion.
- The coastal crest level along Whirinaki has not changed and no land lowering was identified (Appendix A HB profiles 19 – 21).
- The inundation model did not identify overtopping at Whirinaki, apart from a small area at the South of North Shore Road where the rock protection is now placed.
- It is unlikely that the changes following Cyclone Gabrielle would influence the modelled inundation levels or depths.

4.3 Bay View

- The Bay View profiles covered in the 2023 LiDAR show no functional change to the coastal crest level (Appendix A profiles HB16 - HB18).
- It is unlikely that the changes following Cyclone Gabrielle would influence the modelled inundation levels.

5 Comparison of ground levels in the lower Heretaunga Plains

5.1 Overview

The change in ground level in the Heretaunga Plains comparison is presented in Figure 5.1. This shows areas in red on the inland hills where land slides occurred. Areas in blue between the Ngaruroro and Tutaekuri show silt deposition. Some erosion or riverbanks and stop banks is indicated in red. Silt deposition near Te Awa and Awatoto is identified in blue. Some erosion to the beach face and river mouth gravel banks is identified in red. Gravel berms near river mouth areas are known to be dynamic and are likely to recover following the event.

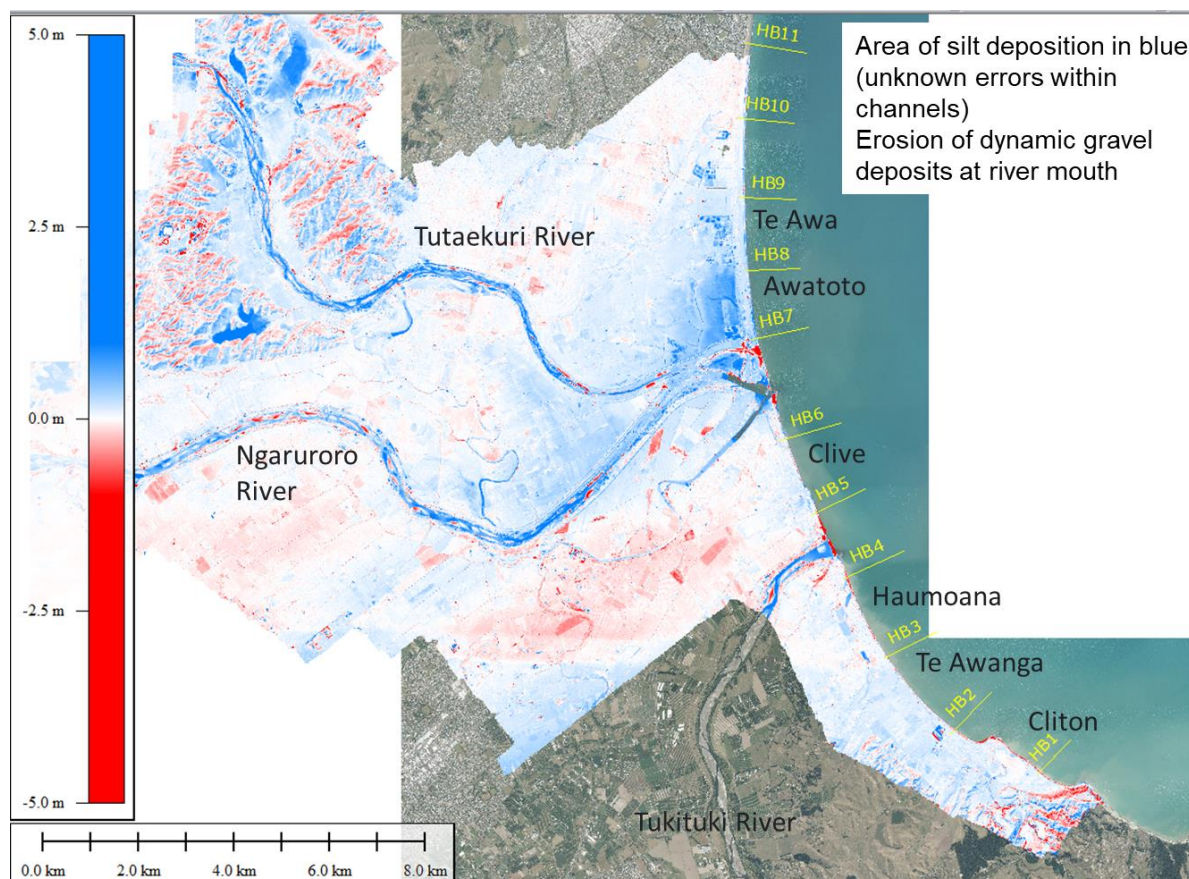


Figure 5.1: Difference plot showing the change in terrain level 2023 minus 2021 with erosion in red and accretion in blue. Colour scale clipped at ± 5 m.

The sections below summarise the ground level changes for different coastal communities covered in the Heretaunga Plains LiDAR comparison. This was informed by reviewing cross sections of the terrain profiles and the modelled inundation levels at each of the HBRC beach profile locations. These profile figures are presented in Appendix A.

5.2 Te Awa

- Overtopping of the gravel barrier is modelled for 2100 in the inundation assessment, causing some ponding on the lower terrain hinterland.
- The beach crest level from the 2023 LiDAR survey is generally consistent with 2021 LiDAR at HB10 and HB9 profiles (Appendix A profiles HB9 – HB10).
- Terrain levels landward of the gravel barrier are generally consistent between the 2021 and 2023 surveys.

- Some minor differences in the terrain level are likely influenced by driftwood debris, ponding water, and geoprocessing processing limitations.
- It is unlikely that changes to the terrain post Cyclone Gabrielle would influence the inundation level or depth.

5.3 Awatoto

- Overtopping of the gravel barrier is modelled for 2100 in the inundation assessment, causing some ponding on the lower terrain landward of the coastal barrier in Figure 5.2.
- The beach crest level from the 2023 LiDAR survey is generally consistent with 2021 LiDAR at HB8 and HB7 profiles but the levels may be offset slightly as indicated in Figure 3.1.
- Silt deposition is evident on the lower terrain landward of the gravel barrier. The 2023 terrain is up to 0.6 m above the 2021 terrain level in some areas of Awatoto due to silt deposition.
- Some minor differences in the terrain level at the barrier crest are likely influenced by driftwood debris, ponding water, gravel movement, and geoprocessing processing limitations.
- It is unlikely that changes to the terrain post Gabrielle would influence the amount of wave overtopping inundation for Awatoto based on minor changes to the crest level.
- If silt deposits remain, the inundation water level would be sitting on a higher base and the modelled inundation level from the model could be underpredicted. Therefore, modelled inundation depths relative to the new ground level would be more representative in this location.
- We understand that silt is being removed for much of this area due to contamination.

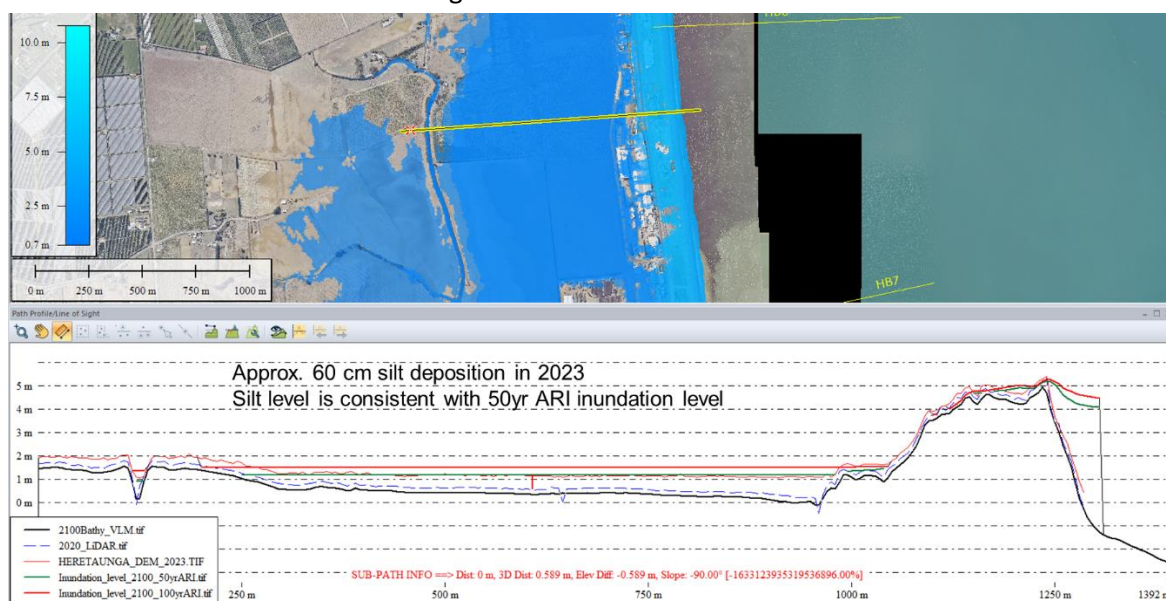


Figure 5.2: Profile at Awatoto showing inundation levels for 2100 with reference to 2021 and 2023 LiDAR. The black profile is the 2021 terrain adjusted for VLM to 2100.

5.4 Clive

- Some overtopping of stop banks and sea exclusion banks is modelled for Clive, resulting in inundation to the lower terrain land.
- The change in terrain post Cyclone Gabrielle identified some erosion of the dynamic gravel berm in areas seaward of the sea exclusion banks (Appendix A profiles HB6 and HB5).
- Terrain at the stop banks and lower land appears consistent between 2021 and 2023.
- Changes are unlikely to influence the modelled inundation levels or depths.

5.5 Haumoana

- Overtopping modelled in the inundation assessment for much of Haumoana (Appendix A profiles HB4 and HB3 profiles).
- The seaward gravel berm was overtopped and beached in areas close to the Tukituki River mouth.
- The 2023 LiDAR surveys shows some berm lowering in this location.
- Beach levels south of the river mouth show some erosion and some accretion (lower and upper beach) between 2021 and 2023 which is expected on dynamic gravel systems.
- No significant changes to crest or terrain level identified.
- It is unlikely that changes would influence modelled inundation levels or depths.

5.6 Te Awanga

- Coastal inundation is modelled for much of Te Awanga for 2100 (Appendix A, profile HB2).
- The 2023 terrain shows some erosion on the upper beach (5 m horizontal) and an overwash deposit on the crest. This is likely to be a dynamic and temporary feature.
- Changes to terrain are unlikely to influence the modelled inundation levels or depths.

5.7 Clifton

- Coastal inundation is modelled for much of Clifton for 2100 (Appendix A, HB1 profile).
- The 2023 terrain shows some erosion on the upper beach and lowering of the crest that is likely to be spatially and temporally dynamic.
- Changes to terrain are unlikely to influence the modelled inundation levels or depths.

6 Conclusion

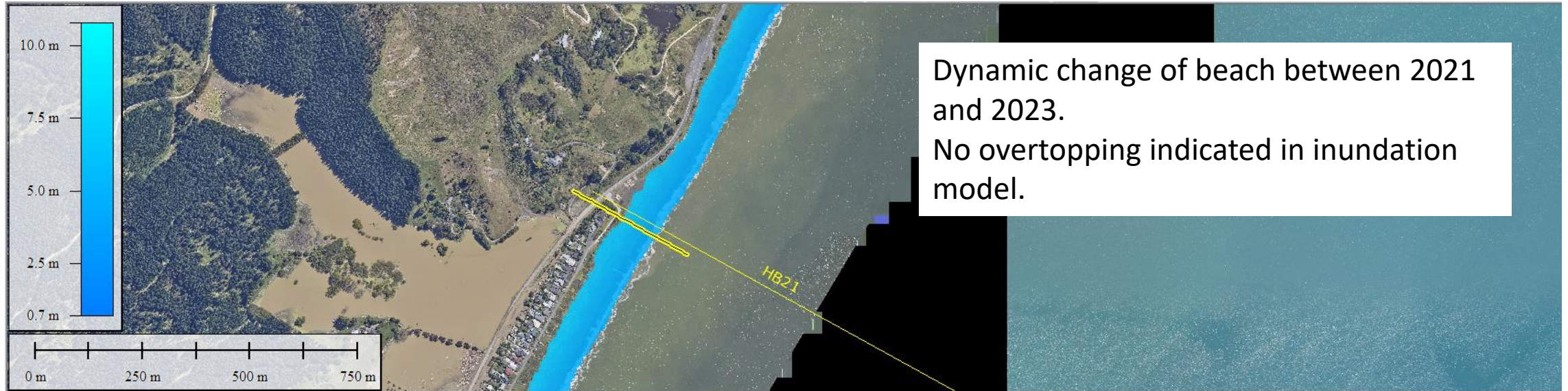
The changes in terrain level between 2021 and 2023 were significant at some lower reach flood plains, river channels and river mouth locations. However, these are unlikely to significantly influence the modelled coastal inundation levels and depth for 2100 based on work undertaken in 2022. One area of potential influence on inundation level is Awatoto, where ground levels in an area of modelled coastal inundation have increased by 0.6 m due to silt deposition. If this higher terrain level is maintained, it is recommended that modelled inundation depth above the new terrain height is used in this location. If silt is removed to the original terrain level, the inundation level should be reasonable.

We do not recommend any additional coastal inundation modelling as a result of changes to terrain level following Cyclone Gabrielle.

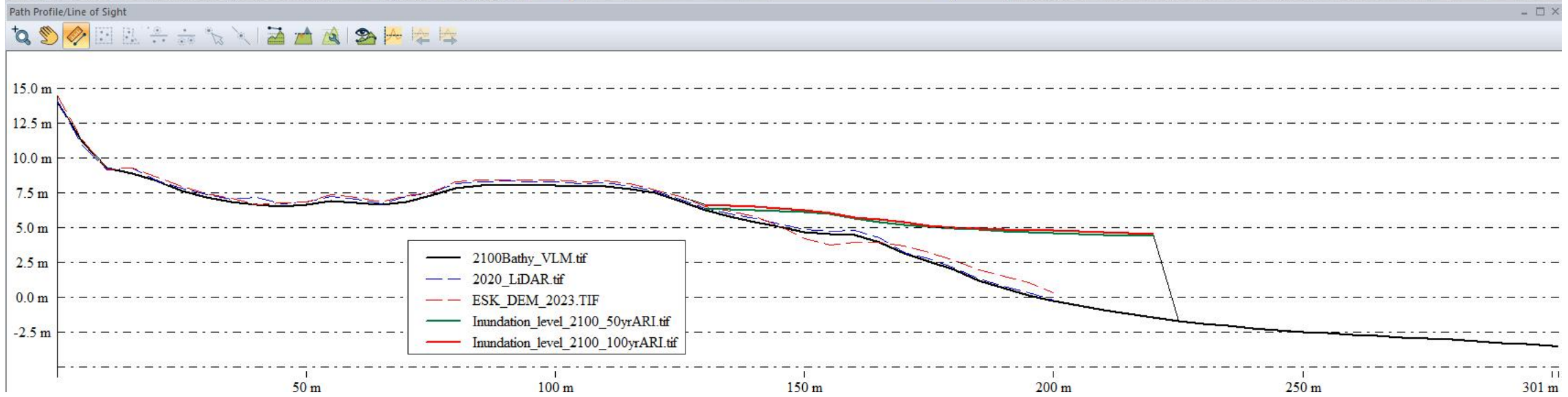
Appendix A Comparison profiles

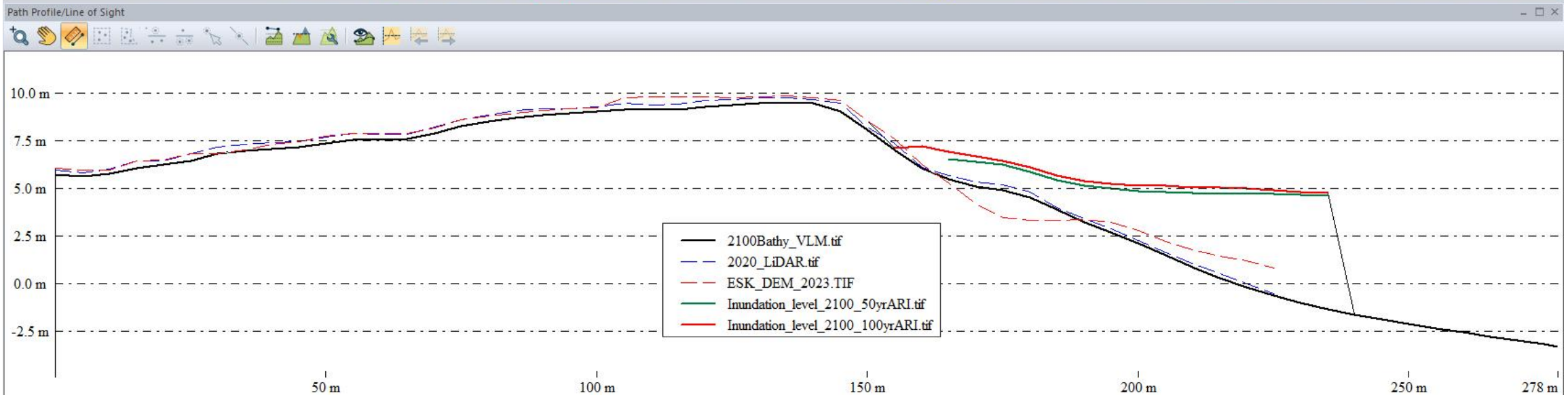
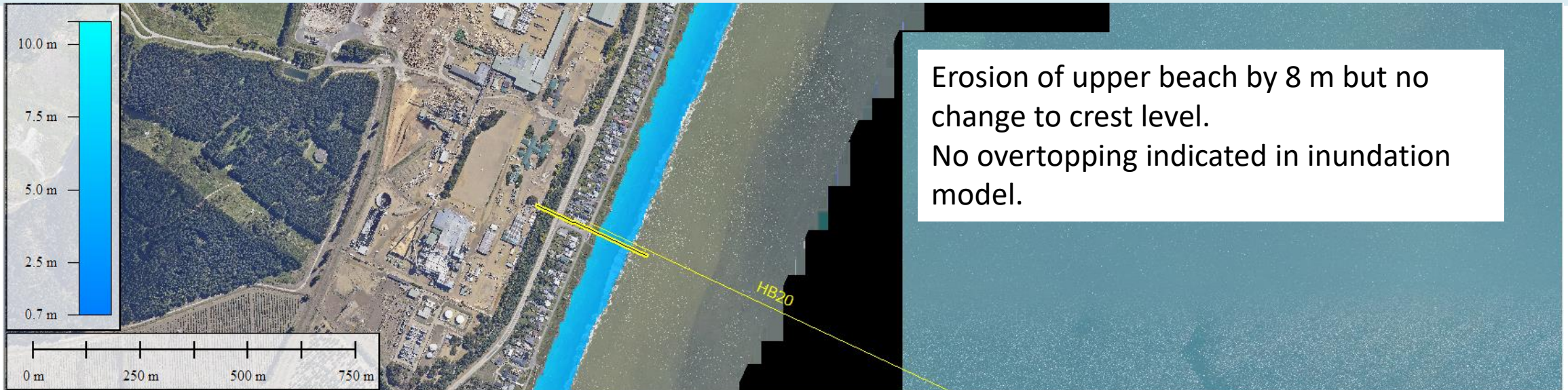
The following pages show profile comparisons for each of the HB beach profile locations, with annotations commenting on the change in terrain (2021 – 2023) and the potential influence on modelled inundation.

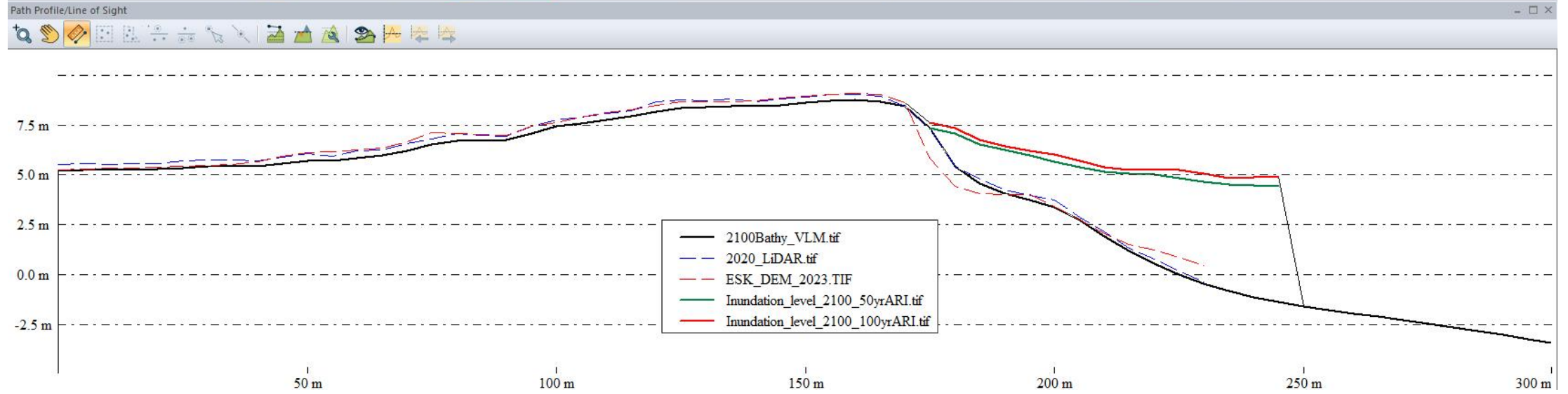
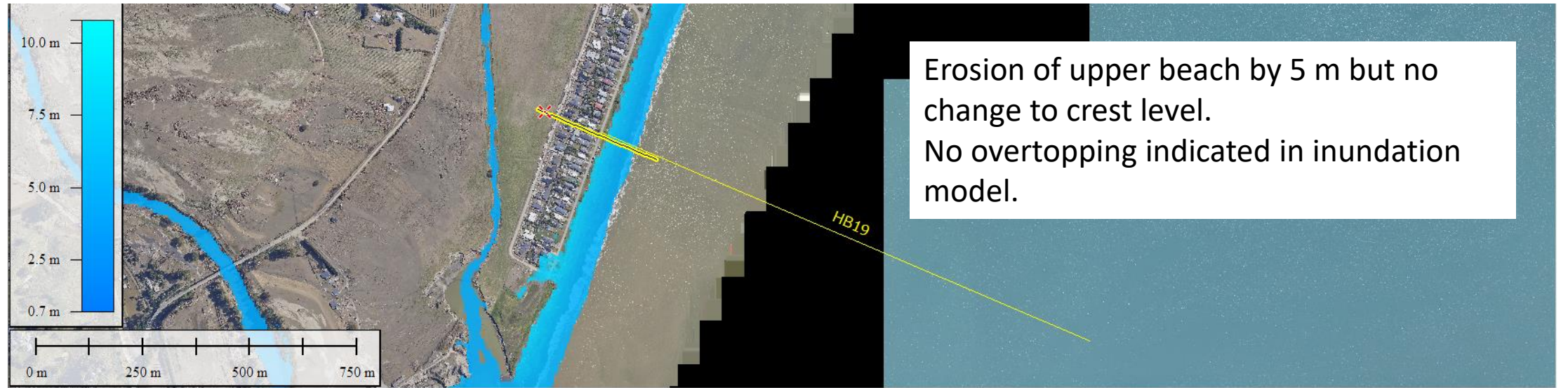
- Bold red and green lines show the maximum inundation water level for 2100.
- Light red and blue lines show the terrain level from 2023 and 2021 surveys respectively.
- The bold black line shows the topo-bathymetry profile used in the inundation model for 2100, which is offset to account for vertical land movement.



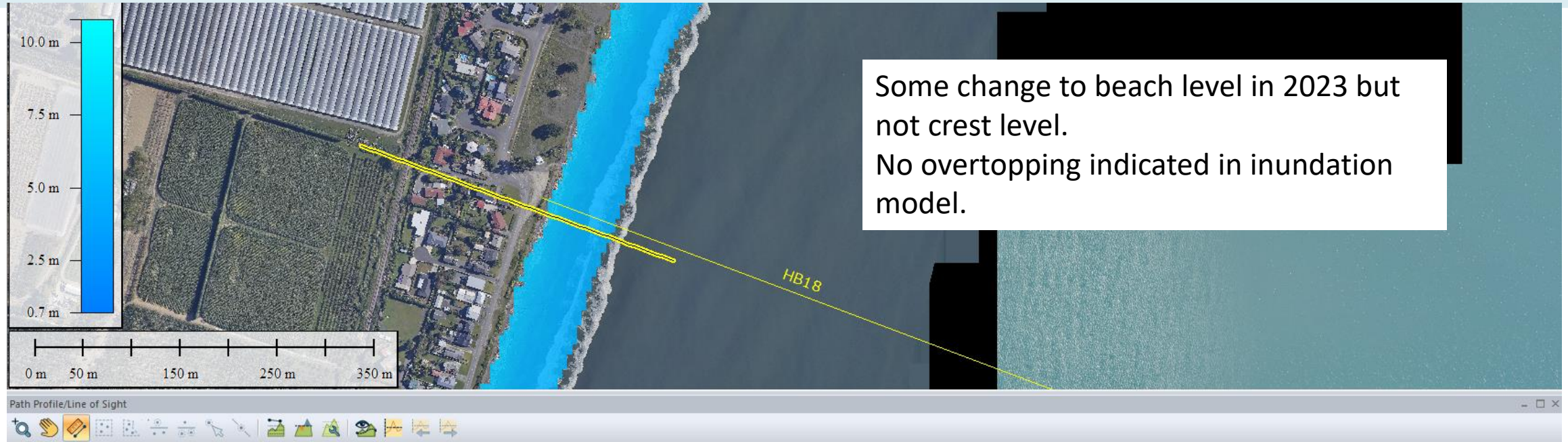
Dynamic change of beach between 2021 and 2023.
No overtopping indicated in inundation model.



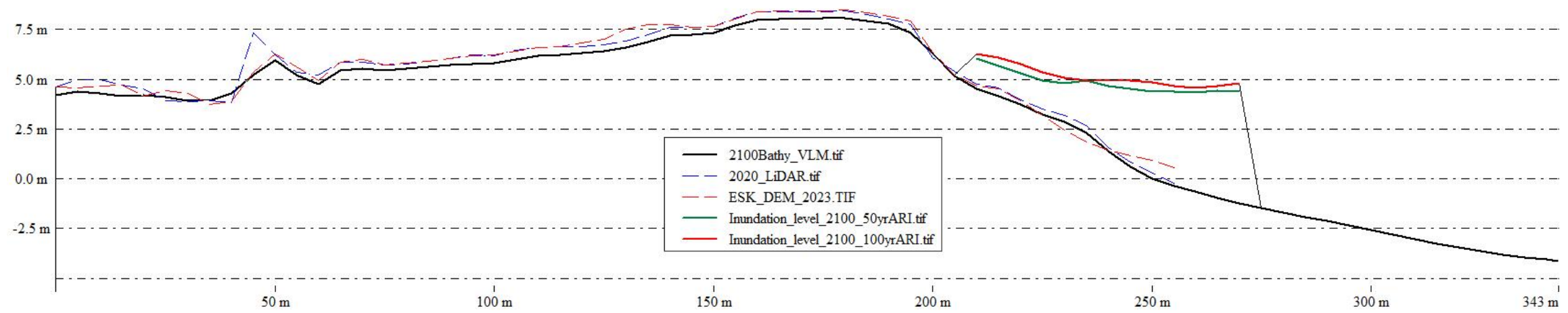




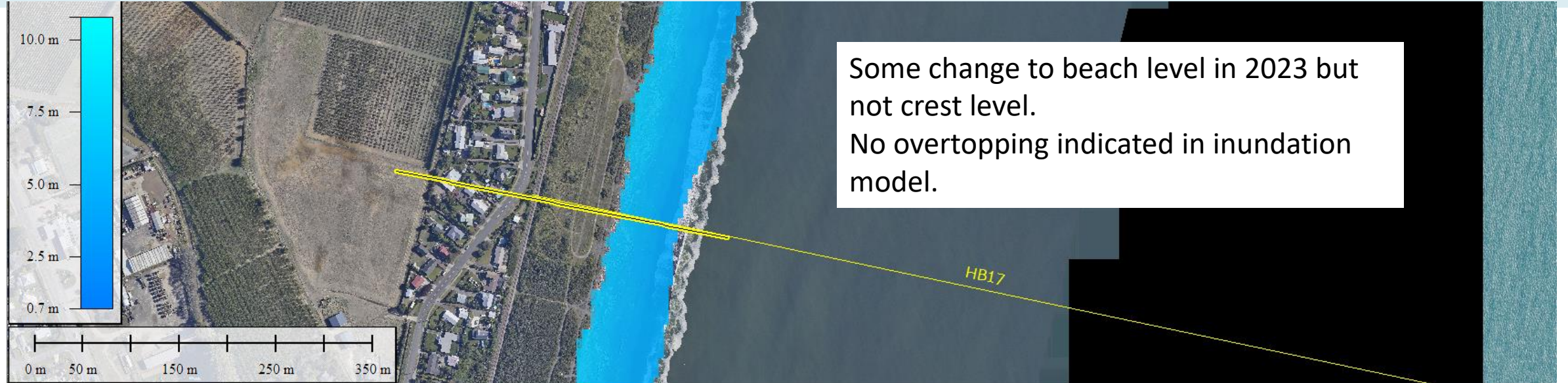
HB18: Bay View



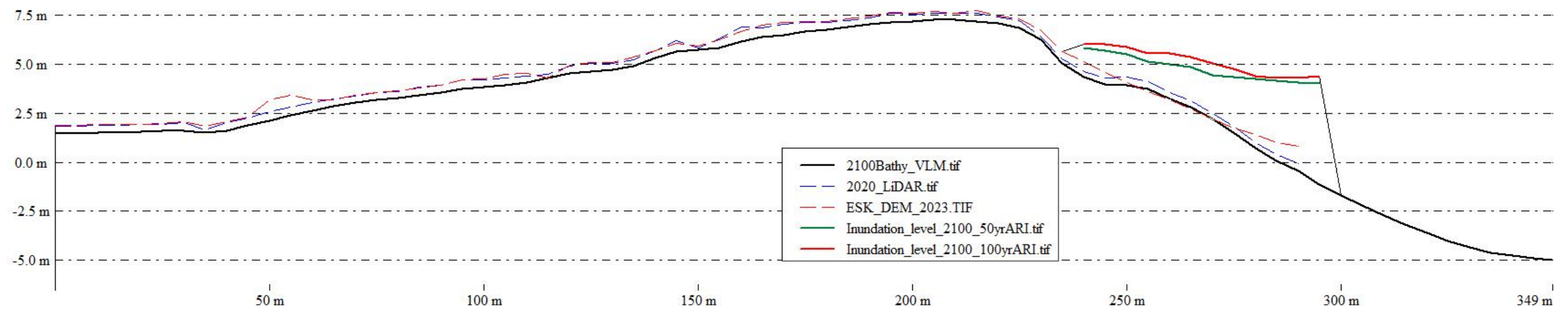
Some change to beach level in 2023 but not crest level.
No overtopping indicated in inundation model.



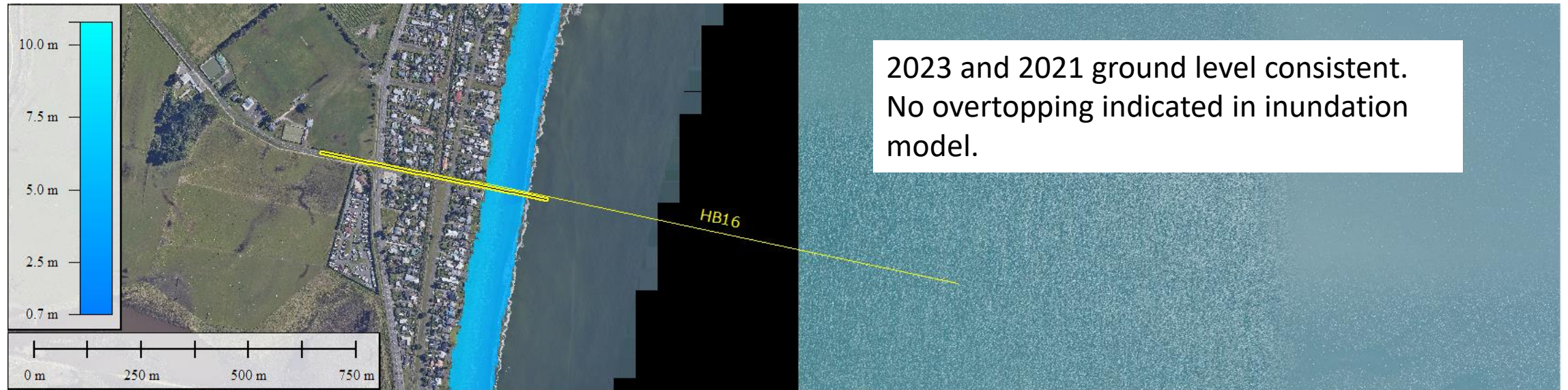
HB17: Bay View



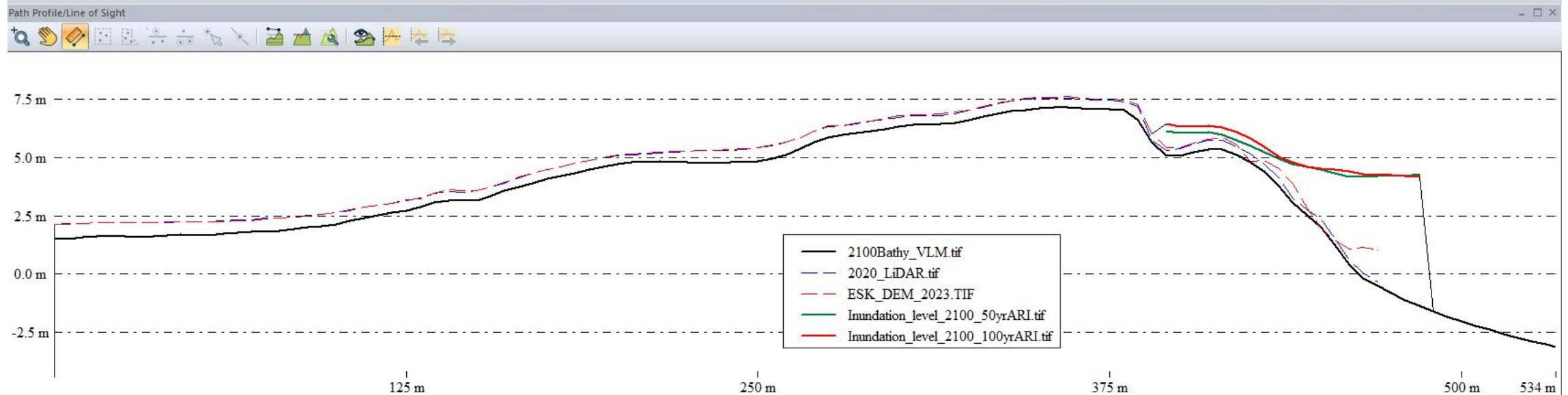
Some change to beach level in 2023 but not crest level.
No overtopping indicated in inundation model.

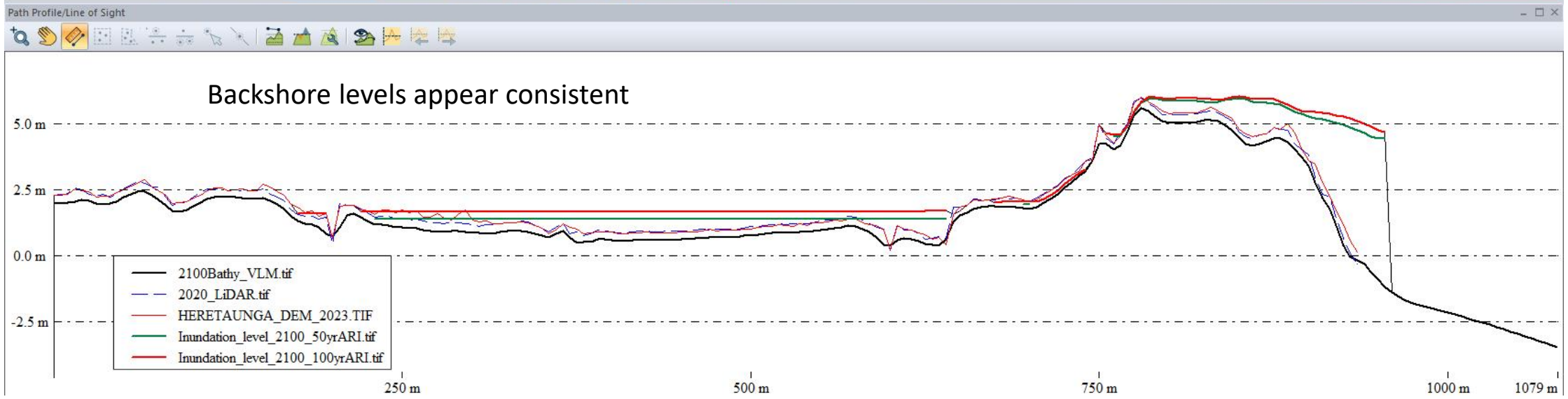
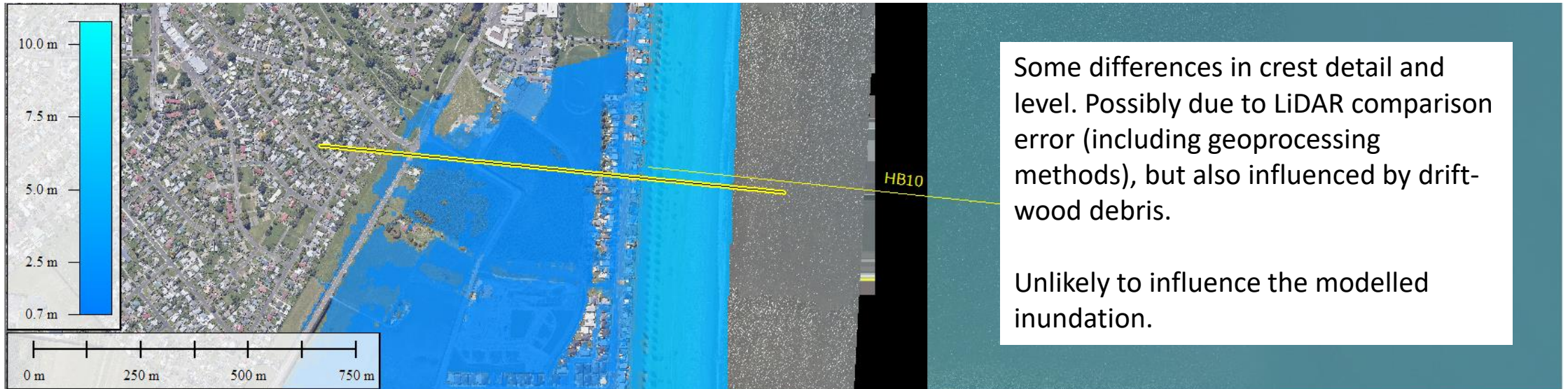


HB16: Bay View



2023 and 2021 ground level consistent.
No overtopping indicated in inundation model.



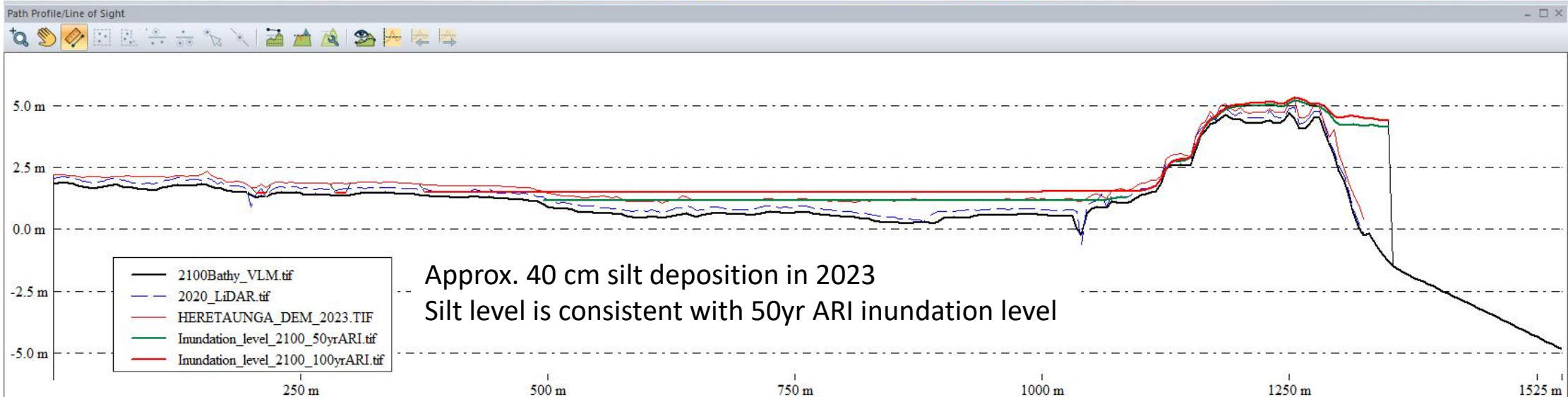
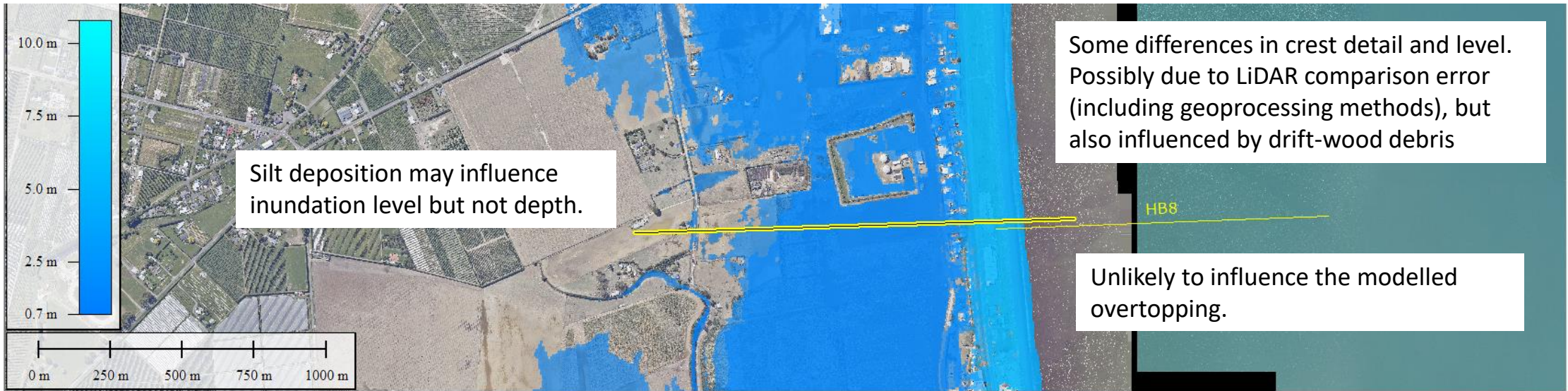




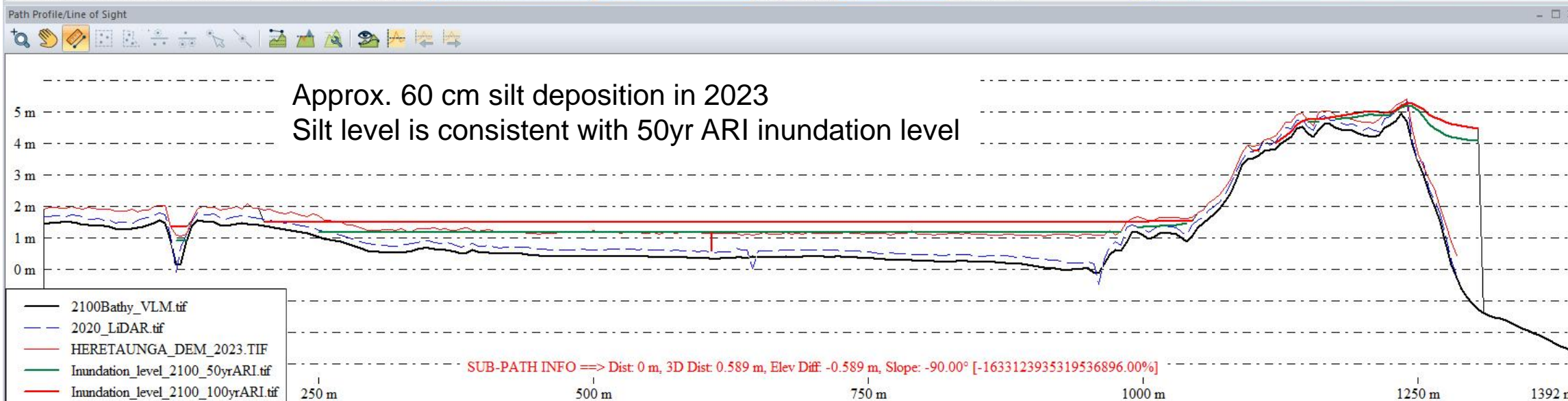
Some differences in crest detail and level. Possibly due to LiDAR comparison error (including geoprocessing methods), but also influenced by drift-wood debris.

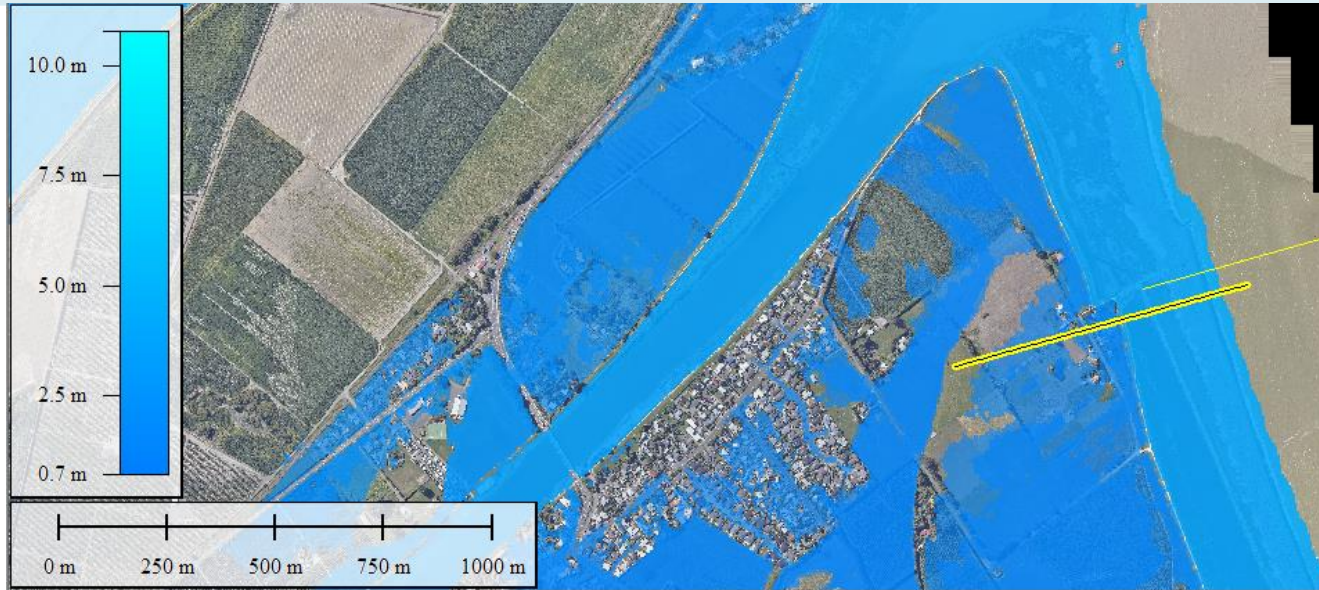
Unlikely to influence the modelled inundation.





HB7a: Awatoto

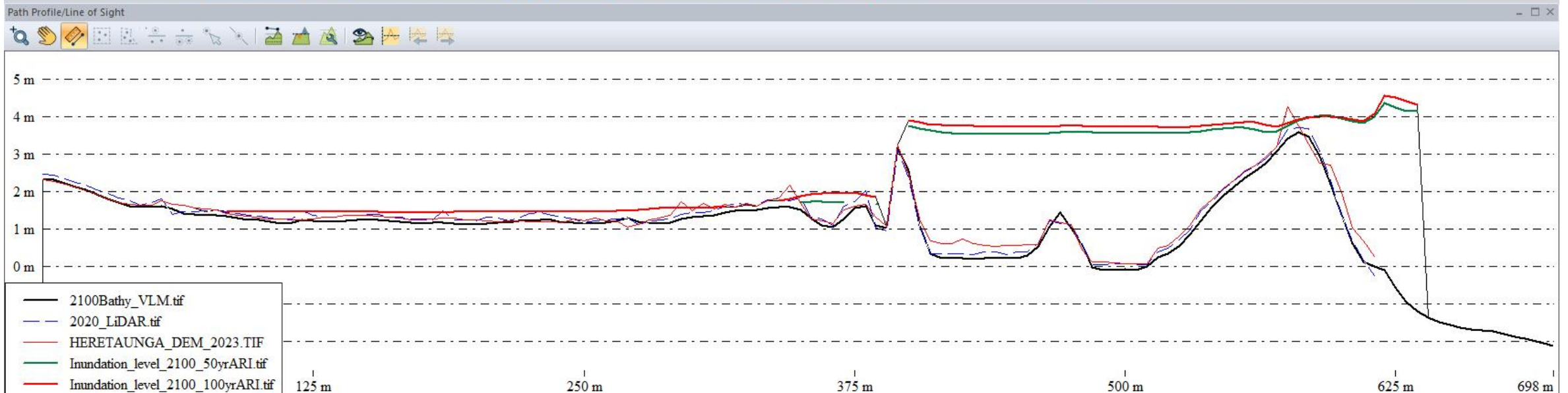


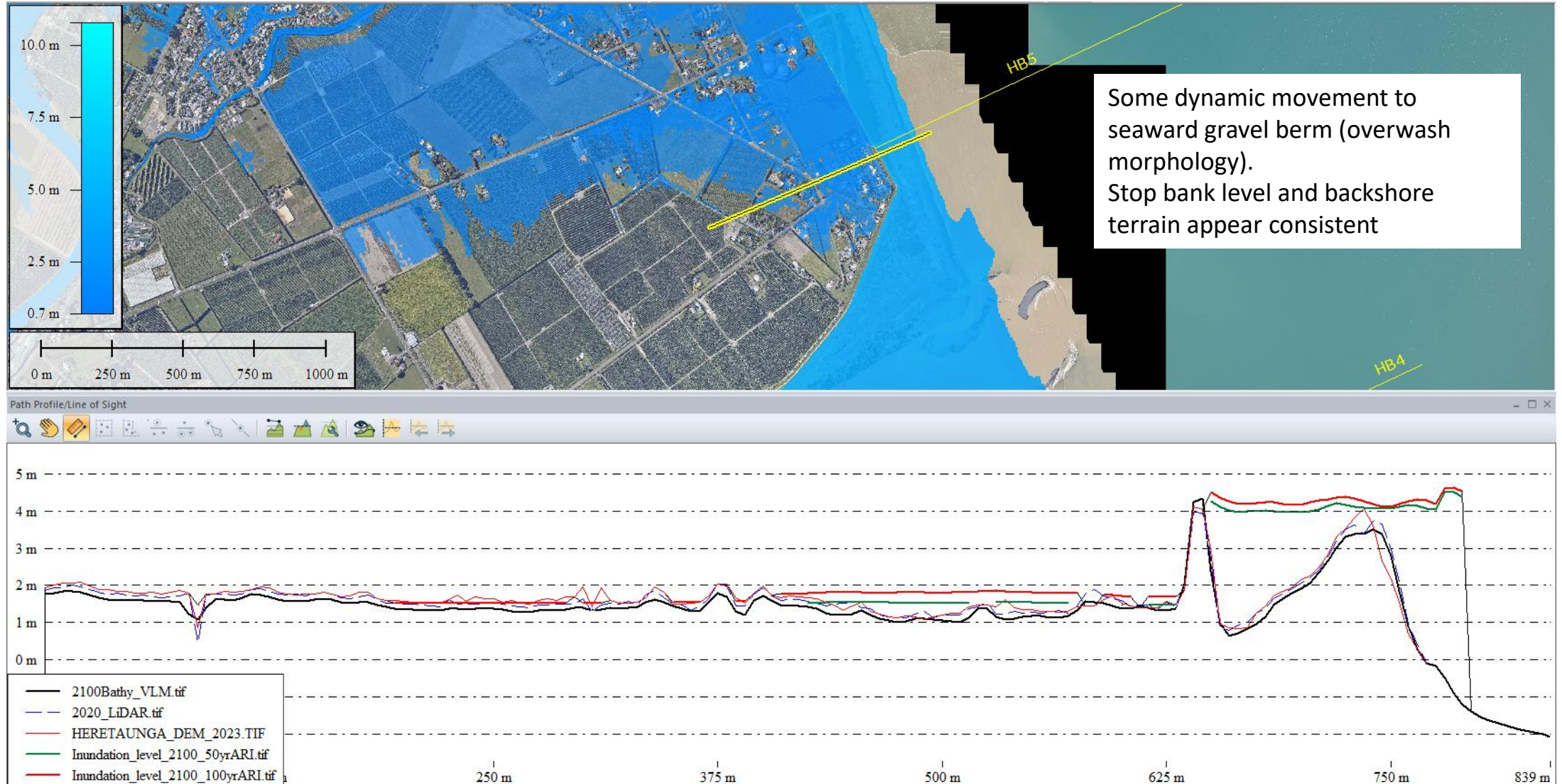


Subtle changes at crest likely due to overwash dynamics or objects (e.g. drift debris) on the seaward gravel berm.

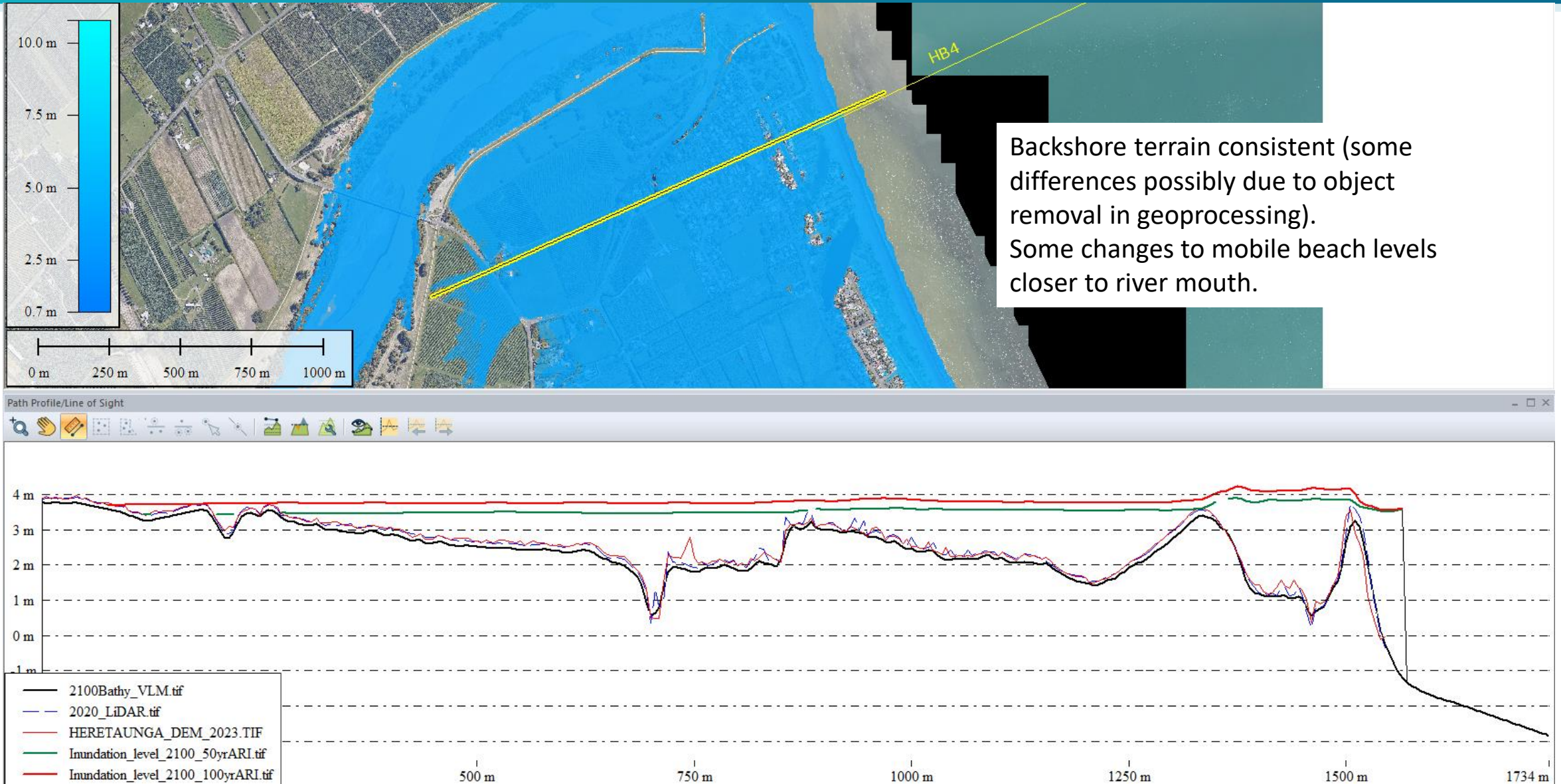
Stop banks and backshore terrain appear consistent.

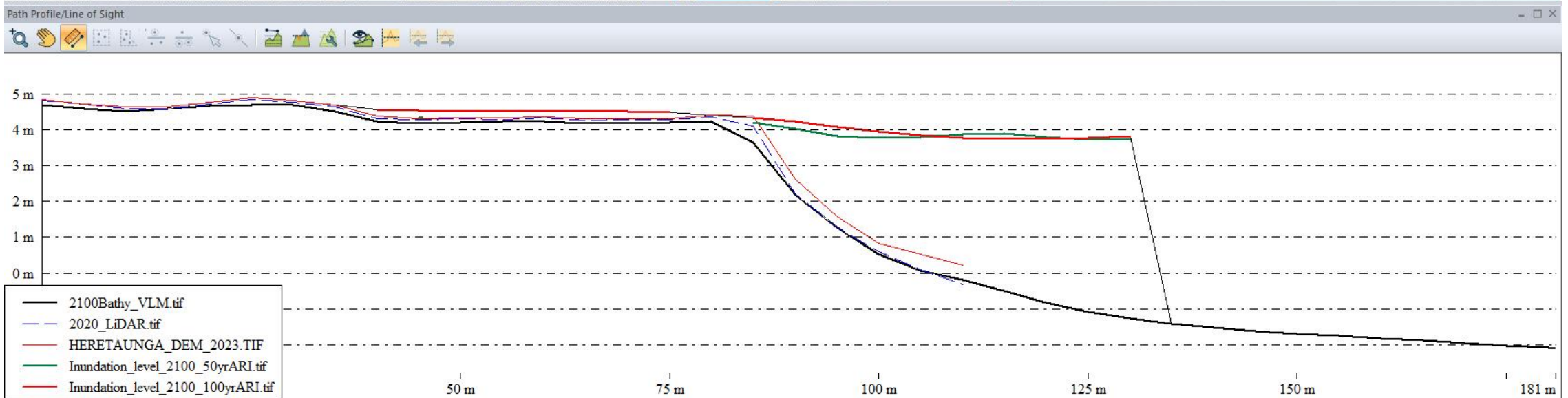
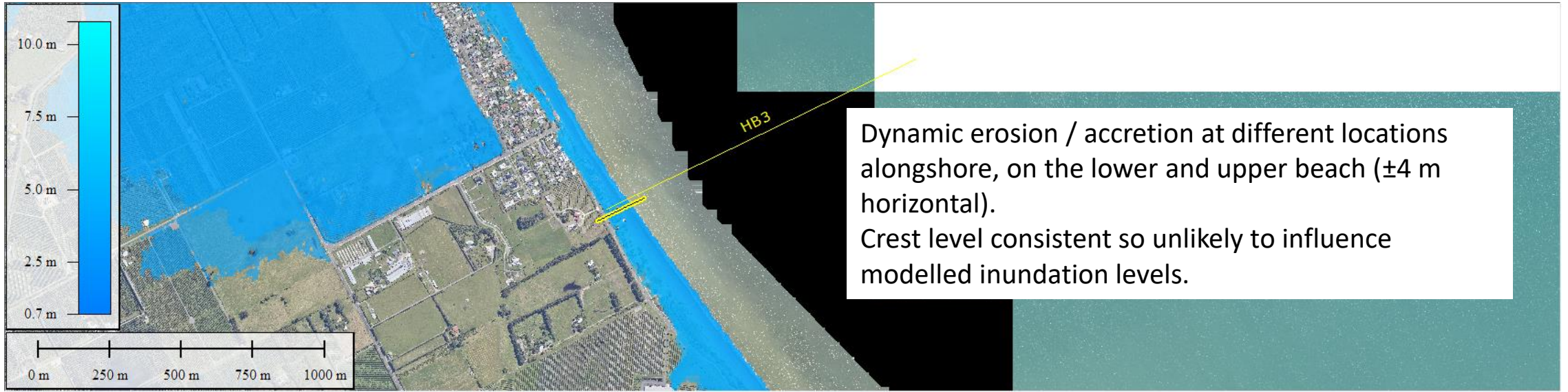
Differences unlikely to influence inundation model.

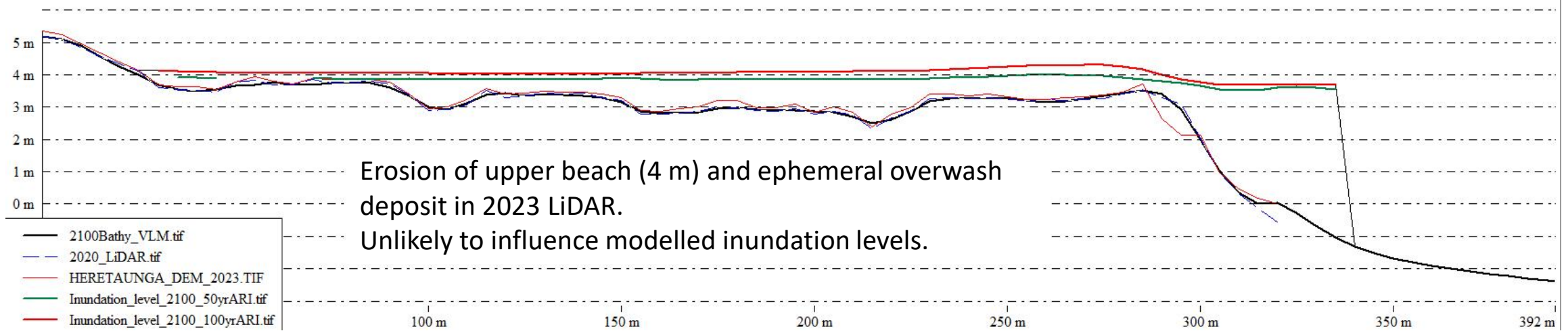
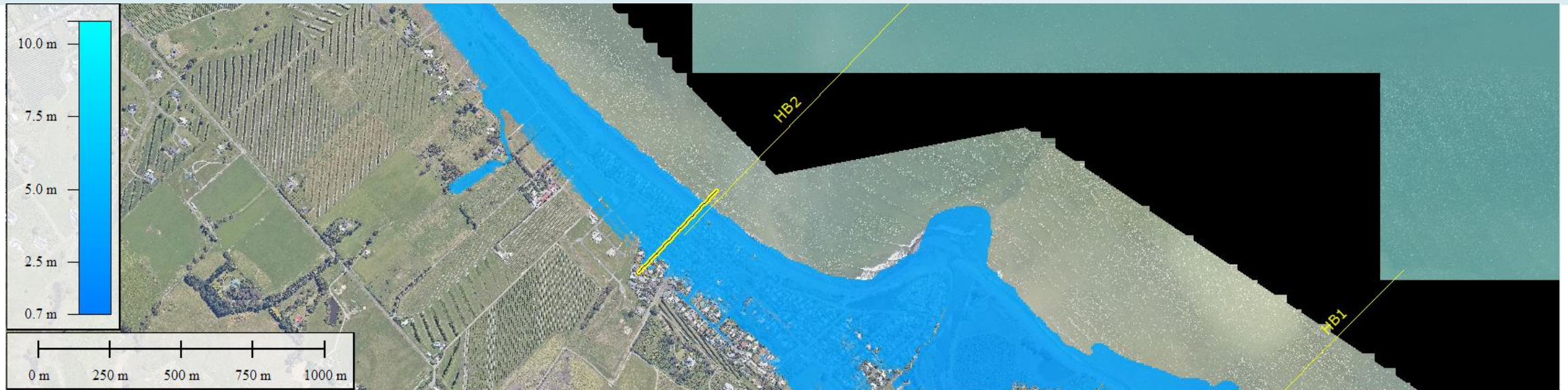


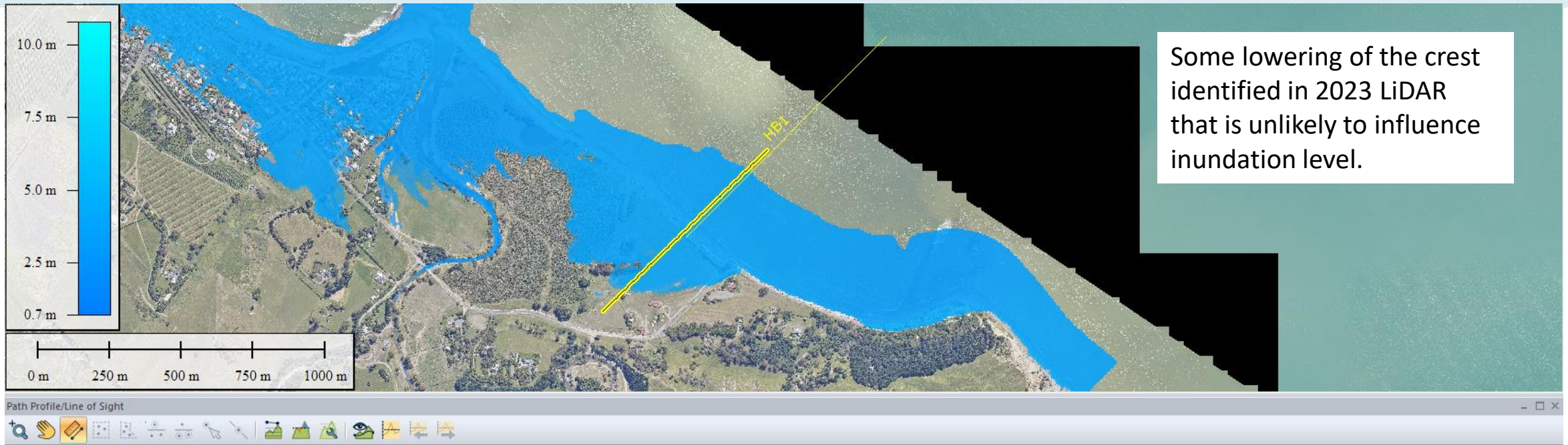


HB4: Haumoana

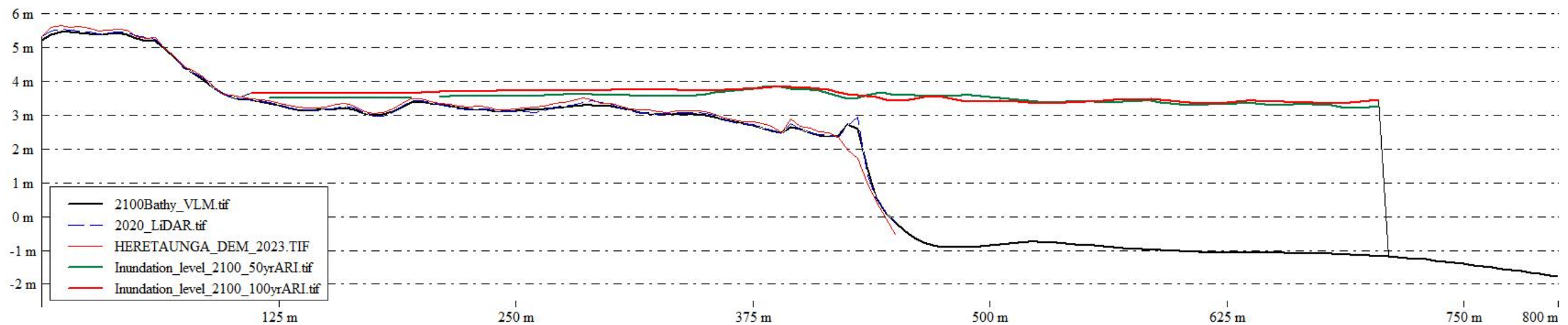








Some lowering of the crest identified in 2023 LiDAR that is unlikely to influence inundation level.



www.tonkintaylor.co.nz

